



**UNIVERSITY OF NAIROBI**

**FACULTY OF ENGINEERING**

**DEPARTMENT OF ELECTRICAL AND INFORMATION ENGINEERING**

**A MICROCONTROLLER-BASED MPPT CHARGE CONTROLLER**

**PROJECT INDEX: PRJ 124**

**BY**

**ABONYO CARLVIN .W.OMONDI**

**F17/38980/2011**

**SUPERVISOR: MR.C. OMBURA**

**EXAMINER: DR. DHARMADHIKARY**

**Project report submitted in partial fulfilment of the requirement for the award of**

**the degree of**

**Bachelor of Science in ELECTRICAL AND ELECTRONICS ENGINEERING from the**

**University of Nairobi 2016**

**Submitted on: 24/05/2016**

# DECLARATION OF ORIGINALITY

**FACULTY/ SCHOOL/ INSTITUTE:** Engineering

**DEPARTMENT:** Electrical and Information Engineering

**COURSE NAME:** Bachelor of Science in Electrical & Electronics Engineering

**TITLE OF NAME OF STUDENT:** Abonyo Calvin Willard Omondi

**REGISTRATION NUMBER:** F17/38980/2011

**COLLEGE:** Architecture & Engineering

**WORK:** MICROCONTROLLER BASED MPPT CHARGE CONTROLLER

- 1) I understand what plagiarism is and I am aware of the university policy in this regard.
- 2) I declare that this final year project report is my original work and has not been submitted elsewhere for examination, award of a degree or publication. Where other people's work or my own work has been used, this has properly been acknowledge and referenced in accordance with the University of Nairobi's requirements.
- 3) I have not sought or used the services of any professional agencies to produce this work.
- 4) I have not allowed, and shall not allow anyone to copy my work with the intention of passing it off as his/her own work.
- 5) I understand that any false claim in respect of this work shall result in disciplinary action, in accordance with University anti-plagiarism policy.

**Signature:** .....

**Date:** .....

Approved by:

Supervisor: Mr. C. Ombura

**Signature:** .....

## **DEDICATION**

To my family for their support during my university education and to my classmates who have helped in push my limits and take on challenges to be better as an engineer.

## **ACKNOWLEDGEMENT**

This project would not have been such a huge success if I did it on my own and I would like to appreciate all who took part in it.

First and foremost, I would like to express my gratitude to Mr Ombura, my supervisor, for his guidance in the implementation of this project. He was instrumental in guiding me to get the knowledge required to implement the project. I would also like to thank the lab technicians Mr.Kimani, Mr.Ng'ang'a among others for their advice, being punctual and helpful in the lab as I tested and troubleshooted the project and help towards the overall success of this project.

Finally, I would also like to extend my gratitude towards my friends, family and classmates, for their support in debugging problems and encouragement when challenges were met.

Above all, I would like to give thanks to the Almighty God for giving me strength to turn challenges into opportunities while giving me good health in the course of the project.

# TABLE OF CONTENTS

|  |      |
|--|------|
| LIST OF FIGURES .....  | v    |
| LIST OF TABLES .....   | vi   |
| ABBREVIATIONS AND ACRONYMS .....   | vii  |
| ABSTRACT .....   | viii |
| 1 INTRODUCTION.....  | 1    |
| 1.1 General background.....  | 1    |
| 1.2 Problem statement .....  | 1    |
| 1.3 Project justification .....  | 1    |
| 1.4 Objectives of the project.....   | 2    |
| 1.5 Scope of project.....  | 2    |
| 1.6 Methodology .....  | 2    |
| 1.7 Project report organization .....  | 3    |
| 2 LITERATURE REVIEW.....   | 5    |
| 2.1 Introduction .....   | 5    |
| 2.2 Solar energy harnessing .....  | 7    |
| 2.3 Solar Panel Technologies .....   | 8    |
| 2.4 PV cell characteristics .....  | 11   |
| 2.5 Charge controllers .....   | 15   |
| 2.6 DC-DC Voltage regulators .....   | 17   |
| 2.7 MPPT Algorithms .....  | 19   |
| 2.7.1 Hill climbing / Perturb and observation .....                              | 19   |
| 2.7.2 Incremental conductance.....   | 20   |
| 2.7.3 Fractional open-circuit voltage and fractional short-circuit voltage ..... | 22   |
| 2.7.4 Fuzzy logic control .....  | 22   |
| 2.8 Batteries .....  | 24   |
| 2.8.1 Three stage lead-acid battery charging.....                                | 25   |
| 2.9 Market Research .....  | 28   |
| 3 DESIGN AND IMPLEMENTATION .....  | 31   |
| 3.1 Microcontroller.....   | 32   |
| 3.2 Sensing networks .....   | 34   |

|       |  |    |
|-------|--|----|
| 3.2.1 | Voltage sensors.....   | 34 |
| 3.2.2 | Current sensors .....  | 35 |
| 3.2.3 | Temperature sensors .....  | 36 |
| 3.3   | System Interface .....   | 38 |
| 3.4   | Buck converter design .....  | 40 |
| 3.5   | Power Supply .....   | 46 |
| 3.6   | MPPT Charge Control Algorithm.....                                       | 47 |
| 3.7   | System Protection .....  | 49 |
| 3.8   | Complete Schematic .....   | 52 |
| 3.9   | Printed Circuit Board.....   | 53 |
| 4     | TESTING, RESULTS AND ANALYSIS .....                                      | 54 |
| 4.1   | Solar Panel Testing.....   | 54 |
| 4.2   | Battery Testing.....   | 55 |
| 4.3   | Sensor Testing .....   | 55 |
| 4.4   | Software Testing.....  | 57 |
| 4.5   | Analysis .....   | 60 |
| 5     | FINANCIAL ANALYSIS .....   | 61 |
| 6     | CONCLUSION AND RECOMMENDATIONS.....                                      | 64 |
| 6.1   | Recommendations for further work.....                                    | 64 |
| 6.2   | Conclusion.....  | 65 |
|       | REFERENCES.....  | 67 |
|       | APPENDICES .....   | 69 |
|       | Appendix One: MPPT Charge Algorithm Code used in the ATMEGA328P.....     | 69 |
|       | Appendix Two: IC Datasheets .....  | 82 |
|       | Appendix Three: PCB traces.....  | 85 |
|       | Appendix Four: Pictures of MPPT Charge Controller in various modes ..... | 86 |

## LIST OF FIGURES

|  |    |
|--|----|
| Figure 2-1: PV Cell characteristics.....   | 11 |
| Figure 2-2: PVcell I-V and P-V characteristics.....  | 12 |
| Figure 2-3: PV cell I-V curve different temperatures.....                                  | 13 |
| Figure 2-4: PV cell P-V curve different temperatures.....                                  | 13 |
| Figure 2-5: PV cell I-V curve different irradiances.....                                   | 14 |
| Figure 2-6: PV cell I-V curve different irradiances.....                                   | 14 |
| Figure 2-7: Extra wattage produced by MPPT for a 120W solar panel.....                     | 16 |
| Figure 2-8: DC-DC Converter Topologies.....  | 18 |
| Figure 2-9: States of a buck converter.....  | 18 |
| Figure 2-10: P&O Flowchart.....  | 20 |
| Figure 2-11: P-V curve slope characteristics of a PV module.....                           | 20 |
| Figure 2-12: Incremental Conductance Flowchart.....  | 21 |
| Figure 2-13: Fuzzy logic control rule base table.....                                      | 23 |
| Figure 2-14: Three stage lead-acid battery charging at individual cell level.....          | 27 |
| Figure 2-16: THE KID MPPT solar charge controller.....                                     | 28 |
| Figure 2-17: SunSaver-20L PWM charge controller.....                                       | 29 |
| Figure 3-1: Block diagram of the designed MPPT charge controller.....                      | 31 |
| Figure 3-2: Synchronous buck operation.....  | 40 |
| Figure 3-3: Buck converter waveforms.....  | 40 |
| Figure 3-4: Flowchart showing MPPT by P&O being used in the bulk charging stage.....       | 47 |
| Figure 3-5: Flowchart showing the basic three stage charging being used.....               | 48 |
| Figure 3-6: MPPT Charge Controller Schematic.....  | 52 |
| Figure 3-7: MPPT Charge Controller PCB Schematic.....                                      | 53 |
| Figure 4-1: PV power and current as a function of PV Voltage; 1415hrs on 5/04/2016.....    | 54 |
| Figure 4-2: PV power and current as a function of PWM; 1415hrs on 5/04/2016.....           | 55 |
| Figure 4-3: PV wattage at different periods of the day on 5/04/2016.....                   | 55 |
| Figure 4-4: Breadboard implementation of MPPT Charge controller; 1555hrs on 5/04/2016..... | 58 |
| Figure 4-5: PCB circuit of MPPT Charge controller 12/05/2016.....                          | 59 |

## LIST OF TABLES

|  |    |
|--|----|
| Table 2-1: Solar Panel technologies.....   | 8  |
| Table 4-1: Voltage Sensor test.....  | 56 |
| Table 4-2: Current Sensor test .....   | 56 |
| Table 4-3: Battery state test .....  | 57 |
| Table 4-4: Charge algorithm test .....   | 57 |
| Table 4-4: MPPT Charge controller efficiency test .....  | 57 |
| Table 4-5: Temperature compensation testing at $3\text{mv}/^{\circ}\text{C}$ /Cell deviation from $25^{\circ}\text{C}$ ..... | 58 |
| Table 5-1: Financial Analysis.....   | 61 |



## ABBREVIATIONS AND ACRONYMS

|                  |   |
|------------------|---|
| ADC              | Analog to Digital Converter                         |
| DC               | Direct current                                      |
| GND              | Ground  |
| IC               | Integrated Circuit                                  |
| I                | Current   |
| I/O              | Input/ Output                                       |
| SPI              | Serial Peripheral Interface                         |
| LDR              | Resistor  |
| MAX              | Maximum   |
| MCU              | Microcontroller                                     |
| MOSFET           | Metal Oxide Semiconductor Field Effect Transistor   |
| VCC              | Supply voltage                                      |
| SoC              | State of Charge                                     |
| PCB              | Printed Circuit Board                               |
| PV               | Photovoltaic panels                                 |
| CMOS             | Complementary Metal Oxide Semiconductor             |
| RISC             | Reduced Instruction Set Controller                  |
| LVD              | Low Voltage Disconnect                              |
| PWM              | Pulse Width Modulation                              |
| V <sub>mpp</sub> | Voltage at maximum power point                      |
| I <sub>mp</sub>  | Current at maximum power point                      |
| STC              | Standard Test Conditions                            |
| V <sub>oc</sub>  | Open circuit voltage                                |
| I <sub>sc</sub>  | Short circuit current                               |
| Insolation       | Incident solar radiation                            |
| MPPT             | Maximum Power Point Tracking                        |
| AGM              | Absorbed Glass Mat                                  |
| LCD              | Liquid Crystal Display                              |
| LED              | Light Emitting Diode                                |
| DIP              | Dual Inline Package                                 |
| DMM              | Digital Multimeter                                  |
| SDA              | Serial Data   |
| SCL              | Serial Clock  |
| IDE              | Integrated Development Environment                  |
| RGB              | Red Green Blue LED                                  |
| AWG              | American Wire Gauge                                 |
| EEPROM           | Electrically Erasable Programmable Read Only Memory |

## **ABSTRACT**

This paper presents detailed design, implementation and testing of an economical microcontroller based MPPT charge controller with a maximum charging rate of 20A to be used in a standalone PV systems which is able to monitor the power generated by the photovoltaic array and deliver the maximum amount into charging the battery under varying atmospheric conditions whilst simultaneously charging the battery in three stages for higher charging efficiency and healthy battery operation. The charge controller is also designed to display the system status by LCD and LEDs for user friendliness.

The MPPT charge controller was designed using a DC/DC buck converter whose switch was controlled by a Pulse-Width-Modulated (PWM) signal generated by the microcontroller to regulate its output. The microcontroller generates the PWM signal after its MPPT algorithm analyzes the sensor inputs connected to the solar panel and battery and decides the on the PWM signal that would make the solar panel operate at its maximum power point whilst also accounting for the battery's charging stage .Basically the solar panel is deemed the energy source, the DC-DC converter is used for maximum power transfer by optimal resistance matching of source to battery and the microcontroller has MPPT algorithm used to track maximum power operation of the solar panel; the MPPT algorithm varies the duty cycle appropriately and that alters the load seen by the solar panel hence making it output different voltage and current for more power to go into charging the battery.

The performance and characteristic of the MPPT charge controller are hence analyzed.

# 1 INTRODUCTION

## 1.1 General background

Renewable energy sources are fast becoming an alternative to traditional fossil fuels due to their advantages of being clean and inexhaustible mainly. Solar power is one of the renewable energy sources and although it has a high potential its generation efficiency (conversion of solar energy to electricity) is low with most commercial solar panels having efficiencies of less than 30%. With this already low power generation efficiency of solar panels it is only necessary that the maximum power is sourced from that generated by solar panels to ensure high efficiency in delivering power to the load to make solar power an effective alternative and justify its high installation costs too. Since the I-V characteristics of solar panels vary with atmospheric conditions such as irradiance, more power can be got out of solar panels by direct methods e.g. solar tracking to track the sun as it moves across the sky or by indirect methods e.g. Maximum power point tracking the latter being in the purview of this project.

Using MPPT charge controllers reduces the number of PV modules that need to be installed to generate a certain power by maximizing the power generated from the critical number of PV modules needed to generate the power at high efficiency.

## 1.2 Problem statement

There are inherent power losses that occur when the solar is connected directly to a load/battery without matching their internal impedances for which in addition to the non-linear (I-V) operating characteristics of a PV module and variations in its output power with solar insolation and operating temperature; an MPPT charge controller is used in most solar power harvesting systems to ensure maximum rated power is drawn from the solar panel and delivered to the battery while charging it in a healthy mode to increase its lifespan and for efficiency purposes under varying atmospheric conditions.

Many are available commercially for high current ratings and relatively expensive so we are building a simple cheap, adaptable, elementary and durable one from first electronic principles that does the job quite as well and has the lucrative advantage that it can be deployed in rural homes and developing areas of the world for enterprises and households cheaper than conventional MPPT charge controllers from the leading industrial manufacturers.

## 1.3 Project justification

The project was designed to address the challenges of low efficiencies in solar harvesting some of the causes being significant energy loss when the solar panel is directly connected to a battery and the non-linear I-V operating characteristics of solar panels which vary with atmospheric characteristics such as insolation and ambient temperature. Several MPPT charge controllers have been proven to boost efficiency while increasing the maximum charging current delivered to load by 30% in

comparison to PWM charge controllers -which do not track maximum operating power point of PV modules - and the project aims at building an economical microcontroller based MPPT charge controller to be part of the solution.

## **1.4 Objectives of the project**

The main objectives of the study are outlined below:

- To design an efficient MPPT charge controller with a maximum charging rate of 20A.
- To implement a fast and fairly accurate maximum power point tracking algorithm, several of which will be discussed, that also charges a battery in stages for healthy battery status.
- To design the MPPT charge controller system to be Plug-and-Play, user-friendly and display the vital operational parameters of the system.

## **1.5 Scope of project**

The MPPT charge controller is to be designed using a DC/DC buck converter whose switch was controlled by a Pulse-Width-Modulated (PWM) signal generated by the microcontroller to regulate its output. The microcontroller generates the PWM signal after its MPPT algorithm analyzes the sensor inputs connected to the solar panel and battery and decides the on the PWM signal that would make the solar panel operate at its maximum power point whilst also accounting for the battery's charging stage .Basically the solar panel is deemed the energy source, the DC-DC converter is used for maximum power transfer by optimal resistance matching of source to battery and the microcontroller has MPPT algorithm used to track maximum power operation of the solar panel; the MPPT algorithm varies the duty cycle appropriately and that alters the load seen by the solar panel hence making it output different voltage and current for more power to go into charging the battery.

## **1.6 Methodology**

As stated before, the aim of the project is to design and build an MPPT charge controller to deliver maximum power from the solar panel. The project consists of three main structures which are the input, controller and output.

The first step in developing the Maximum Power Point Tracker is to decide the type of solar panel and battery ranges it would be connected to, based on the maximum charging current desired. The DC/DC converter topology for the MPPT will then be selected and designed based on the maximum solar panel voltage, the battery voltage and the switching frequency by the microcontroller using the least power consuming but efficient components.

The microcontroller will then be chosen and should be low-power, have fast processing speed to run the algorithm in shortest time while also multitasking communication with the various I/O devices in real-time and contain enough programming space for all project objectives. The sensors in the MPPT charge controller are the devices that are going to be in charge of monitoring and communicating the system status to the microcontroller will then be designed. The current and voltage sensors are going to be needed in the design to calculate power which is vital in achieving maximum power point tracking. These sensors on the battery side, in addition to the battery temperature sensor, will also be used to determine the battery charging status ensuring healthy battery operation. The sensors are to be designed to be as sensitive as possible while consuming minimal power

The design of the software will then be done using an MPPT & charge control algorithm to ensure that the solar panel is operating at the highest power point while charging the battery efficiently. The charge control part of the algorithm will implement a 3-stage charging process for the lead-acid battery based on the battery voltage and solar panel output voltage. It will have the bulk, absorption and float charging stages with the MPPT algorithm being implemented in the bulk charging state. The actual quantitative set-points of the operating modes will be based on characteristics of the battery and PV module that will be implemented finally. The software should be able to display the vital parameters quickly and easily through the LCD and LEDs incorporated to the system so that the user can interpret the status of the system.

In order to ensure a proper design and easier debugging, a printed circuit board (PCB) will be made for the MPPT charge controller and the parts soldered on. Finally, a financial feasibility study was done on the components and design as a whole to assess the viability of making the MPPT charge controller in a low cost manner to ensure it could be readily made for economical mass-markets. After all these steps were completed the design was deemed ready for use. The entire system was simulated meticulously to ensure the design performed as desired. The PCB board was then tested with the solar panel and battery load to ensure the system met expectations.

## **1.7 Project report organization**

The project is divided into 6 chapters:

- Chapter 1:** This covers the introduction of the project report describing the justification for doing the project, the objectives, methodology and scope of the work.
- Chapter 2:** This covers the literature review and research regarding solar panel and battery workings, the necessity of maximum power point tracking, various MPPT algorithms .It basically focuses on the material background data needed to be understood to design and build the various components of an efficient MPPT charge controller.
- Chapter 3:** This chapter involves explains the design and implementation of the MPPT charge controller that will satisfy the project goals.

- Chapter 4:** This chapter describes the results got after tests are done on the MPPT charge controller after the physical implementation.
- Chapter 5:** This chapter gives a financial feasibility assessment of the components used for the MPPT charge controller.
- Chapter 6:** This chapter gives the conclusion of the project and future works recommendation.

## 2 LITERATURE REVIEW

### 2.1 Introduction

With increasing global population, energy demand has grown exponentially leading to depletion of natural resources we have heavily been relying on e.g. coal, oil and natural gas. This has not only depreciated the longevity of these resources but has also detrimentally affected our global climate. Clean, renewable energy sources are thus becoming more desirable throughout the world in an effort to reduce greenhouse emissions. The main renewable sources are biomass, geothermal, tidal, hydro, solar, and wind. Unfortunately, solar energy is not as efficient as traditional energy sources such as coal, but advances in the electronics field can be used to create more stable and efficient sources to compensate the problems associated with using solar panels.

PV power systems have the following advantages:

- i. Their installation is static (i.e. no moving parts)
- ii. They are simple and quick compared to other renewable sources.
- iii. They have longevity, ( are durable typically more than 20 years)
- iv. They have low operational and maintenance costs hence they provide a significant solution for powering remote areas.
- v. They are not noisy.
- vi. Suitable for Distributed Generations (DGs) which permits small-scale generators to be installed at the distribution level of the power system close to the end which come in handy when there is insufficient transmission capacity, constraints in building new transmission lines and untapped emerging electricity markets hence boosting the Grid from remote areas .
- vii. Solar energy is abundant, virtually available everywhere in the world and is the most plentiful energy source. Earth receives 3.85 million Exajoules of energy per year at the surface, about 50% of total incident solar radiation or insolation.
- viii. PV modules are pollution free-they have “zero-emission” factor

However, PV power systems have some disadvantages:

- i. Solar energy is not constant even during the daytime. Due to Earth’s atmosphere and its atmospheric conditions, it is approximated that only 50% of solar energy that is directed to the planet reaches its surface the other half is reflected back and absorbed by elements in the atmosphere such as dust and water vapor.
- ii. Solar energy is not available at night.
- iii. The current available technologies place on the efficiency at which this energy is harvested and utilized. Even though there are numerous solar panel and solar cell technologies available,

the highest efficiency at which these devices convert solar energy to electricity is lower than 30% and the costs per kilo-watt-hour (kWh) are not usually competitive enough to face off petroleum energy sources.

- iv. Their installation cost is high and they still need dc/dc converters to charge batteries and inverters for load interface. Since Photovoltaic (PV) modules still have relatively low conversion efficiency

With the cost of the solar cells decreasing, the shift to solar energy use is increasingly becoming viable. This is particular true in tropical and desert countries where there is abundant solar energy available throughout the year. Also as solar power increases in popularity, the need for this power to become more efficient is incumbent. Photovoltaic sources are used vastly in many operations such as battery charging, water pumping ,powering equipment in marine boats ,electric and recreational vehicles, home power supply, hybrid system incorporating solar and other renewable energy sources, swimming-pool heating systems, in space and powering satellites, military applications, solar power plants and some applications where nonlinear power source is needed.

PV systems can be divided into two categories: stand-alone and grid-connection systems. In stand-alone systems PV array feeds the loads directly without connecting to the grid utility system which is profitable because of the modest system configuration and control scheme. This kind of energy source, due to the proximity between the generation and the consumption, is an attractive alternative for telecommunication stations and rural systems that are off the grid .Secondary batteries more so lead acid batteries are widely used in stand-alone PV systems to store the excess generated energy and supply the load in case of minimal to no solar energy production at night. The popular type used is the valve regulated lead–acid (VRLA) battery, because of its fair cost, maintenance-free operation, high safety operation and high efficiency characteristics compared to flooded lead acid batteries. The performance and longevity of VRLA batteries depend, to a large extent, on the quality of their chargers. Designing a VRLA battery charger for stand-alone PV systems is a balancing act. One should consider the charging voltage and current in order not to overcharge and damage the battery as well as the maximum power point of PV power generation system which depends on different operating conditions such as array temperature and solar irradiance. Therefore a MPPT algorithm with charge control functionality should be implemented to maximize the energy transferred to the battery bank.

In light of the pros, cons and applications of using solar energy; this project looks into using a technique that develops high efficiency converters more so for battery charge controllers which simultaneously are designed to extract the maximum possible power from the PV module by Maximum Power Point Tracking, (MPPT) hence improving efficiency and reducing overall cost of the system. The key data and knowledge pertinent to the cause of the project and needed to design an MPPT charge controller are discussed below till the end of this chapter.



## 2.2 Solar energy harnessing

Solar energy can be harvested in two different ways, directly using photovoltaics or by using Concentrated Solar Power (CSP). The CSP process is an indirect method and involves the use of mirrors and lenses to intensify sunlight and its thermal energy is used to heat up water and produce steam. Steam is then used to drive steam turbines which produce electricity.

Photovoltaic cells are devices that absorb sunlight and convert that solar energy into electrical energy by photoelectric effect. Solar cells are commonly made of silicon. Pure silicon is a poor conductor of electricity and has four outer valence electrons that form tetrahedral crystal lattices; hence the silicon has to be purposefully injected with impurities, a process called doping, to improve its electrical characteristics. The electron clouds of the crystalline sheets are stressed to create P-type and N-type silicon by adding trace amounts of elements containing three or five outer shell electrons respectively (based on the prevalence of free electrons). The combination of N-type and P-type silicon leads to formation of an electrostatic field at their boundary (junction). Electrons at the junction from the either side mix and form a barrier that prevents electrons on the negative side to cross to the positive side.

When equilibrium is reached an electric field separates the sides into valence and conduction bands. The potential difference between the lowest energy level on the conduction band  $E_c$  and the highest energy level on the valence band  $E_v$  is called band gap energy or  $E_g$ . Electrons with enough input energy can jump this band gap from their usual steady state spot on the valence band to an excited state on the conduction band. These electrons cause the direct current that the solar cells produce. Solar energy packets or photons that contain different amounts of energy correspond to different wavelengths of the solar spectrum. Consequently photons with higher energy levels than  $E_g$  are also absorbed but their excess energy is reflected or dissipated in the form of heat (wasted energy) and photons with lower energy levels than  $E_g$  are not able to get absorbed at all.

When photons (sunlight) hit a solar cell, its energy breaks the inherent band gap energy thus frees electron-holes pairs sending free electrons to the negative side and holes to the positive side. If an external current path is provided electrons, trying to reinstate electrical neutrality, will flow through it to their original positive side to combine with holes that the electric field sent there hence doing work. The electron flow provides the current, and the cell's electric field causes a voltage. Typically, PV cells produce low power (approximately 1-3Watts); hence several cells are connected together (in series to increase voltage or in parallel to increase current) to form modules and panels for higher power applications. Solar panels can be joined to create a solar array. The panels are built of aluminum for durability. The cells are usually placed behind tempered glass for safety, durability and protection of cells against weather conditions. A clear resin is used to insulate the back of the solar cells and also keep them in place against the top panel glass. Some light is lost due to reflection, which is why antireflection coating is used on top of every solar cell.

## 2.3 Solar Panel Technologies

There are many different types of solar cells and various materials used to make them, but the two most popular technologies used in today's solar energy market are silicon, which is considered a first-generation technology and thin film which is considered a second-generation technology. Thin-films include solar cells like: amorphous silicon (TF-Si), Copper Indium Gallium DE Selenide (CIGS), and Cadmium Telluride (CdTe)

**Table 2-1: Solar Panel technologies**

|                  | BRIEF  | ADVANTAGES  | DISADVANTAGES   |
|------------------|--|---|---|
| mono-crystalline | Produced using the Czochralski process where seed crystal silicon is dipped into molten silicon and withdrawn very slowly. This process produces a two meter long cylindrical single-crystal ingot as the molten silicon crystallizes around the seed. The silicon can be intrinsic or doped with impurities depending on its future use. The ingot is then sliced into thin wafers. | <ul style="list-style-type: none"> <li>- The most efficient, with percentages averaging around 11% - 16% due to the lack of imperfections and cell structure this type of solar panel</li> <li>- They have been proven to last longer than the rest of the silicon technology</li> <li>- They have most watts per square foot of panel used, since these panels are so efficient</li> </ul> | <ul style="list-style-type: none"> <li>- Has a higher price per panel because a lot of silicon material is wasted in the process considering the square shape of solar cell which means more silicon is used to compensate the waste and the manufacturing process is complicated</li> <li>- They are very fragile and care must be given during the shipping and installation processes</li> </ul> |
| polycrystalline  | In this fabrication process molten silicon is usually casted and then cooled in a rectangular shape for a more profitable outcome. The block is then sliced similarly to the mono-crystalline ingot to create the thin solar cells. As the name implies the ingot is made of multiple crystals resembling pieces of  | <ul style="list-style-type: none"> <li>- These types of silicon cells are cheaper and therefore cost less to produce in comparison to mono-crystalline cells are the most common type of solar panel in home installations today, due to their low cost and average power efficiency</li> </ul>   | <ul style="list-style-type: none"> <li>- The lower grade semiconductor used in fabrication and the imperfections drop the solar cell performance. Efficiency is the main disadvantage of polycrystalline solar panels dropping to 10-14% because of the energy loss at the junction points between two adjacent crystals and increases in electron-</li> </ul>                                      |

|  |   |   |   |
|--|---|---|---|
|  | shattered glass due to the manufacturing process  | - This process is a faster and a lot easier to implement  | hole recombination rate due to the impurity concentration & abnormal structure.   |
| amorphous silicon (TF-Si)                | <p>-Amorphous silicon or other non-silicon semiconductors are used, instead of crystal silicon. The semiconductor is placed between flexible laminate, glass or steel plates. The flexible laminate is most commonly used to produce these panels.</p> <p>-Thin film solar panels are cheaper and faster to produce since the entire panel is considered a solar cell, unlike traditional panels constructed of numerous solar cells. The manufacturing process makes these panels the most readily available solar panel on the market</p> | <p>- The flexible laminate makes these panels bendable and thus easier to mount on uneven surfaces &amp; more durable to extreme weather condition like a hailstorm</p> <p>- In case of damage the thin films panels with continue to work at a lesser rate, while crystalline silicon panels stop working altogether if a single cells is damaged</p> <p>- Thin film panels weigh less than crystalline silicon panels thus easier installing for residential use.</p> <p>- Thin film panels perform better in hotter climates.</p> <p>- Thin film panels perform better than the competition in shade or low light conditions</p> | <p>- Thin film technology efficiency ranges between 6% - 9%. This means that in order to produce the same amount of electricity twice as many thin film panels are needed in comparison with polycrystalline panels and almost three times as many when compared to mono-crystalline.</p> |
| Copper Indium Gallium DE Selenide (CIGS) | -The semiconductor in this type of panel is composed of copper, indium, gallium and selenium. The CIGS compound, which has a  | - Unlike silicon, CIGS efficiency is not affected as much as the panel temperature increases. CIGS panel efficiency ranges from 10%-15%   | -These panels are usually very expensive and hard to find due to their vacuum based fabrication process   |

|                          |   |   |  |
|--------------------------|---|---|--|
|                          | high optical absorption coefficient , is layered on a glass back plate which has a high optical absorption coefficient, therefore very little is needed to produce the panels. As a result CIGS panels are very light in comparison to crystalline silicon panels |   |  |
| Cadmium Telluride (CdTe) | -used in thin film technology to Improve the low efficiency experienced with amorphous silicon. . They are the most common type of Thin film solar panel on the market and the most cost-effective to manufacture.  | -CdTe panels perform significantly better in high temperatures and in low-light conditions similarly to CIGS panels   | - Have efficiency range between 7% - 12% on average<br>The limited supply of Tellurium and toxicity of Cadmium make these panels expensive and dangerous for the environment.                          |
| Gallium Arsenide (GaAs)  | The semiconductor compound used to make these panels is Gallium Arsenide, a mixture of Gallium and Arsenic  | -The main benefit of GaAs panels is their efficiency. GaAs efficiency can range between 20% - 25%. mainly due to the nearly ideal GaAs band gap<br>-GaAs panels are very useful in space applications because of its resistance to radiation damage and insensitivity to heat | -GaAs in a single crystal form is very expensive and Gallium is a rare material<br>-Arsenic is very poisonous hence the panels are dangerous if damaged to the point that the semiconductor is exposed |

## 2.4 PV cell characteristics

The building block of PV arrays is the solar cell, which is basically a p-n semiconductor junction that directly converts light energy into electricity and the PV module can be modeled as shown by the schematic of Fig 2-1.

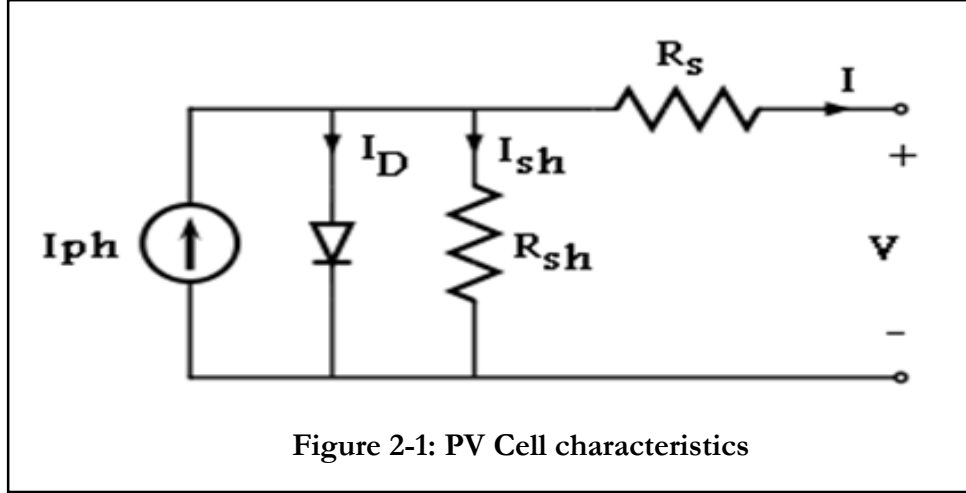


Figure 2-1: PV Cell characteristics

The characteristic equation of this model of a single PV module is given as

$$I = I_{ph} - \frac{V + IR_s}{R_{sh}} - I_0 \exp \left[ \left( \frac{V + IR_s}{AV_t} \right) - 1 \right] \quad \text{Equation 1.0}$$

If there are  $N_p$  parallel modules each one including  $N_s$  serial-connected PV cells the equation becomes:

$$I = N_p I_{ph} - \frac{\frac{N_p V}{N_s} + IR_s}{R_{sh}} - N_p I_0 \exp \left[ \left( \frac{\frac{V}{N_s} + IR_s}{AV_t} \right) - 1 \right] \quad \text{Equation 1.0.1}$$

Where

$$I_0 = I_{or} \left[ \frac{T}{T_r} \right]^3 \exp \left[ \frac{q E_{go}}{Bk} \left( \frac{1}{T_r} - \frac{1}{T} \right) \right] \quad \text{Equation 1.1}$$

$$I_{ph} = [I_{scr} + K_i(T - 25)] \frac{\lambda}{100} \quad \text{Equation 1.2}$$

And

|                                      |  |
|--------------------------------------|--|
| <b>I and V</b>                       | cell output current and voltage;                             |
| <b>I<sub>0</sub></b>                 | cell reverse saturation current;                             |
| <b>V<sub>t</sub></b>                 | Thermal voltage ( $V_t = kT/q$ );                            |
| <b>T</b>                             | cell temperature in C;                                       |
| <b>k</b>                             | Boltzmann's constant;  |
| <b>q</b>                             | Electronic charge;   |
| <b>K<sub>i</sub> (A/°C) = 0.0017</b> | short circuit current temperature coefficient at $I_{scr}$ ; |
| <b>λ</b>                             | solar irradiation in $W/m^2$ ;                               |
| <b>I<sub>scr</sub></b>               | short-circuit current at 25 °C and 1000 $W/m^2$ ;            |

|                                |   |
|--------------------------------|---|
| <b>I<sub>ph</sub></b>          | light-generated solar cell current;         |
| <b>E<sub>go</sub></b>          | band gap for silicon;                       |
| <b>B=A=1.92</b>                | ideality factors;                           |
| <b>T<sub>r</sub>=301.18 °K</b> | reference temperature;                      |
| <b>I<sub>or</sub></b>          | cell saturation current at T <sub>r</sub> ; |
| <b>R<sub>sh</sub></b>          | shunt resistance;                           |
| <b>R<sub>s</sub></b>           | series resistance.                          |

Eqn 1.0 can be simplified by assuming ideal conditions I.e. R<sub>s</sub>=0 and R<sub>sh</sub> =∞ yielding Equation 1.3

$$I = I_{ph} - I_o \exp \left[ \left( \frac{V}{AV_t} \right) - 1 \right] \quad \text{Equation 1.3}$$

Under open circuit conditions V=V<sub>oc</sub> and I=0 this can be solved to give Equation 1.4

$$V_{oc} = \frac{AkT}{q} \ln \left( \frac{I_{ph}}{I_{os}} + 1 \right) \quad \text{Equation 1.4}$$

From Equation1.3 the maximum power point can be calculated by P=VI giving Equation1.5

$$P = V \left( I_{ph} - I_o \exp \left[ \left( \frac{V}{AV_t} \right) - 1 \right] \right) \quad \text{Equation1.5}$$

And since at maximum power point the gradient is zero we obtain the following equations at MPP

$$\frac{dP}{dV} = I_{ph} - I_o \left[ \exp \left( \frac{V}{AV_t} \right) + V \left( \frac{q}{AV_t} \right) e^{\frac{V}{AV_t}} - 1 \right] \quad \text{Equation1.6}$$

$$I_{ph} - I_o \left[ \exp \left( \frac{V_{mp}}{AV_t} \right) + V \left( \frac{q}{AV_t} \right) e^{\frac{V_{mp}}{AV_t}} - 1 \right] = 0 \quad \text{Equation1.7}$$

The typical output characteristics of the PV module is shown in Figure 2-2. Solar panels have a common characteristic regarding their Voltage-Current relationship. Figure 2-2 shows the typical Voltage-Current curve of solar cells. As it can be seen, their operation is not linear and there is a tradeoff between voltage and current.

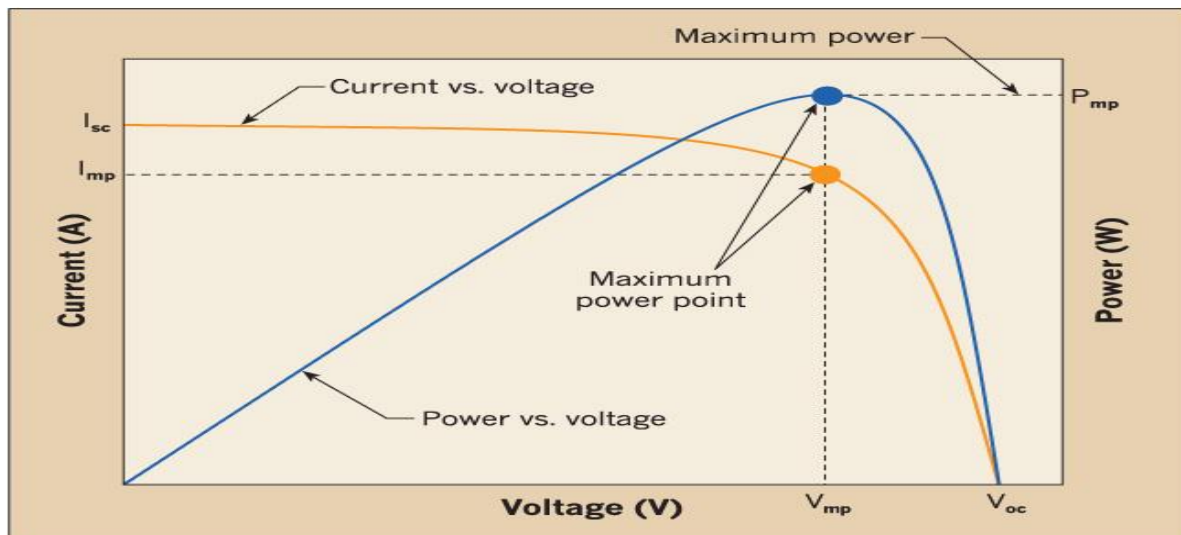


Figure 2-2: PVcell I-V and P-V characteristics.

When no load is connected, the voltage across the terminals is called the open circuit voltage ( $V_{oc}$ ). Similarly, when the load has an impedance of zero (short-circuited terminals), the current that flows through the terminals of the panel is called the short-circuit current ( $I_{sc}$ ). Solar panels range from mini solar cells that can produce less than 1W of power to industrial solar panels that can produce several thousands of watts. It all depends on the applications for which it is intended.

Usually most solar panels, the I-V and P-V curves are tested at standard test conditions (STC) of temperature of 25°C and solar insolation (irradiance) of 1000W/m<sup>2</sup>. However, the I-V and P-V curves of Figure 2-2 change as these two parameters vary as seen also from Equation 1.7 where maximum power point varies with  $I_{ph}$  dependent on irradiance and  $V_t$  dependent on temperature. For the case of temperature, as the semiconductor temperature goes up so does its conductivity, the higher conductivity reduces the electric field at the silicon p-n junction, which in turn reduces the voltage across a solar cell. A smaller cell voltage leads to a smaller power output, intuitively lowering efficiency. Solar panels will usually have a temperature coefficient ( $K_i$ ), which is usually the rate of power reduction for every degree above normal operating temperature of 25°C.

Figure 2-3 shows temperature effects on the I-V curves on a solar panel. It is seen that the higher the temperature the less the area under the curve and hence less power and efficiency. Pumping a coolant through the backside of the panels is an active method or attaching a heat sink or cooling fins is a passive way of dissipating heat from the panels. Figure 2-4 shows the resultant P-V curve for a typical commercial 250W solar panel. Solar panels are thus most efficient in cold sunny days in contrast.

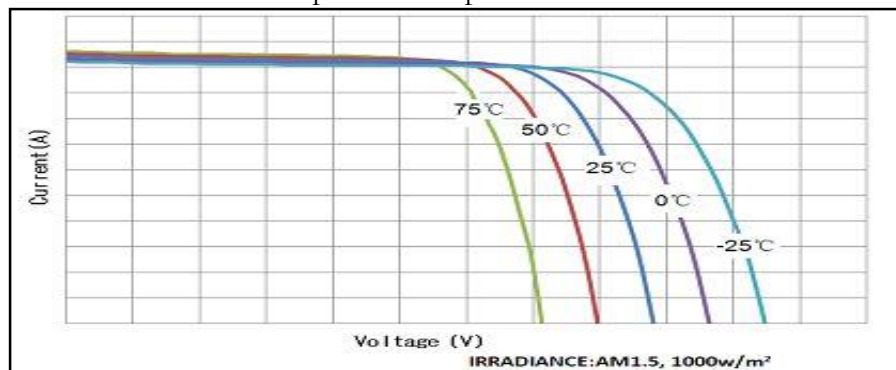


Figure 2-3: PV cell I-V curve different temperatures

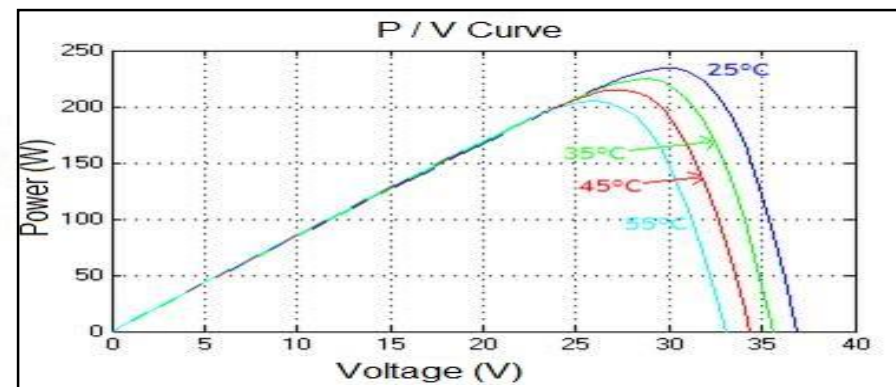
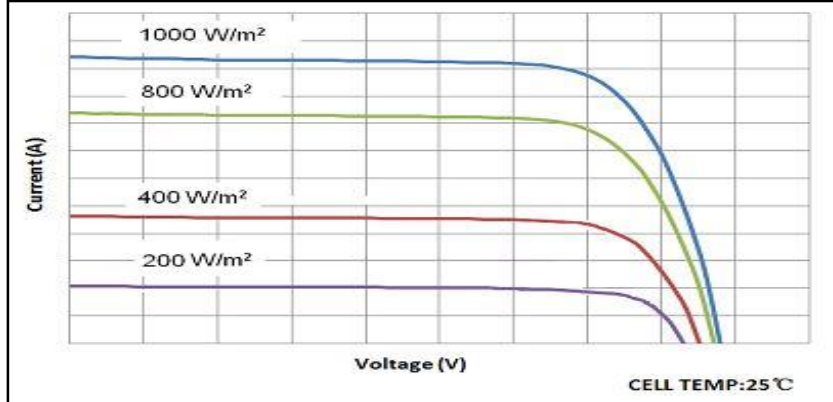
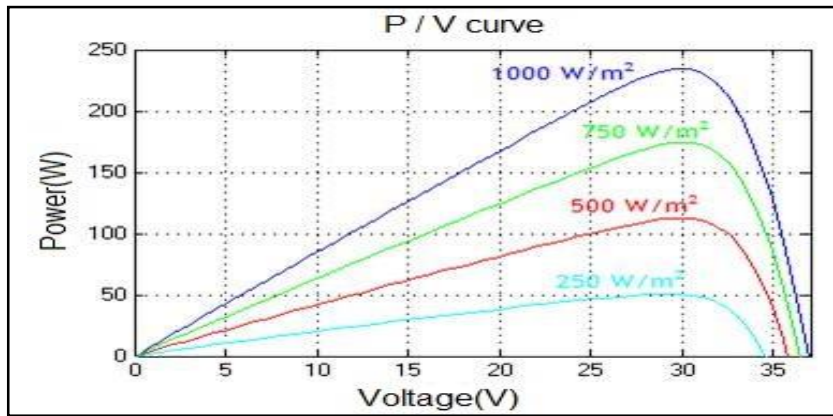


Figure 2-4: PV cell P-V curve different temperatures.

As for solar insolation (irradiance); solar radiation is the electromagnetic (EM) radiation emitted from the sun. Insolation is expressed by the amount of energy received on a given surface in a given time. It is expressed by watts per square meter ( $\text{W/m}^2$ ). Solar insolation is observed as the reason why solar panels produce more output during midday as compared to mornings and evenings. Figure 2-5 shows the impact of irradiance on the I-V curve of a solar panel. It is seen that more irradiance increases the area under the curve which means more power and efficiency, this can be demonstrated by the P-V curve of Figure 2-6 for a typical 250W solar panel. Efficiency can be improved in cases of low solar irradiance using direct methods like solar tracking and light concentration or indirect methods such as the one in the purview of this project which is implementation of an MPPT charge controller.



**Figure 2-5: PV cell I-V curve different irradiances.**



**Figure 2-6: PV cell I-V curve different irradiances.**

As seen from the above, the output of a solar is a non-linear curve and is characterized by the fill factor, which helps determine the maximum power a solar cell can provide. This factor, abbreviated “FF,” is the ratio of the maximum output power of the solar cell to the product of the open circuit voltage and short circuit current of the cell; efficiency of the solar cell is the ratio of maximum power to the incident power

$$FF = \frac{P_{max}}{(V_{oc} \cdot I_{sc})} \quad \text{Equation 2.0}$$

$$Efficiency = \frac{V_{oc} \cdot I_{sc} \cdot FF}{P_{in}} \quad \text{Equation 2.1}$$



## 2.5 Charge controllers

Charge controllers aim to provide the correct voltage and current ratings for a rechargeable battery by monitoring and regulating the solar panel output voltage to match the batteries. This output voltage regulation is very important in battery charging because batteries require a specific charging method with various voltage and current levels for each specific stage, these charging methods are needed to prolong battery life and performance.

Some common charge controller protection features to prevent battery damage are undercharge and overcharge protection. Undercharge protection entails disconnecting the battery when the charge is too low to continue powering connected loads, similarly, the charge controller stops providing energy to the battery when it is fully charged to prevent overcharge. This is where the charge controller does most of the work. Simple charge controllers disconnect the battery once the battery surpasses a threshold level and reconnect it once the battery level falls below a certain preset charge level. Other protection features include protection against over-voltage and completely draining ("deep discharging") a battery and regulating charging/discharging rates to protect battery life and improve its life span. From the above it is seen that the gist of a charge controller is a DC to DC converter that converts the solar panel voltage to a voltage suitable for charging the battery while protecting it. Implementing a DC to DC converter rather than a linear regulator (or just connecting the battery directly to the solar panel) ensures considerably higher power efficiency.

Standard charge controllers will typically be used in a situation where the input voltage from the solar panel is higher than the voltage from the battery. In this case the voltage will be reduced by the controller while the current that the panel is outputting will stay the same. This will result in power loss from the total power generated from the panels. More sophisticated charge controllers include the PWM and MPPT types.

Pulse-Width Modulating (PWM) charge controllers use complex algorithms to determine the amount of charge going to a battery and tapering according to the battery's condition (State of charge) and recharging needs. The controller periodically checks the battery's state of charge (SoC) to determine how fast to send pulses, and how long (wide) the pulses will be. In a discharged battery, the pulses would be very long and almost continuous, or the controller may go into "totally on" mode. When a battery voltage reaches the regulation set point, the PWM algorithm slowly reduces the charging current by slowly tapering off charging as the battery becomes full to avoid heating and gassing of the battery, however the charging still delivers the maximum amount of power to the battery in the shortest time. PWM is often used as one method of float charging where instead of a steady output from the controller, it sends out a pulse train of short charging pulses to the battery. In a fully charged battery with no load, it may just spike every few seconds and send a short pulse to the battery (trickle charge).

PWM has the advantages of increasing battery life span, minimizing stress on battery, reducing battery overheating and ability to desulphate a battery but the drawback of PWM is it isn't as highly efficient as MPPT for higher panel ratings and colder operating conditions; the greater the voltage variation

between battery voltage and the  $V_{mp}$  (Peak maximum solar panel voltage) of the array, the greater the energy dissipated by a PWM controller during in the battery's bulk charging state. MPPT charge controllers use fast processing e.g. Microcontrollers, to compute the highest instantaneous possible power output (Operation at the knee point of the P-V curve of Figure2-2) by suitably adjusting the load impedance seen by the panel under operation in addition to monitoring the different battery charging stages.

Therefore in the same conditions as above for standard charge controllers, where the input voltage is higher than the output voltage, the MPPT charge controller will lower the voltage and simultaneously increase the current to the batteries. As  $P=VI$ , this results in higher power transfer efficiencies, which means less solar power is lost during the storage process. MPPT Charge controllers are designed to maximize the output efficiency of a solar panel, the main aim of such tracker is to vary the module operating current and voltage such that the maximum output power is achieved in a rapid but precise manner especially under variable atmospheric conditions it implements this through a DC-DC converter with variable duty cycle.

An MPPT will provide the maximum possible power to the battery while still using the full output of the solar panel by ensuring maximum current the PV can produce at the time is delivered. Figure 2-7 demonstrates this with a typical setting of a 120W solar panel with a  $V_{mp}$  of 17V charging a 12V battery with a float voltage of 13.5V

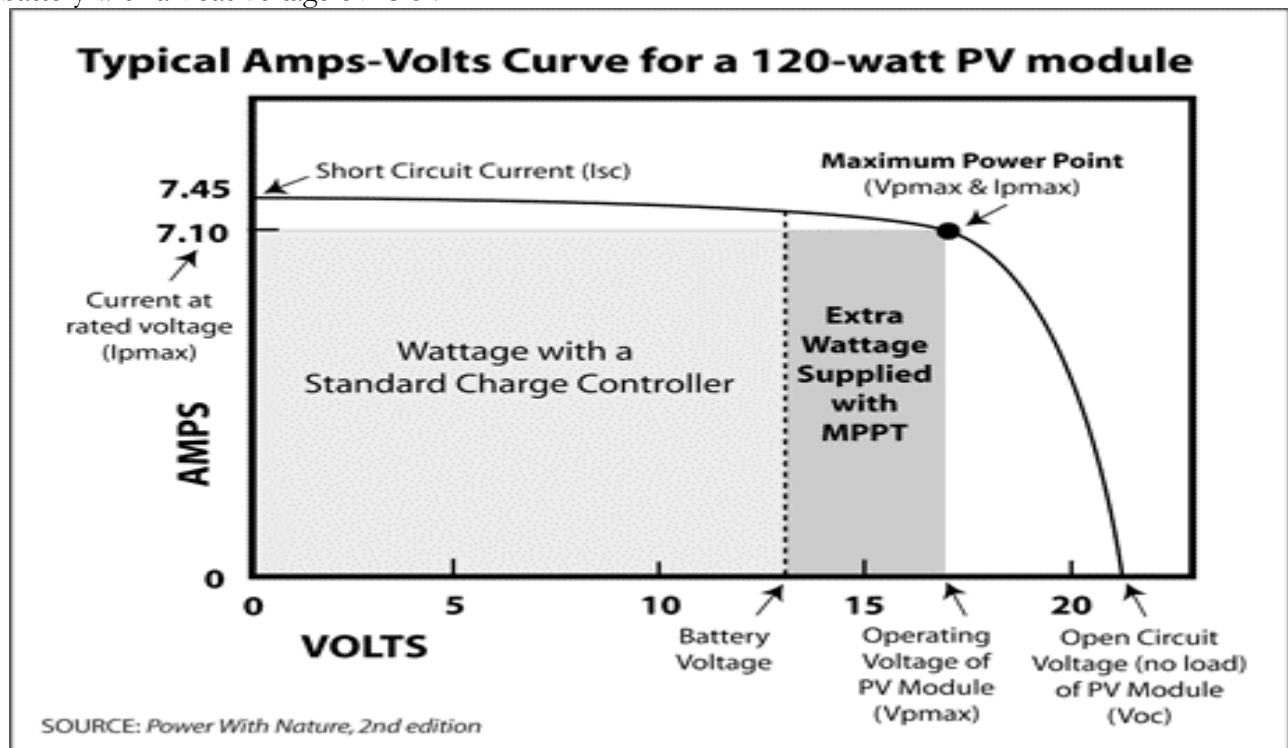


Figure 2-7: Extra wattage produced by MPPT for a 120W solar panel.

## 2.6 DC-DC Voltage regulators

The DC voltage from the panel will vary depending on solar insolation based on the time of day and solar panel temperature as discussed in the section on PV cell characteristics. The battery voltage will vary depending on the load connected to it. In order to maintain optimal battery charging, it is extremely important that the panel voltage and current matches the required battery charging stage at that particular moment. A DC to DC converter is an electronic circuit that performs an energy conversion in order to step down, step up a voltage. The main advantage that it has over ordinary linear regulators is that power losses are minimized as linear regulators dissipate excess power as heat and do not offer any current step-up/down capabilities too, switching voltage regulators thus have higher efficiencies and since their heat loss is less their thermal management is easy. A DC-to-DC regulator is needed to increase or decrease the input panel voltage to the required battery level.

These regulators are also known as switching regulators where a power switch, a rectifier and the filter elements- an inductor for storing charge and capacitor- are arranged in different topologies and but for efficient power transfer from input to output. The switches are either passive or active. MOSFETs have fast and efficient switching capabilities hence can be used as the power switch, the pulse width modulation (PWM) signal is used to control the frequency and duty cycle of the ON and OFF time of the “power switch”. This technique modulates the width of a square waveform from 0% (fully off) to 100% (fully on). The average voltage of the modulated waveform is a function of its Duty cycle. Duty Cycle of a square waveform is defined as the ratio between the time of high state (ON state) and the period of the waveform. The higher the duty cycle the more power is transferred from input to output. Using a variable PWM can account for varying DC supplies, such as a solar panel. One of the advantages of the PWM is that the signal remains digital from the source, in this case from the microcontroller to the MOSFET's, suppressing the need for any analog-to-digital signal conversion. Generally digital signals are less influenced by outside noise.

Some of the common DC-to-DC converter topologies used today are the: Buck, Boost, Buck/Boost; their schematics are shown in Figure 2-8. These regulators do not produce power they are essentially power converters can be compared with same analogy as power transformers. Thus the adjusted voltage level affects the current level, ideally maintaining power level constant (although they consume a little power based on their efficiencies). By  $P=VI$ , current and voltage are both directly proportional to power, it is intuitive that in buck mode the voltage is lowered (stepped down) as the current increased. While in boost mode the voltage is increased (stepped up) as the current decreases. Hence for boost converters DC input voltage is less than DC output voltage and can be used where PV

voltage is less than battery voltage; in buck converters the DC input voltage is greater than the DC output voltage and can be used where PV voltage is greater than the battery voltage.

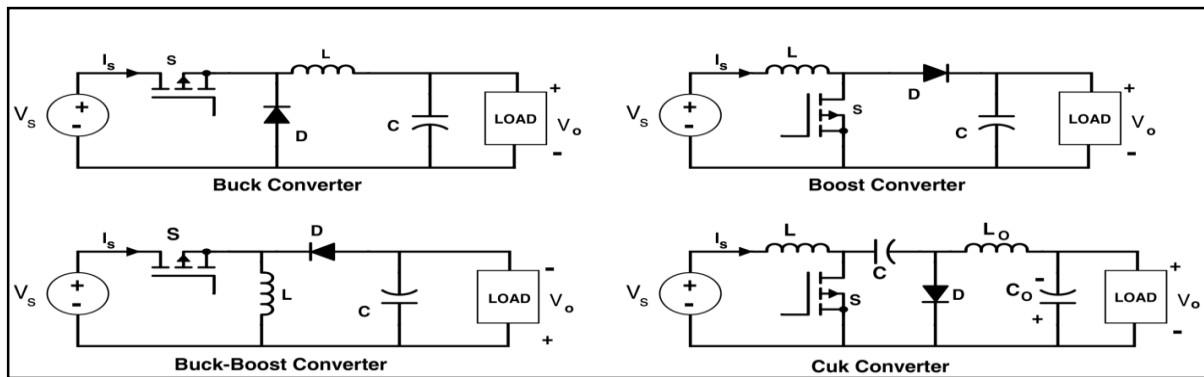


**Figure 2-8: DC-DC Converter Topologies**

A buck converter is used for this project. Initially at off-state, when the switch is open, the no current flows in the circuit. In the on-state, when the switch is closed, the current level starts rising and the inductor produces voltage to oppose the current change across its terminals. This voltage drop counteracts the source voltage hence reducing the net load voltage. Eventually the rate of change of current decreases subsequently causing decrease in inductor voltage and increase in load voltage. In this time, the inductor stores energy as magnetic field energy. If the switch is opened with the current still changing, then there will always be a voltage drop across the inductor making the load voltage always less than the input voltage source.

When the switch is opened again (off-state), the input voltage source is no longer connected to the circuit, and the current decreases. The changing current produces a voltage change across the inductor, however now not opposing but aiding the source. The energy that had been stored in the inductor's magnetic field aids current flow via the load, the inductor discharges its stored energy into the rest of the circuit. By using a fast switching speed and using corrective circuit elements, a stable output of voltage and current is obtained with minimal ripple, giving less voltage and more current than at the source.

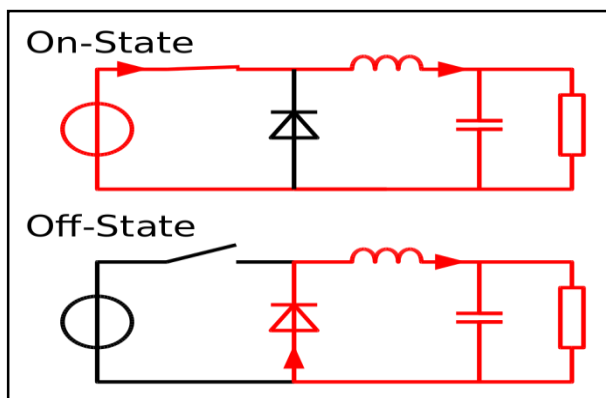


**Figure 2-9: States of a buck converter.**

## 2.7 MPPT Algorithms

This project is based on improving efficiency of solar panels by the indirect method of Maximum Power Point Tracking (MPPT) as discussed under PV cell characteristics. The non-linear power curve of Figure 2-2 for a PV panel was seen to change primarily as dictated by the factors of solar insolation level and operating temperatures. This means the maximum power point shifts a lot from the rated point; this is why a capable MPPT algorithm must not be static and must be constantly tracking the power point. Maximum power point tracking has been shown to increase the efficiency of the system by approximately 30% over charge controllers that do not implement MPPT.

In a nutshell, the MPPT charge controller algorithm should be able to monitor voltages from both the photovoltaic array and the battery in order to determine the various charging states of a battery whilst still maintaining maximum efficiency from the solar panel. Additional power harvested from the panel is then made available as increased battery charge current. There are several MPPT algorithms that have been designed in order to perform this task and the major and common ones are discussed below. These techniques differ in many aspects like complexity, convergence speed, hardware implementation, sensors required, cost, range of effectiveness and need for parameterization.

### 2.7.1 Hill climbing / Perturb and observation

This method, also known as Perturb and Observation (P&O), perturbs the reference variable  $r[k]$  (i.e. voltage, current or duty cycle) using a trial and error approach to get closer to the optimum point; this algorithm periodically changes the reference variable  $r[k]$  by a fixed step-size along the direction of increasing power. It is referred to as a hill climbing method, because it depends on the rise of the curve of power against voltage below the maximum power point, and the fall above that point. First, the panel's output voltage  $V_{pv}[k]$ , and output current  $I_{pv}[k]$  are sensed to calculate the output power  $P[k]$ . This power is then compared to the previously calculated power  $P[k-1]$ , and the perturbation direction of the reference variable is increased if there's a relative increase in power and is reversed if there's a relative decrease in power (i.e. the tracking direction is away from the maximum power point). After the peak power is reached the power at the next instant decreases and hence after that the perturbation reverses.

Hill climbing involves a perturbation in the duty ratio of the power converter, and P&O a perturbation in the operating voltage of the PV array. In the case of a PV array connected to a power converter, perturbing the duty ratio of power converter perturbs the PV array current and consequently perturbs the PV array voltage. What characterizes this method is its simplicity and speed where no complex calculations are involved. However, it mainly suffers from steady state power oscillations as it continues perturbing the reference variable even when the steady state (Maximum power point) is reached leading to inefficiencies when radiation is low and when the P-V curve begins to flatten out.

The oscillation can be minimized by reducing the perturbation step size. However, a smaller perturbation size slows down the MPPT. A solution to this conflicting situation is to have a variable perturbation size that gets smaller towards the MPPT. The algorithm may also perform several

perturbations in the wrong direction when there is drastic sudden weather changes. To ensure that the MPP is tracked even under sudden changes in irradiance, using a three-point weight comparison P&O method that compares the actual power point to two preceding ones before a decision is made about the perturbation sign; using a high sampling rate is also key.

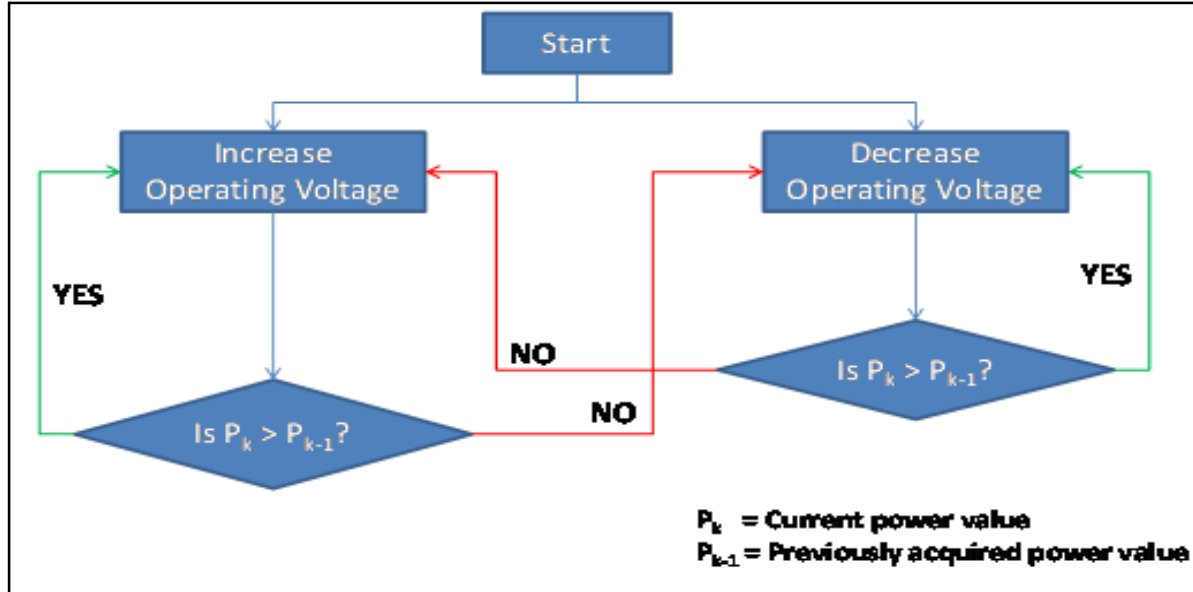


Figure 2-10: P&O Flowchart

### 2.7.2 Incremental conductance

This method, calculates the derivative of the output power with respect to voltage ( $dP/dV$ ) to predict the direction of the reference variable update. This method requires more computation in the controller, but can track changing conditions more rapidly than the perturb and observe method (P&O). The power-voltage (P-V) characteristics of PV modules and its derivative  $dP/dV$  are shown in Figure 2-11.

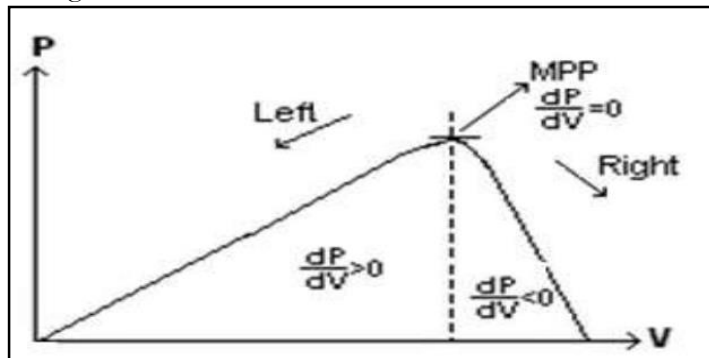


Figure 2-11: P-V curve slope characteristics of a PV module

It is noticed that the function  $dP/dV$  (the gradient of the P-V curve) is positive to the left of the maximum power point (MPP), negative to the right side of the MPP, and zero at the MPP. Consequently, this algorithm periodically calculates  $dP/dV$  using Equation 3.0. The incremental conductance method computes the maximum power point by comparison of the incremental conductance ( $I \Delta / V \Delta$ ) to the array conductance ( $I / V$ ).

Since  $\frac{dP}{dV} = d\left(\frac{IV}{dV}\right) = I + V \frac{dI}{dV} \approx I + V \frac{\partial I}{\partial V}$  **Equation 3.0**

We see  $\frac{\partial I}{\partial V} = \frac{-I}{V}$  At MPP  $\frac{\partial I}{\partial V} < \frac{-I}{V}$  To right of MPP and  $\frac{\partial I}{\partial V} > \frac{-I}{V}$  To left of MPP

The reference variable (e.g. voltage) is moved to the right (if  $dP/dV > 0$ ), to the left (if  $dP/dV < 0$ ), or held constant if ( $dP/dV = 0$ ). The MPP can thus be tracked by comparing the instantaneous conductance ( $I/V$ ) to the incremental conductance ( $\Delta I/\Delta V$ ) as shown in the flowchart in Figure 12. If the incremental conductance is greater than the instantaneous conductance the algorithm should continue to increase the voltage until the maximum power point is determined. Once the MPP is reached, the operation of the PV array is maintained at this point unless a change in  $\Delta I$  is noted, indicating a change in atmospheric conditions and the MPP. The increment size determines how fast the MPP is tracked. Fast tracking can be achieved with bigger increments but the system might not operate exactly at the MPP and oscillate about it instead; so there is a tradeoff.

This method has two advantages over the P&O method especially that it stops updating the reference variable when the MPP is reached (using incremental conductance a discrete value for the maximum power point can be obtained and the system will remain at this point until it undergoes a change in the environmental conditions affecting the power), thus reducing power oscillations around MPP. Also, it calculates the correct direction to update the reference variable (by calculating the derivative and creating the inequality, the algorithm will know which direction to move along the curve in order to reach the maximum power point.), rather than the trial and error.

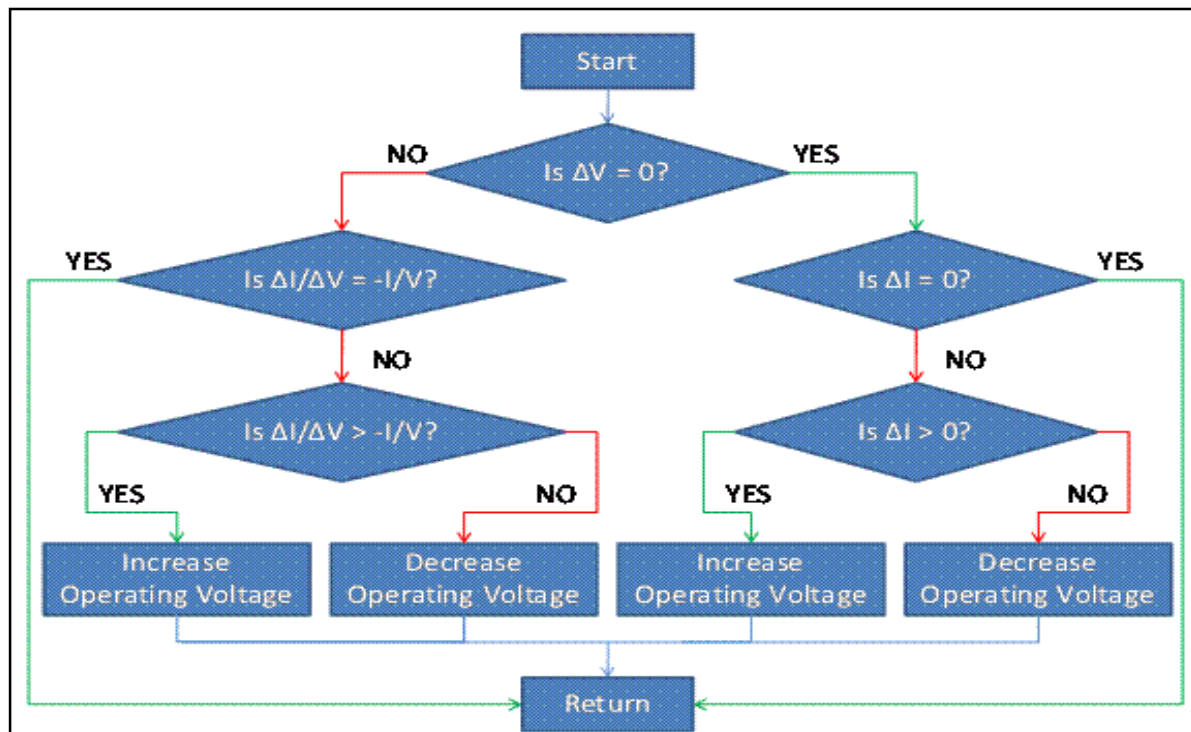


**Figure 2-12: Incremental Conductance Flowchart**

### 2.7.3 Fractional open-circuit voltage and fractional short-circuit voltage

The near linear relationship between  $V_{MPP}$  and  $V_{OC}$  of the PV array, under varying irradiance and temperature levels, has given rise to the fractional  $V_{OC}$  method

$V_{MPP} \approx K1 V_{OC}$  where  $K1$  is a constant of proportionality. Since  $K1$  is dependent on the characteristics of the PV array being used, it usually has to be computed beforehand by empirically determining  $V_{MPP}$  and  $V_{OC}$  for the specific PV array at different irradiance and temperature levels. The factor  $K1$  has been reported to be between 0.71 and 0.78. Once  $K1$  is known,  $V_{MPP}$  can be computed using with  $V_{OC}$  measured periodically by momentarily shutting down the power converter. However, this incurs some disadvantages, including temporary loss of power. The operating point of the PV array is thus kept near the MPP by regulating the array voltage and matching it to the fixed reference voltage  $V_{ref} = K1 V_{OC}$ . Since this is only an approximation, the PV array technically never operates at the MPP. Depending on the application of the PV system, this can sometimes be adequate. Even if fractional  $V_{OC}$  is not a true MPPT technique, it is very easy and cheap to implement as it does not necessarily require microcontroller control. However,  $K1$  is no more valid in the presence of partial shading (which causes multiple local maxima) of the PV array and proposes sweeping the PV array voltage to update  $K1$ . This obviously adds to the implementation complexity and incurs more power loss.

Similarly Fractional  $I_{SC}$  results from the fact that, under varying atmospheric conditions,  $I_{MPP}$  is approximately linearly related to the  $I_{SC}$  of the PV array,  $I_{MPP} \approx K2 I_{SC}$  where  $K2$  is a proportionality constant. Just like in the fractional  $V_{OC}$  technique,  $K2$  has to be determined according to the PV array in use. The constant  $K2$  is generally found to be between 0.78 and 0.92. An additional switch usually has to be added to the power converter to periodically short the PV array so that  $I_{SC}$  can be measured using a current sensor

### 2.7.4 Fuzzy logic control

Fuzzy logic controllers have the advantages of working with imprecise inputs, not needing an accurate mathematical model, and handling nonlinearity. Fuzzy logic control generally consists of three stages: fuzzification, rule base table lookup, and defuzzification. During fuzzification, numerical input variables are converted into linguistic variables based on a membership function similar to Fig.13. In this case, five fuzzy levels are used: NB (negative big), NS(negative small), ZE (zero), PS (positive small), and PB (positive big). The inputs to a MPPT fuzzy logic controller are usually an error  $E$  and a change in error  $\Delta E$ . The user has the flexibility of choosing how to compute  $E$  and  $\Delta E$ . Since  $dP/dV$  vanishes at the MPP, we can use the approximation

$$E(k) = \frac{P(k) - P(k-1)}{V(k) - V(k-1)} \quad \text{Equation 4.0}$$

$$\partial E(k) = E(k) - E(k-1) \quad \text{Equation 4.1}$$



Or one may also use the approximation of the  $\Delta P$  and  $\Delta I$  curve as shown in Fig13. Once  $E$  and  $\Delta E$  are calculated and converted to the linguistic variables, the fuzzy logic controller output, which is typically a change in duty ratio  $\Delta D$  of the power converter, can be looked up in a rule base table such as Figure 2-13. The linguistic variables assigned to  $\Delta D$  for the different combinations of  $E$  and  $\Delta E$  are based on the power converter being used and also on the knowledge of the user. In the defuzzification stage, the fuzzy logic controller output is converted from a linguistic variable to a numerical variable still using a membership function.

MPPT fuzzy logic controllers have been shown to perform well under varying atmospheric conditions. However, their effectiveness depends a lot on the knowledge of the user or control engineer in choosing the right error computation and coming up with the rule base table

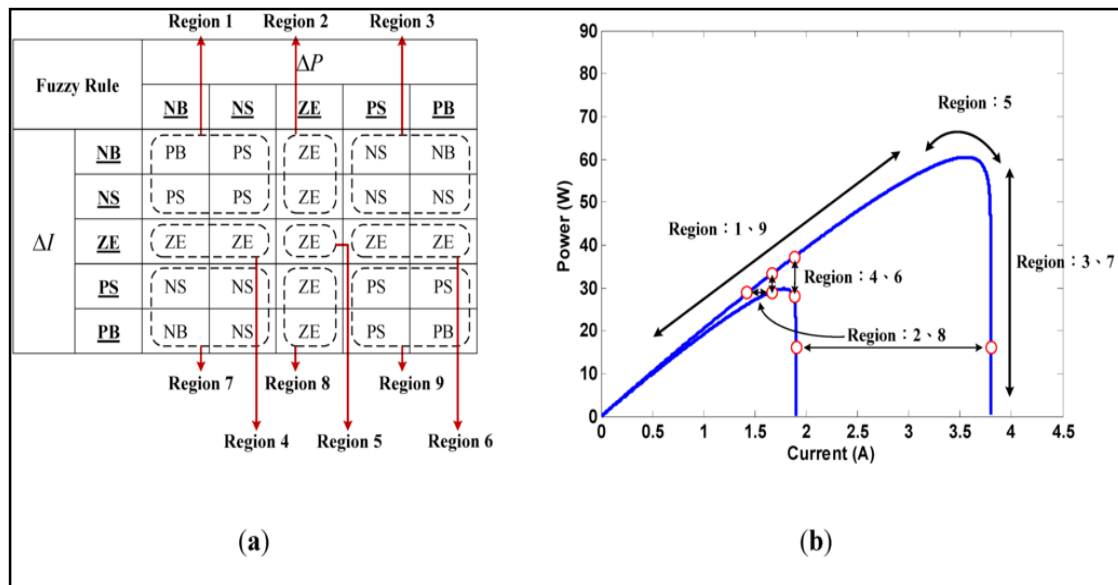


**Figure 2-13: Fuzzy logic control rule base table**

Other MPPT Algorithms:

- Neural network-Neural networks commonly have three layers: input, hidden, and output layers. The number of nodes in each layer vary and are user-dependent. The input variables can be PV array parameters like  $V_{OC}$  and  $I_{SC}$ , atmospheric data like irradiance and temperature, or any combination of these. The output is usually one or several reference signal(s) like duty cycle signal used to drive the power converter to operate at or close to the MPP. How close the operating point gets to the MPP depends on the algorithms used by the hidden layer and how well the neural network has been trained. The links between the nodes are all weighted. Since most PV arrays have different characteristics, a neural network has to be specifically trained for the PV array with which it will be used. The characteristics of a PV array also change with time, implying that the neural network has to be periodically trained to guarantee accurate MPPT.

- Ripple Current Correlation(RCC)- When a PV array is connected to a power converter, the switching action of the power converter imposes voltage and current ripple on the PV array. As a consequence, the PV array power is also subject to ripple. Ripple correlation control (RCC) makes use of ripple to perform MPPT. RCC correlates the time derivative of the time-varying PV array power  $\dot{P}$  with the time derivative of the time-varying PV array current  $\dot{I}$  or voltage  $\dot{U}$  to drive the power gradient to zero, thus reaching the MPP.

- DC-Link Capacitor Droop Control.

- Array reconfiguration.

- Linear current control.

- $dP/dV$  or  $dP/dI$  Feedback Control.

Some of the most popular Artificial Intelligence algorithms are Fuzzy logic and Artificial Neural Networks, these algorithms perform better than traditional P&O algorithm. Yet there is a tradeoff between quick settling time and steady state error. Further improvement of artificial intelligence algorithm which will be able to track maximum power point with minimum number of iteration with more than 98% accuracy under all diversity factors of temperature and irradiance being taken into account have been suggested by methods such as Particle Swarm Optimization.

## 2.8 Batteries

As mentioned beforehand, batteries are used to store the excess power harnessed by the solar panel and can be used as a reserve to supply a load at night or when there's very low solar irradiance. Batteries convert chemical energy directly to electrical energy. Batteries are classified into primary and secondary forms. Primary batteries irreversibly transform chemical energy to electrical energy. When the supply of reactants is exhausted, energy cannot be readily restored to the battery while secondary batteries can be recharged; that is, they can have their chemical reactions reversed by supplying electrical energy to the cell, approximately restoring their original composition.

Secondary batteries, also known as secondary cells, or rechargeable batteries, must be charged before first use; they are usually assembled with active materials in the discharged state. Rechargeable batteries are (re)charged by applying electric current, which reverses the chemical reactions that occur during discharge/use. Devices to supply the appropriate current are called chargers, in this project the device is a MPPT charge controller. The oldest form of rechargeable battery is the lead–acid battery. This technology contains liquid electrolyte in an unsealed container, requiring that the battery be kept upright and the area be well ventilated to ensure safe dispersal of the hydrogen gas it produces during overcharging.

The lead–acid battery is relatively heavy for the amount of electrical energy it can supply. Its low manufacturing cost and its high surge current levels make it common where its capacity (over approximately 10 Ah) is more important than weight and handling issues. In a photovoltaic power

supply system, Lead acid battery is commonly used because of its features such as wide operating temperature range, low self-discharge, long service life and easy maintenance. A deep-cycle battery is a lead-acid battery designed to be regularly deeply discharged using most of its capacity (discharge between 45% and 75% of its capacity). Deep-cycle lead-acid batteries generally fall into two distinct categories: flooded (FLA) and valve-regulated lead-acid (VRLA), more commonly known as a sealed battery (SLA) or maintenance free battery; with the VRLA type further subdivided into two types: Absorbed Glass Mat (AGM) and Gel. Gel batteries contain a putty-like substance, while AGM batteries contain special acid-saturated fiberglass mats however AGM batteries are generally more powerful and cost-effective, but gel batteries offer more longevity. Deep cycle battery plates have thicker active plates than cranking batteries. The thicker battery plates resist corrosion through extended charge and discharge cycles. Due to their construction, the Gel and AGM types of VRLA can be mounted in any orientation, and do not require constant maintenance. Deep-cycle AGMs are also commonly used in off grid solar and wind power installation as an energy storage bank.

Other portable rechargeable batteries include several sealed "dry cell" types that are useful in applications such as mobile phones and laptop computers. Cells of this type (in order of increasing power density and cost) include nickel–cadmium (NiCad), nickel–zinc (NiZn), nickel metal hydride (NiMH), and lithium-ion (Li-ion) cells.

Li-ion batteries offer some of the highest energy densities as well as the lowest weight of all battery chemistries and constitute the largest global share of world dry-cell rechargeable batteries. They have a high cell voltage, low self-discharge rate, fast charging rate, and relatively good lifetime when deep-cycled. The two limiting factors afflicting Li-ion are cost and safety. Li-ion batteries tend to have one of the highest cost-per-watt ratios, much higher than lead-acid chemistries. In addition, it is imperative to build protection circuitry into the battery pack so that thermal runaway does not cause the battery to light on fire and/or explode. Lithium is also highly reactive with water so care must always be taken to not overexpose these batteries to water. A battery is rated with the following attributes: voltage, capacity in ampere-hours (Ah), cold cranking amps (CCA), specific energy, specific power, and C-rate

### **2.8.1 Three stage lead-acid battery charging**

Lead acid batteries are usually charged in three stages for healthy operation as explained below.

1. The BULK stage involves about 80% of the recharge, wherein the charger current is held constant (in a constant current charger), and voltage increases. As the battery becomes increasingly charged, its opposition or resistance to a charge current increases, this will cause the current flow to tail off. Considering Ohms Law where  $Voltage = I \text{ (current in Amps)} \times R \text{ (resistance in Ohms)}$  shows that if we want to maintain a constant current in a circuit with rising resistance, we must raise the voltage. The bulk charge continues until the voltage output by the charger reaches a specific level. At that point, it switches to the absorption charge. This first stage is typically where the highest voltage and amperage the charger is rated for will actually be used. The properly sized charger will give the battery as much current as it will accept up to charger capacity (25% of battery capacity in amp hours), and not raise a wet battery over 125° F, or an AGM or GEL (valve regulated) battery over 100° F.

The level of charge that can be applied without overheating the battery is known as the battery's natural absorption rate. For a typical 12 volt AGM battery, the charging voltage going into a battery will reach 14.6-14.8 volts, while flooded batteries can be even higher. For the gel battery, the voltage should be no more than 14.2-14.3 volts. If the charger is a 10 amp charger, and if the battery resistance allows for it, the charger will put out a full 10 amps. This stage will recharge batteries that are severely drained. There is no risk of overcharging in this stage because the battery hasn't even reached full yet.

2. The ABSORPTION stage (the remaining 20%, approximately) has the charger holding the voltage at the charger's absorption voltage (between 14.1 VDC and 14.8 VDC, depending on charger set points) and decreasing the current until the battery is fully charged. As the battery becomes increasingly charged, its opposition or resistance to a charge current increases, this will cause the current flow to tail off. Considering Ohms Law once again where  $Voltage = I \text{ (current in amps)} \times R \text{ (resistance in ohms)}$  If voltage is held constant and resistance increases, current must decrease. During the absorption charge, the three stage charger monitors the falling current until a specified point is reached that indicates that the battery is about ninety eight percent charged. The lower current going into the battery safely brings up the charge on the battery without overheating it. This stage takes more time. For instance, the last remaining 20% of the battery takes much longer when compared to the first 20% during the bulk stage. The current continuously declines until the battery almost reaches full capacity. Actual Equalization control over charge is mostly limited to flooded type lead-acid batteries.

3. The FLOAT stage is where the charge voltage is reduced to between 13.1 VDC and 13.5 VDC (which is the maximum voltage a 12 volt battery can hold) and held constant, while the current is reduced to less than 1% of battery capacity, a point where it's considered a trickle. That's where the term "trickle charger" comes from. It's essentially the float stage where there is charge going into the battery at all times, but only at a safe rate to ensure a full state of charge and nothing more. This mode can be used to maintain a fully charged battery indefinitely.

During the float charge, the voltage is dropped to a level lower than what was applied during the absorption charge. The float charge serves two purposes. First, it brings the battery from a 98 percent state of charge (SoC) to a 100 percent state of charge. Second, it maintains the battery in a 100 percent state of charge condition. There are a couple ways of maintaining the battery at 100 percent state of charge. The first is to simply apply a voltage that is theoretically ideal to the type of battery being charged. The idea is that this voltage is low enough to keep the electrolyte from boiling off, yet high enough to counteract the phenomenon known as self-discharge. The problem with this is that it does not account for the affect that temperature has on batteries, nor does it account for those small differences caused by battery age and construction. The second is to actually monitor the state of charge and apply voltage when it's needed. Indeed, some of the smarter chargers use temperature sensors. Others monitor the voltage of the cells and send a short pulse of charge using a technique called and a pulse width modulation.

Heat is the worst enemy of batteries, including lead acid. The chemical reactions that occur within batteries vary with temperature. These variations cause a battery charged or maintained at standard

voltages to be undercharged if cold, and overcharged if hot. Adding temperature compensation on a lead acid charger to adjust for temperature variations is said to prolong battery life by up to 15 percent. The recommended compensation is a 3mV drop per cell for every degree Celsius rise in temperature. If the float voltage is set to 2.30V/cell at 25°C (77°F), the voltage should read 2.27V/cell at 35°C (95°F). Going colder, the voltage should be 2.33V/cell at 15°C (59°F). These 10°C adjustments represent 30mV change.

Figure 2-14 shows the three charging stages at cell level for a 12V Lead-acid battery with 6cells. Lead-acid batteries are sluggish to charge, usually taking between 12 and 16 hours to reach 100% capacity. This is, in reality, not such a bad thing for solar cell applications. The sun usually shines for many hours during a given day, delivering power at a rate that is slow enough to allow efficient charging of lead-acid batteries. Lead-acid batteries also have a high overcharge tolerance compared to lithium-ion

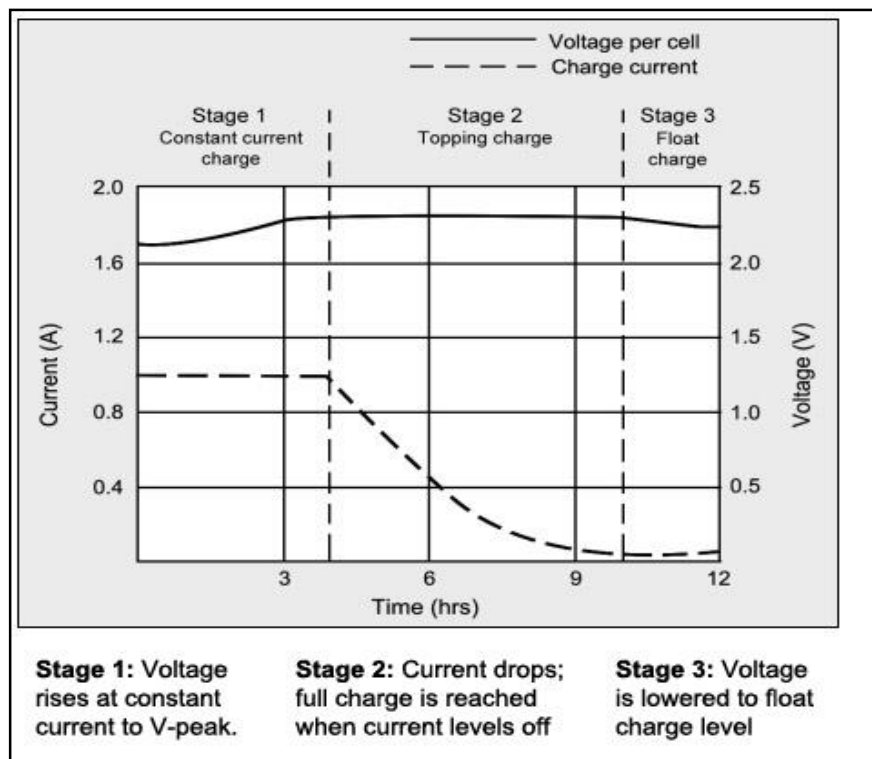


Figure 2-14: Three stage lead-acid battery charging at individual cell level.

An additional fourth stage “Equalization” is incorporated but limited only to flooded type batteries. Equalizing is an overcharge performed on flooded lead acid batteries after they have been fully charged. It reverses the buildup of negative chemical effects like stratification, a condition where acid concentration is greater at the bottom of the battery than at the top. Equalizing also helps to remove sulphate crystals that might have built up on the plates. If left unchecked, this condition, called sulphation, will reduce the overall capacity of the battery.

For the absorption and float charging stage; implementation of MPPT is not rewarding as the controller can easily reach constant voltage stage. Thus, having the system operating at MPP at these stages will only result in overcurrent charging which can shorten the battery life. MPPT is most effective for the bulk charging state.

## 2.9 Market Research

Investigating and studying the design of the readily available commercial MPPT charge controller products is important to understanding of how maximum power point tracking charge controllers function and some of the value added features and protection features incorporated in them. The MPPT charge controllers in the market already that met project goals and specifications in terms of maximum charging current were analyzed to see how changing our design can improve our charge controller feature performance. The MPPT charge controllers existing in the market that closely match the project's design scope of 20A maximum battery charging current are discussed below:

### *Midnite Solar Inc.'s THE KID by Mario MPPT Solar Charge Controller*

From its manual The KID is the most versatile medium-sized charge controller on the market. It is ideal for small renewable energy systems. The KID also allows for true input paralleling Its average market price is \$439.



**Figure 2-16: THE KID MPPT solar charge controller**  
Features

- MPPT Tracking.
- True paralleling – Input and output for two KIDs, with smart current sharing.
- Up to 150V input (Maximum Solar panel array open-circuit voltage Voc).
- 12V, 24V, 36V, 48V nominal battery output; battery voltage range of 9V-64V.
- 4 stage battery charging-Bulk, absorption, float as well as Equalization.
- Reverse polarity protected.
- Up to 30A battery output.

- Battery temperature sensor standard with marine version, has adjustable and automatic battery temperature compensation.
- Front panel exchangeable fuses for input and battery.
- 3 LED bar graph for battery status at a glance also has LCD display.
- Keypad access to extensive menu items and set points, has adjustable setting for equalization voltage and duration.
- RS232 openly published protocols as well as USB communication enabled.
- Sealed for harsh environments.
- Includes wall mount adapter and boat mount bracket for marine versions.
- Battery types: Flooded, GEL, AGM, Calcium SMF, Lithium BMS, Custom.

### ***Morning Star's SunSaver Solar Controllers***

This is not an MPPT charge controller however it is the PWM charge controller used by the solar panel in the school specifically SS-20L-12V(The 20A and 12V version with LVD). Its average market price is \$75



**Figure 2-17: SunSaver-20L PWM charge controller**

Some of its features are:

#### Electrical Features

- System voltage-12V
- Min. battery voltage-1V
- Regulation voltage :Sealed battery-14.1V ,Flooded battery-14.4V
- Max. solar voltage-30V
- Self-consumption <8mA
- Transient surge protection-1500W per connection

#### Electronic protections

- Solar: Overload, short-circuit, high voltage
- Battery: High Voltage
- Reverse polarity, high temperature, lightning and transient surges for all
- Reverse current at night

#### Battery charging

- 4 stage series PWM charging method (Bulk, absorb, float, equalize)
- Temperature compensation
- Coefficient for 12V battery :  $-30\text{mV}/^{\circ}\text{C}$
- Range :  $-30^{\circ}\text{C}$  to  $+60^{\circ}\text{C}$
- Set points: Absorption, float, equalize
- 1 Status LED to show Charging or not charging & Solar error conditions and 3 Battery LED's to show battery level and Charging stage

Other sampled MPPT products are Morning Star's ProStar MPPT Solar Charge Controller, its average market price is \$350 without a meter accessory option and Blue Sky Energy's Solar Boost 2512i-HV and 2512iX-HV. The 2512i-HV goes for \$213 while the 2512iX-HV goes for \$254

From the above products we see that MPPT greatly increases the value and efficiency for solar energy harvesting making MPPT charge controllers in this 20A max. charging bracket to go for >\$200 compared to PWM charge controllers in the same range going for <\$100. As an example the SunSaver SS-20L-12V PWM charge controller with a maximum charging current of 20A goes for \$75 while the SS-MPPT-15L from the same company with a less maximum charging current of 15A but with MPPT tracking goes for \$205. It is seen that MPPT functionality doubles or even triples the cost of a PWM charge controller which shows how useful it is in maximum power extraction and efficiency operation.



### 3 DESIGN AND IMPLEMENTATION

The block diagram of the MPPT to be implemented is as illustrated below in Figure 3-1.

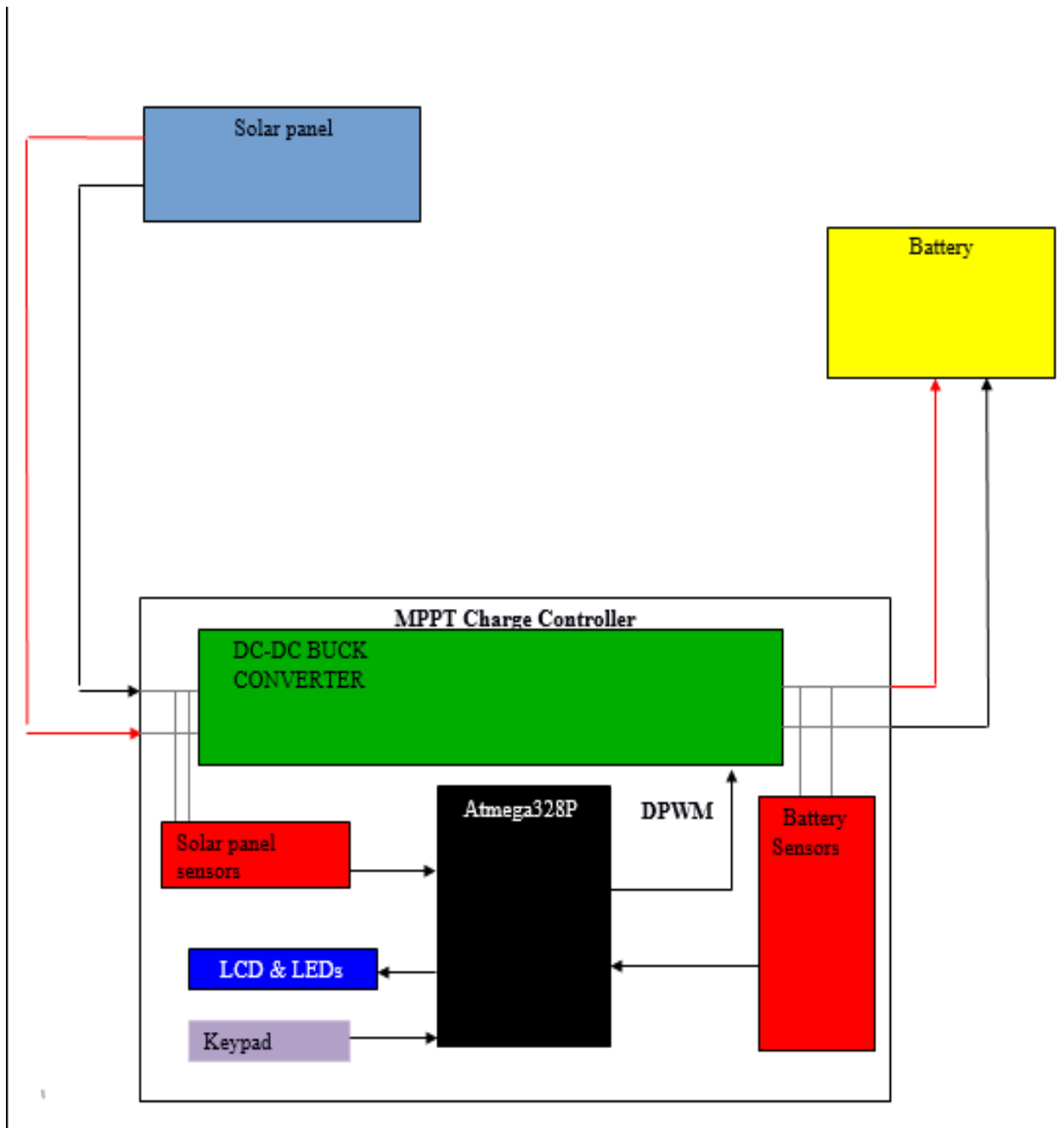


Figure 3-1: Block diagram of the designed MPPT charge controller.

### 3.1 Microcontroller

The Atmel ATmega328P –PU microcontroller was chosen as the microcontroller of choice. The ATmega328P is a low-power CMOS 8-bit microcontroller based on the AVR enhanced RISC architecture. It contains the pertinent hardware and software requirements to meet all design goals, providing enough digital and analog pins to handle all sensors, LCD, while at the same time being able to control the MPPT circuit using pulse-width modulation (PWM) outputs. A list of specifications for the ATmega328P is given below:

- 8-bit microcontroller
- Up to 20 MHz clock
- 32 KB flash memory
- 1 KB EEPROM
- 2 KB SRAM(Static Random Access Memory)
- 6 PWM channels
- 6 analog inputs (10-bit built-in ADC)
- 14 digital input/output pins
- Programmable Serial USART
- Master/slave SPI Interface
- Two-Wire (TWI) or Inter-Integrated Circuit (I2C) communication
- 5V DC power
- Low-power modes
- Throughputs approaching 1 MIPS per MHz allowing the system designer to optimize power consumption versus processing speed
- DIP or SMT packages
- Power-on Reset and Programmable Brown-out Detection
- Internal Calibrated Oscillator
- Temperature Range:-40°C to 85°C
- Operating Voltage: 1.8 - 5.5V
- Low Power Consumption at 1 MHz, 1.8V, 25°C
- Write/Erase Cycles: 10,000 Flash/100,000 EEPROM
- Low Power Consumption ,at 1MHz, 1.8V, 25°C :Active Mode-0.2mA ,Power Down Mode-0.1μA ,Power Save Mode-0.75μA (Has Six Sleep Modes: Idle, ADC Noise Reduction, Power-save, Power-down, Standby, and Extended Standby)

The six analog pins will all be utilized in the MPPT charge controller. Two analog current sensors and two analog voltage sensors each for the battery and solar panel took four of the analog pins (PC0-PC3). I2C employs a clock and data bus, and the LCD is connected to the remaining two analog pins (PC4/SDA and PC5/SCL).

The Arduino was chosen as to be used as an ISP (In System Programmer) because:

- The Arduino boot loader allows direct programming through USB, eliminating the need of a separate hardware programmer to implement new code. Using an external programmer is both time consuming and the user risks damaging the IC (bending pins, electrostatic discharge) every time the chip is removed from a socket. This would be extremely inconvenient in final design, for the charge controller will be contained in a small housing in the final product and thus removing the microcontroller every time programming is needed would not be ideal.
- The Arduino hardware platform already has the power and reset circuitry setup as well as circuitry to program and communicate with the microcontroller over USB (The serial monitor window can also be enabled to view what the Arduino I/O ports are receiving/transmitting which is good for troubleshooting).
- The Arduino programming language was chosen due to relatively shorter learning curve and a large and active online support community which facilitates faster learning and debugging. The language and IDE are completely free and open source, and many resources concerning sensors, LEDs, communication tutorials, etc. are readily available on the Arduino website with some already as examples inclusive in the IDE package...
- The Arduino offers libraries that have been written for common sensors and other peripherals which will aid in the learning and programming the devices to be used in implementing the MPPT charge controller.
- The language is both easy to use and robust, providing all the functionality needed for interfacing with analog sensors (analogread & analog write), I2C components, and TTL serial peripherals among others. The simplest of these are functions to control and read the I/O pins (analogread & digitalread) rather than having to fiddle with the bus/bit masks normally used to interface with the Atmega I/O (This is a fairly minor inconvenience). More useful are things such as being able to set I/O pins to PWM at a certain duty cycle using a single command (analogwrite) or doing Serial communication.

## 3.2 Sensing networks

### 3.2.1 Voltage sensors

For Voltage sensing, voltage divider networks were used to sense the solar panel and battery voltages. From the ATMEGA 328P data sheet the specified operating voltage for the (I/O) pins is 5V, the maximum DC current per I/O pin is 40mA; therefore a ratio of resistors is used to scale down the voltages so that the maximum voltage fed from the voltage divider is 5V to avoid damaging the analog (I/O) ports while limiting current drawn within the limits. Using the voltage divider equation (Equation 6.0), the resistance values were found.

$$V_{out} = \frac{R_2}{R_1 + R_2} * V_{in} \quad \text{Equation 6.0}$$

The resistors had to be sufficiently large enough to limit the current drawn hence the ( $I^2R$ ) power losses, so resistors in  $K\Omega$  range were chosen. Capacitors were added in parallel with the second resistor  $R_2$  to act as filters smoothen hence preventing noise spikes making it to the microcontroller. The voltage across  $R_2$  ( $V_{out}$ ) is the one to be measured by the ATMEGA328P. For the solar panel voltage divider network, Equation 6.0 is carried out taking the worst-case scenario of  $V_{in} = V_{oc}$  (open-circuit voltage of the solar panel) to give a  $V_{out} = 5V$  as a safety measure; similarly for the battery voltage divider network the worst case scenario was taken with  $V_{in} = V_{absorption}$  of the battery.

Since the Atmega328P has a 10-bit ADC it allocates the analog read values to  $2^{10}$  (1024) levels (0-1023) and also since the recommended voltage of the analog I/O pins is 0-5V, the 5V input maps to the 1024<sup>th</sup> level, the ADC sensitivity to voltage is therefore 5/1024 V/ADC level. To get the sensed voltage from the ADC output to be used for computation by the ATMEGA328P in the MPPT algorithm we need to calculate  $V_{in}$  by using the formula

$$V_{sensed} = \frac{(ADCvalue * 5 / 1024) * (R_1 + R_2)}{R_2} \quad \text{Equation 6.1}$$

The resistor ratings used after being measured by a DMM to account for tolerances were: For the solar panel side resistors of  $R_1 = 81.1K$ ,  $R_2 = 9.75K$  were used while for the battery side  $R_3 = 20.08K$ ,  $R_4 = 9.85K$  were used.

- ✓ The above enabled the worst case solar input voltage  $V_{oc} = 45V$  and worst case battery voltage  $V_{batt} = 15V$  to be scaled down to under 5V which i.e. 4.83V and 4.93V which were safe for the microcontroller under worst case conditions. The series pair of resistors in Kilo Ohms also made sure the input current into the microcontroller was scaled down to 0.5mA which is very safe for the microcontroller I/O pins.
- ✓ Capacitors were placed across the sensor input to the microcontroller to smoothen the input and filter noise.

### 3.2.2 Current sensors

Allegro Microsystems Hall Effect sensors were considered to be suitable for the project. The Hall Effect is the production of a voltage difference (the Hall voltage) across an electrical conductor, transverse to an electric current in the conductor and a magnetic field perpendicular to the current. Practically, the current to be sensed is passed through the copper conduction path of the Allegro Sensors, the copper current carrying conductor then generates a magnetic field that is monitored by the hall IC and converted into a proportional analog voltage based on the sensitivity of the IC. Device accuracy is optimized through the close proximity of the magnetic signal to the Hall transducer. A precise, proportional voltage is provided by the low-offset, chopper-stabilized BiCMOS Hall IC, which is programmed for accuracy after packaging. This output voltage can be interfaced and digitized via ADC converters of the ATMEGA328P.

The Allegro current sensors are of three types 0-50A, 50-200A, 0->1000A; to narrow the scope the 0-50A range of the current sensors was chosen because it covered project requirements and had better current sensitivity than the other two groups. The ACS 712 series was chosen because it had  $V_{cc}=5V$ , it was bidirectional and had 5, 20 and 30A versions. The 20A version was chosen based on the project objective current range to design an MPPT with a maximum charging current of 20A for which the 5A version was inadequate and though the 30A version would have sufficed to cater margins, the 20A version had better sensitivity meaning the MPPT charge controller would be more accurate.

Other feature advantages of ACS712 -20A version are:

- Low-noise analog signal path
- Device bandwidth is set via the new FILTER pin
- 5  $\mu s$  output rise time in response to step input current
- 80 kHz bandwidth
- Total output error 1.5% at  $T_A = 25^\circ C$
- Small footprint, low-profile SOIC8 package
- 1.2 m $\Omega$  internal conductor resistance
- 2.1 kVRMS minimum isolation voltage from pins 1-4 to pins 5-8
- 5.0 V, single supply operation
- 100 mV/A output sensitivity
- Output voltage proportional to AC or DC currents
- Factory-trimmed for accuracy
- Extremely stable output offset voltage
- Nearly zero magnetic hysteresis

- Ratio metric output from supply voltage

From the graph output voltage vs sensed current from the ACS712-20A datasheet it is evident from the gradient that sensitivity is 0.1V/A and that it outputs a voltage of 2.5V when there is no current (0A) flowing assuming no electrical offsets.

Pin7 (VIOUT) is the pin connected to the analog input pin of the ATMEGA328P for the MPPT algorithm to compute the current.

Therefore ideally the measured current in Amperes is given by  $I_{measured} = \frac{V_{measured} - 2.5V}{(0.1V/A)}$

The ATMEGA328P though has a 10 bit ADC hence allocates measured voltage amongst  $2^{10}$  (1024) levels, and since the recommended voltage to the I/O pins is 5V, a 5V analog input is represented by the 1024<sup>th</sup> ADC value .Hence we see that range of current=0A to current=20A maps to the 512<sup>th</sup> to 1024th ADC value .Thus to convert the read ADC Value to a current level to be used for arithmetic computation by the MPPT algorithm we use the following formula

$$I_{sensed} = \frac{(ADCvalue * 5 / 1024) - 2.5}{0.1} \quad \text{Equation 7.0}$$

from which we see the ADC value sensed is converted to the voltage range 0-5V and the ideal null offset of 2.5V deducted ,the result is then converted to amperes based on the sensitivity of 0.1V/A

- ✓ After the current sensors were mounted, the offset voltages ( $V_{IOUT}$  to ground) were measured at open circuits to determine the real offsets at 0A for more accurate current readings. They were found to be 2.48V and 2.476V for the input and output sides respectively, these were programmed into the algorithm for more accurate readings.

### 3.2.3 Temperature sensors

The battery temperature is of importance in its charging for temperature compensation such that the setpoints are lowered as temperatures increases above 25°C and raised as temperatures are lowered below 25°C, it is also important to note battery temperature to avoid overheating of the battery during charging as this destroys battery life and could even explode batteries. The DS18B20 Programmable Resolution 1-Wire Digital Thermometer from Maxim-Integrated is used as the temperature sensor. The DS18B20 digital thermometer provides 9-bit to 12-bit Celsius temperature measurements and has an alarm function with nonvolatile user-programmable upper and lower trigger points. The DS18B20 communicates over a 1-Wire bus that by definition requires only one data line (and ground) for communication with a central microprocessor. In addition, the DS18B20 can derive power directly from the data line (“parasite power”), eliminating the need for an external power supply.

#### Features:

- Unique 1-Wire® Interface Requires Only One Port Pin for Communication
- Reduce Component Count with Integrated Temperature Sensor and EEPROM
- Measures Temperatures from -55°C to +125°C (-67°F to +257°F)
- $\pm 0.5^\circ\text{C}$  Accuracy from -10°C to +85°C
- Programmable Resolution from 9 Bits to 12 Bits
- No External Components Required
- Parasitic Power Mode Requires Only 2 Pins for Operation (DQ and GND)
- Simplifies Distributed Temperature-Sensing Applications with Multidrop Capability
- Each Device Has a Unique 64-Bit Serial Code Stored in On-Board ROM
- Flexible User-Definable Nonvolatile (NV) Alarm Settings with Alarm Search Command Identifies Devices with Temperatures Outside Programmed Limits
- Available in 8-Pin SO (150 mils), 8-Pin  $\mu\text{SOP}$ , and 3-Pin TO-92 Packages

As from the datasheet one of the applications of the DS18B20 is in battery management and power supplies, temperature monitoring control systems making it suitable for this project

The DS18B20 was connected as from its datasheet typical application with the DQ pin connected to PD1 and a 4.7K pull-up resistor connected between it and  $V_{pu}$  (pull-up supply voltage) which in this case was  $V_{cc}=5\text{V}$ . It was placed on at the point where the battery would be warmest, the terminals. The DS18B20 is connected to the battery and used to measure its temperature for healthy charging. The charge controller algorithm uses the measured temperature for temperature compensated charging of  $-3\text{mV}/^\circ\text{C}/\text{Cell}$  with the temperature of  $25^\circ\text{C}$  used as reference. This was the default value but could be adjusted by the keypad. The charge controller turns off the system for temperatures above  $40^\circ\text{C}$ .

- ✓ The TO-92 package was used with a water resistant probe of 50cm to cater for cases where the battery was not too close to the MPPT charge controller and for wet rainy conditions

### 3.3 System Interface

#### LCD

A Liquid Crystal Display (LCD) is implemented in the design to display vital parameters that are system status indicators for user-friendliness. Since LCD panels produce no light of their own, they require external light to produce a visible image. In a "transmissive" type of LCD, this light is provided at the back of the glass and is called the backlight. The LCD is made up of a given number of pixels that are generally arranged in front of the light source. These pixels are turned on and off based on an applied electric field. The LCD used in this design will be programmed to interface with the microcontroller. There are several types of basic level technology LCDs in the market, they include segmented displays, character displays and graphical displays

The Character LCD was chosen in its advantages over segmented and graphical displays in terms of the project goals. The segmented displays offered least power consumption but their characters took too big a space on the screen to display complete comprehensive information to the user for the same size of display as a character LCD used; graphical displays on the other hand offered a wide range of functionality and flexibility in writing custom characters and pictures, this was more user friendly but its use would consume more power and add more complex programming in the design algorithm which isn't a logical trade-off based on the project goals.

A 20x4 character LCD screen met the project goals with the minimal as possible power consumption for the image quality good enough to display all the vital parameters simultaneously in an uncongested manner which was the shortcoming of a 16x2 character LCD. The backlighting feature of the LCD was also important in the design so that the status could be read in any lighting situation.

An I2C is incorporated to serially transmit data to the ATMEGA328P by only connecting to the SDA (PC4) and SCL (PC5) pins instead of traditionally connecting to the (PB4, PB3, PD5, PD4, PD3, PD2) pins hence saving on four I/O pins to be used for other peripherals and future works; it also has an onboard potentiometer to vary the contrast of the LCD, the backlight is important for the user to be able to read the status under any operating conditions.

The screen presents the current and voltage of the solar panel and battery, solar panel power, charging mode, duty cycle as well as the temperature of the battery. It also displays the battery charging status as well as any system warnings or messages.

#### Specifications

- 4 lines with 20 characters per line
- Interface: I<sup>2</sup>C
- I2C Hex Address: 0x3F
- Back lit (green with black characters)



- Supply voltage: 5V
- Adjustable contrast using the onboard potentiometer

### LED indicators

In designing the LED indicators an RGB Common Anode LED was used to display the system status .It can display up to 256 colors depending on the hues (set by PWM ) on its red(R), green(G) and blue(B) pin .It was chosen since as it saved on amount of space required and amount of components required. Since it has a common anode, only one current limiting resistor is used on its anode.

The following are the different LED Color denotations:

Blue: No solar panel/battery connected.

Red: Low battery voltage.

Yellow: Battery charging.

Green: Battery fully charged.

Purple: Battery overvoltage.

- ✓ Without an RGB led, five separate LEDs would have been required, each with its own current limiting resistor. Hence using a RGB LED saves on power dissipation and board space area.

Pin(R) was connected to PD5, Pin (G) was connected to PD6 and Pin (B) was connected to PD3.A green LED was also added on the output side of the LM7805 to indicate when the MPPT charge controller was receiving its output power.

### Keypad

In order to make the MPPT charge controller versatile for various applications, an input system was needed to set to customize the charge controller for different weather conditions and battery types.

A 4\*3 Keypad was chosen to be used as the input interface, it was connected to PD2, PD4, PD7 and PB2-PB5.

- ✓ The keypad was used to adjust the battery type, setpoints for float voltage, absorption voltage, equalization voltage, Low Voltage Disconnect ,float voltage, load mode ,absorption set time and temperature compensation. The Keypad was also used to scroll through the LCD since not all information can fit into the LCD at once. Long pressing '\*' is used to edit the parameters while long pressing '#' is used to scroll through the LCD. Long pressing '1' enables load mode while long pressing '0' disables load mode

### 3.4 Buck converter design

In an asynchronous buck converter e.g. the one in Figure 2-8 a diode is used and its switching is independent of MOSFET switching. In the synchronous buck converter the diode is paralleled to another MOSFET and that MOSFET Q2 is switched on and off synchronously with the primary switch Q1's operation. Its aim is to use a MOSFET as a rectifier that has very low voltage drop compared to a standard rectifier since the diode has a higher voltage drop than a MOSFET which usually have very low  $R_{ds(on)}$  {2m $\Omega$ -200m $\Omega$ }, which correspond to lower switching losses, this increases the buck converter efficiency by minimizing the power loss.

The MOSFET Q2 requires a second PWM signal which is a complement of the primary PWM signal of MOSFET Q1 hence synchronous operation such that when Q1 is ON, Q2 is OFF and vice versa. MOSFET Q2 is clamped by a schottky diode to conduct inductor fly back voltage and thus prevent Q2's body diode from conducting and storing charge, the body diode in a MOSFET is a slow rectifier and would add significant losses if allowed to switch. The schottky diode conducts peak current through the inductor but this current flows for a short time until MOSFET Q2 switches on, the current rating of the schottky diode can thus be a lot less than peak inductor current. A schottky diode is used because its forward voltage drop sits at around 0.3V compared to 0.7V of normal diodes. This is shown in Figure 3-2.

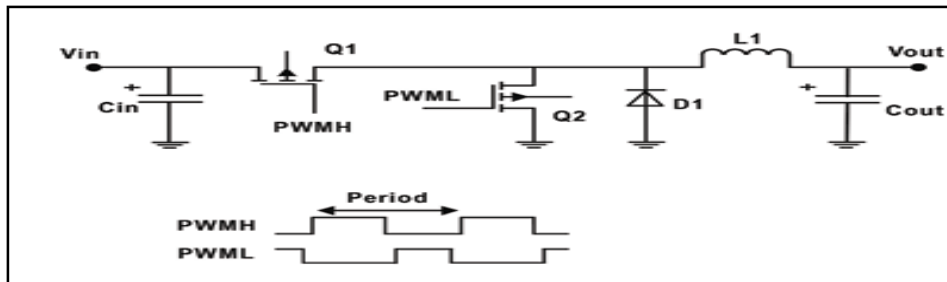


**Figure 3-2: Synchronous buck operation**

The current waveforms in the capacitor and inductor for a whole switching period for a buck converter in Continuous Conduction Mode (CCM) are shown in Figure 3-3.

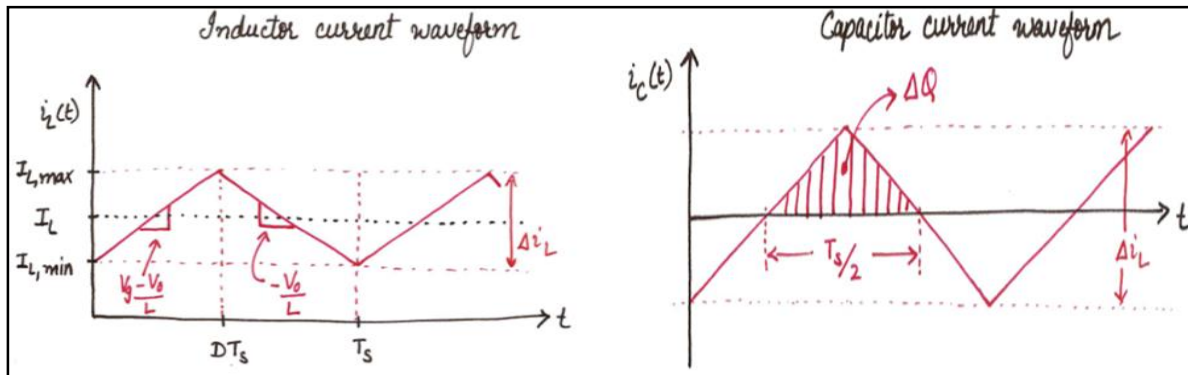


**Figure 3-3: Buck converter waveforms**

From the inductor waveform it is seen that in the On state: the inductor current rises to a maximum value  $I_{L,MAX}$  and from the inductor V-I characteristic it is seen that:

$$L * \partial \frac{Il(t)}{\partial t} = Vin - Vout \quad \text{Equation 9.0}$$

$$Il(t) = \int_0^T \frac{Vin - Vout \partial t}{L} \quad \text{Equation 9.1}$$

$$IL, max = \frac{(Vin - Vout)ton}{L} + IL, min = \frac{(Vin - Vout)DTs}{L} + IL, min \quad \text{Equation 9.2}$$

$$\nabla Il = IL, max - IL, min = \frac{(Vin - Vout)DTs}{L} \quad \text{Equation 9.3}$$

In the Off state: the inductor decreases to its minimum value  $I_{L, min}$  thus

$$L * \partial \frac{Il(t)}{\partial t} = -Vout \quad \text{Equation 9.4}$$

$$Il(t) = \int_0^T \frac{-Vout \partial t}{L} \quad \text{Equation 9.5}$$

$$IL, min = \frac{(-Vout)toff}{L} + IL, max = \frac{-Vout(1-D)Ts}{L} + IL, max \quad \text{Equation 9.6}$$

$$\nabla Il = IL, max - IL, min = \frac{Vout(1-D)Ts}{L} \quad \text{Equation 9.7}$$

Since the rise in current in the On state equals fall in current in the Off state the both  $\Delta I_L$  s from Equations 9.3 and 9.7 must be equal and equating the two we get

$$(VinD - Vout)Ts = 0 \text{ or } D = \frac{Vout}{Vin} \quad \text{Equation 9.8}$$

From Figure 3-2 and 3-3 it is seen that the current that flows through the output capacitor,  $C_{out}$ , is the inductor ripple current. Since the current through the inductor is the sum of load current and inductor ripple current, the output capacitor filters the inductor ripple current so as for load current ( $I_L$ ) to flow to the load. This capacitance is necessary to maintain a regulated output when MOSFET Q1 is off and is necessary to minimize amount of ripple present in the output voltage too. The average current through the capacitor is zero but in one half cycle, half the period, the capacitor is charged and the increase in charge is

$$\nabla Q = \frac{1}{2} \frac{\nabla Il}{2} \frac{Ts}{2} = \frac{\nabla Il Ts}{8} \quad \text{Equation 10.0}$$

The output ripple voltage is given by

$$\nabla V = \frac{\nabla Q}{Cout} = \frac{\nabla Il Ts}{8Cout} = \frac{(1-D)Vout Ts^2}{8LCout} \quad \text{Equation 10.1}$$

The input capacitor is there to buffer the input current at a constant rate and supply requested bursts to the buck converter, it provides the ripple current required for the switching of MOSFET Q1 hence the panel current can be ripple free. The solar panel needs ripple free current to stay at maximum

power point and without  $C_{in}$  the pulsating current produced by switching Q1 would need to be completely supplied by the PV module.  $C_{in}$  thus stabilizes the input voltage and increases efficiency. During the on state, the current flowing through  $C_{in}$  is the difference between the input current  $I_{in}$  and current through inductor in On state  $I_L$ ; the current through  $C_{in}$  in the off state is only  $I_{in}$ . During the Off state (with Q1 in open circuit) the  $C_{in}$  is charged by  $I_{in}$  while during the on (conduction) state it's discharged. All in all the charge added in off state is equal to the charge removed in on state. Thus from the off state:

$$C_{in} \frac{\partial V_{in}}{\partial t} \equiv C_{in} \frac{\nabla V_{in}}{t_{off}} = I_{in} \quad \text{Equation 11.0}$$

$$I_{in} = D I_{out}; t_{off} = (1 - D) T_s \quad \text{Equation 11.1}$$

$$\nabla V_{in} = \frac{I_{in} t_{off}}{C_{in}} = \frac{I_{out} D (1 - D) T_s}{C_{in}} \quad \text{Equation 11.2}$$

### Component selection:

#### **Inductor**

Rearranging Equation 9.7 we get

$$L = \frac{V_{out}(1-D)T_s}{\nabla I_L} \quad \text{Equation 12.0}$$

To calculate the sufficient inductance needed for operation in all duty cycles we calculate the duty cycle from Equation 9.8 corresponding to the worst case scenario i.e. when  $V_{out}$  is at its largest possible value, which is the open-circuit voltage ( $V_{oc}$ ) of the solar panel designed to be connected to the input. A maximum charging current of 20A for a battery of 12V requires a solar panel of 230-240W (yielding 19.2 -20A respectively) .

In this case after research on solar panels in the market 230-240W panels, the high rating solar panels have  $V_{oc}$  up to 40V e.g. the 240W SHARP ND-240QCJ panel has  $V_{oc}=37.5V$ ; however if two 115-120W solar panels are connected to achieve the power most of the individual panels  $V_{oc}$  up to 22.5V hence for series connection a  $V_{oc}=45V$  e.g. Sunshine solar's 120WSSP120M panel has a  $V_{oc}=22.5V$ .

Using  $V_{out} = 12.5V$  for efficient charging of a drained battery and  $V_{oc}=45V$ ,  $D=0.28$ ;

Using a switching frequency of 50KHz which corresponds to  $T_s=20\mu s$ ,  $V_{out}$  (battery voltage) =12.5 and a ripple voltage taken to be 20% of maximum output current of 20A ( $\Delta I_L=6A$ ); from Equation 12.0 we get an inductance of 45.1 $\mu H$ .

The inductor should also be able to handle the peak current of  $(20A + \Delta I_L / 2 = 23A)$  in continuous conduction mode without saturation to be efficient as temperature increases during saturation. Using this parameters, an  $L1=45.1\mu H$  inductor with a saturating current greater than 23A is chosen, the

larger inductor is chosen to cater for high voltage and current peaks during transients. A not too large inductance is chosen so as not to limit response time to load transients. Continuous conduction mode (CCM) of the inductor means that the inductor current does not fall to zero. From these calculations it is seen that the inductor enters discontinuous conduction mode(DCM) when the output current falls below 2A ,the CCM/DCM boundary is when  $\Delta I_L / 2 = I_{out}$ .

Since commercially available inductors are fairly fixed and rigid in inductance size available it was opted to wind a home-made inductor. An iron-powder toroid core was chosen. The formula used to calculate number of turns required is

$$N = \sqrt[2]{(desired' L'(uH)/Al(uH/100turns)} \quad \text{Equation12.01}$$

The characteristics of the iron powder core used were: Outer Diameter(OD)=1.57 inches ,Inner Diameter(ID)=0.95 inches ,Height=0.570inches, Mean Length=10.05cm ,Cross-Section=1.14cm<sup>2</sup> Color: Yellow-white(26mix,μ=75).

Iron powder toroids are usually specified in terms of their outer diameter and mix color hence for our above specifications, our toroid is T-157-26 looking that part number on an  $A_L$  (μH/100 turns) table it yield an  $A_L = 970 \mu H/100$  turns.

- ✓ Substituting this value of  $A_L$  and out required inductance of 45.1 μH in Equation 12.01 we got 21.6 turns which was rounded up to 22turns;on measuring the wound inductor in the lab, a value of 45.23 μH was obtained as the actual inductance used.
- ✓ An enamel coated 16AWG wire stripped at its ends was used to make the turns since it could support the maximum current rating of 20A and being fairly thick in diameter it offered less resistance hence less I<sup>2</sup>R and heating losses.

## Output capacitor

Rearranging Equation10.1 we get

$$C_{out} = \frac{\nabla I L T s}{8 \nabla V} = \frac{(1-D) V_{out} T s^2}{8 \nabla V L} \quad \text{Equation12.1}$$

However capacitors are not ideal and have effective series resistance (ESR) due to losses in dielectrics the output capacitor ripple voltage is thus expressed as  $\nabla V = \frac{\nabla I L T s}{8 C_{out}} + \nabla I L * ESR$

Accounting for this Equation 12.1 becomes

$$C_{out} = \frac{\nabla I L T s}{8(\nabla V - \nabla I L * ESR)} = \frac{(1-D) V_{out} T s^2}{8 L (\nabla V - \nabla I L * ESR)} \quad \text{Equation12.2}$$

Taking an  $ESR=30m\Omega$ ,  $D=0.28$ ,  $T_s=20\mu S$  and ripple voltage of 2% of output voltage of 12.5 V ( $\Delta V=0.25V$ ) we get the rating for  $C_{out}=195\mu F$ . Capacitors also have Effective Series Inductance (ESL) but it's significant at high frequency of MHz. The capacitor voltage rating is also 1.5  $V_{out}=18.75V$  thus 20V would suffice.

✓ The output capacitor  $C_2$  chosen was 220uF by 25V

### Input capacitor

Rearranging Equation 11.2 
$$C_{in} = \frac{I_{out}D(1-D)T_s}{\nabla V_{in}}$$

The input capacitor voltage ripple is limited by  $C_{in}$ , with ripple caused by its ESR added; thus taking into account the ESR we get

$$\nabla V_{in} = I_{out} \left( \frac{D(1-D)T_s}{C_{in}} + ESR \right) \quad \text{Equation 12.3}$$

$$C_{in} = \frac{I_{out}D(1-D)T_s}{\nabla V_{in} - I_{out} * ESR} \quad \text{Equation 12.4}$$

Taking  $I_{out}=20A$ ,  $T_s=20\mu S$ ,  $ESR=30m\Omega$  and a ripple voltage 2% of maximum input voltage ( $\Delta V=0.9V$ )

$C_{in}=369\mu F$ . The capacitor should also have a voltage rating greater than  $V_{in}=45V$ .

✓ The Input capacitor  $C_1$  chosen was 470uF by 50V

### Mosfet

The selected MOSFET should have low static Drain-Source ON resistance - $R_{ds(on)}$  -to minimize conduction losses and temperature rise ,it should have a breakdown threshold voltage ( $V_{(BR)DSS}$ ) greater than the maximum input voltage  $V_{oc}=45V$  and a maximum drain current ( $I_D$ ) greater than maximum output current  $I_{out}=20A$ .

✓ The IRFZ44N was chosen it met the design specifications with the following characteristics  $V_{DSS} = 55V$  ,  $R_{DS(on)} = 17.5m\Omega$   $I_D = 49A$

## Mosfet driver

One significant feature of MOS-gated transistors is their capacitive input characteristic (i.e., the fact that they are turned on by supplying a charge to the gate rather than a continuous current). From the IRFZ44N data sheet, to achieve its  $R_{ds(on)}$  of 17.5mohms,  $V_{gs}=10V$  and  $I_d=25A$ . Since the gate of the MOSFET is connected to the ATMEGA328P PB1 and the source to the cathode of the buck converter diode which is at about the same potential as the battery, the source voltage with respect to the common ground is always equal to the voltage across the battery which in this case is approximately 12V.

The peak amplitude of the microcontroller's (Atmega328P-PU) output PWM waveform is 5V with respect to common ground and this is insufficient to turn on the MOSFET. A driver boost circuitry is therefore needed to amplify the 5V output of the microcontroller to create a  $V_{gs}$  of at least 10V to fully turn on the MOSFET as a switch during the ON period of the duty cycle. There are a couple of circuits capable of doing this such as Opto couplers and Mosfet Drivers.

Since we are driving an NMOS a high-side driver is used. International Rectifier family has a variety of MOSFET Gate Drivers (MGDs) to choose from, the IR2110 is a High Voltage IC designed for driving high speed MOSFETs and IGBT. It was the MOSFET Driver chosen at first but on experimentation it was found not to be as suitable a choice as an optocoupler since it needed boost strap circuitry to drive the high side MOSFET and since in our buck converter the output was at a constant 12V, the boost strap didn't charge since there was no path to ground to charge them. Using a modification of the circuit as per an application note AN978 of the company still proved futile.

An optocoupler was therefore chosen as our MOSFET driver. An optocoupler, also called an opto-isolator is a component that transfers electrical signals between two isolated circuits by using light. An opto-coupler contains a source (emitter) of light, usually a An opto-isolator contains a source (emitter) of light, almost always a near infrared light-emitting diode (LED), that converts electrical input signal into light, a dielectrical channel, and a photosensor, which detects incoming light and either generates electric energy directly, or modulates electric current flowing from an external power supply. The sensor can be a photoresistor, a photodiode, a phototransistor, a silicon-controlled rectifier (SCR) or a triac. The optocoupler is thus used to magnify the amplitude of the PWM signal from the ATMEGA328P to a value big enough to switch the gate whilst still maintaining the frequency and duty cycle.

The PC817 was chosen and its schematic and internal circuitry is shown in the appendix 2.

- ✓ The PC 817 has a maximum collector-emitter voltage of 35V which is enough to create enough  $V_{gs}$  of 10V to charge a 12V or even 24V battery connected at the output of the buck converter

### **Mosfet Driver Circuit modification**

- The microcontroller outputs its PWM waveform from PB1 to the anode Pin1 of PC817 via a current limiting resistor of 300 ohms and the amplified waveform is tapped from Pin3.
- A 1KOhm resistor is placed across the Gate-Source of the MOSFET to prevent accidental turn on of the Mosfet by external noise or its internal capacitance “Miller’-capacitance.
- Rg of 27Ohms is used between Pin3 of the optocoupler and the gate of IRFZ44N as a gate current limiting resistor.

### **3.5 Power Supply**

After all components were connected and seen to be working on breadboard, it was imperative to design a power supply mode to enable the components to be powered in a stand-alone setup. The LM7805 linear voltage regulator was used as it steps down 12V to 5V.

The LM7805 input pin was connected to the battery positive via a switch and diode to protect polarity, its output pin was used to supply 5V to power the ATMEGA 328P, I<sup>2</sup>C module and ACS-current sensors.

A green LED was also added on the output side of the LM7805 to indicate when the MPPT charge controller was receiving its output power.



### 3.6 MPPT Charge Control Algorithm

The algorithm used for Maximum power point tracking was P&O (Perturb and Observe) and a three stage charging algorithm was used to charge the battery. These are the main algorithms snippets shown in Figure 3-4 and Figure 3-5. The full code is provided in Appendix 1, the logic of the algorithm is well defined by comments in the code (the pin out connections and system status indicators that show the relevant information from the main flowchart to the user)

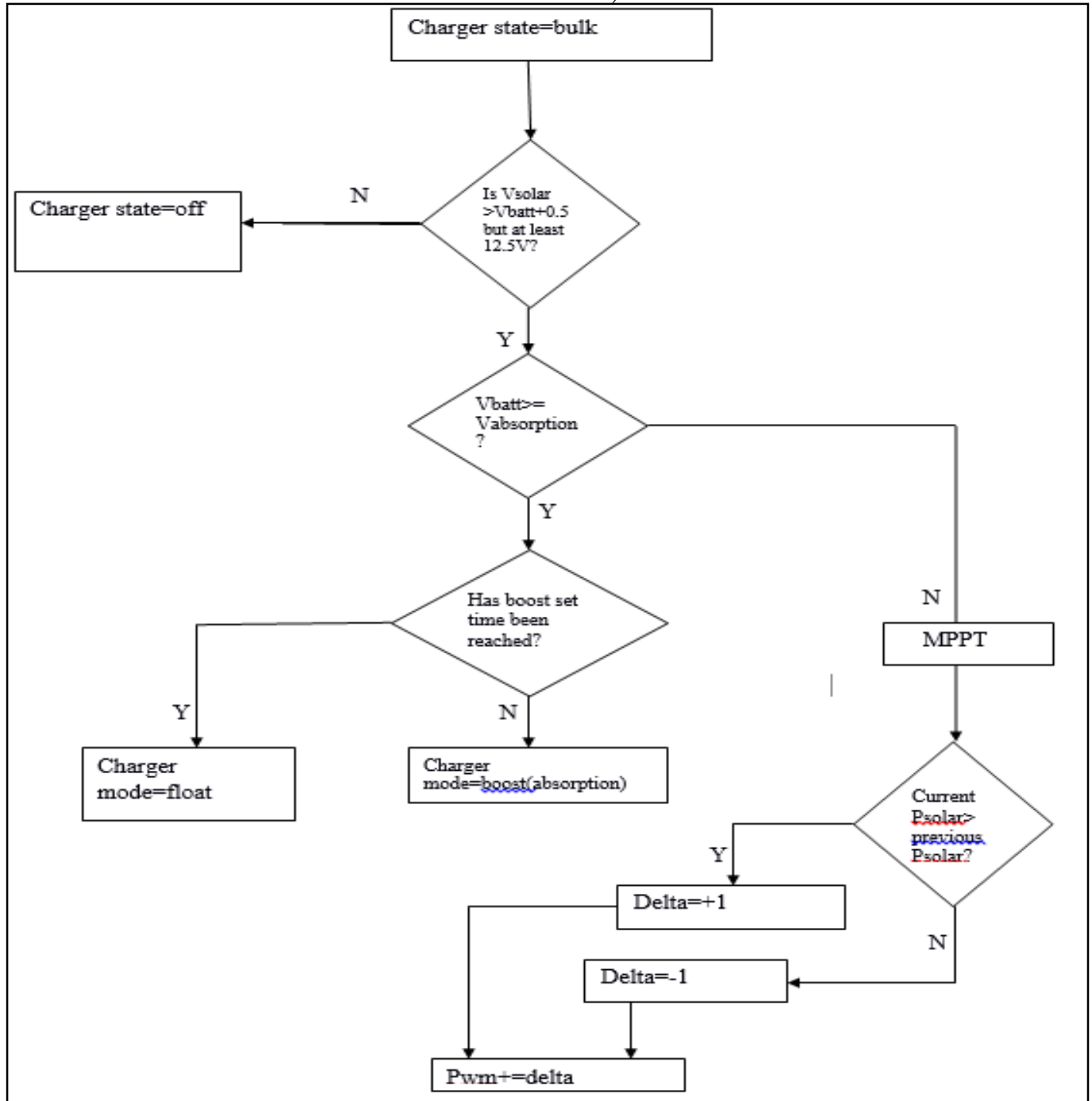


Figure 3-4: Flowchart showing MPPT by P&O being used in the bulk charging stage

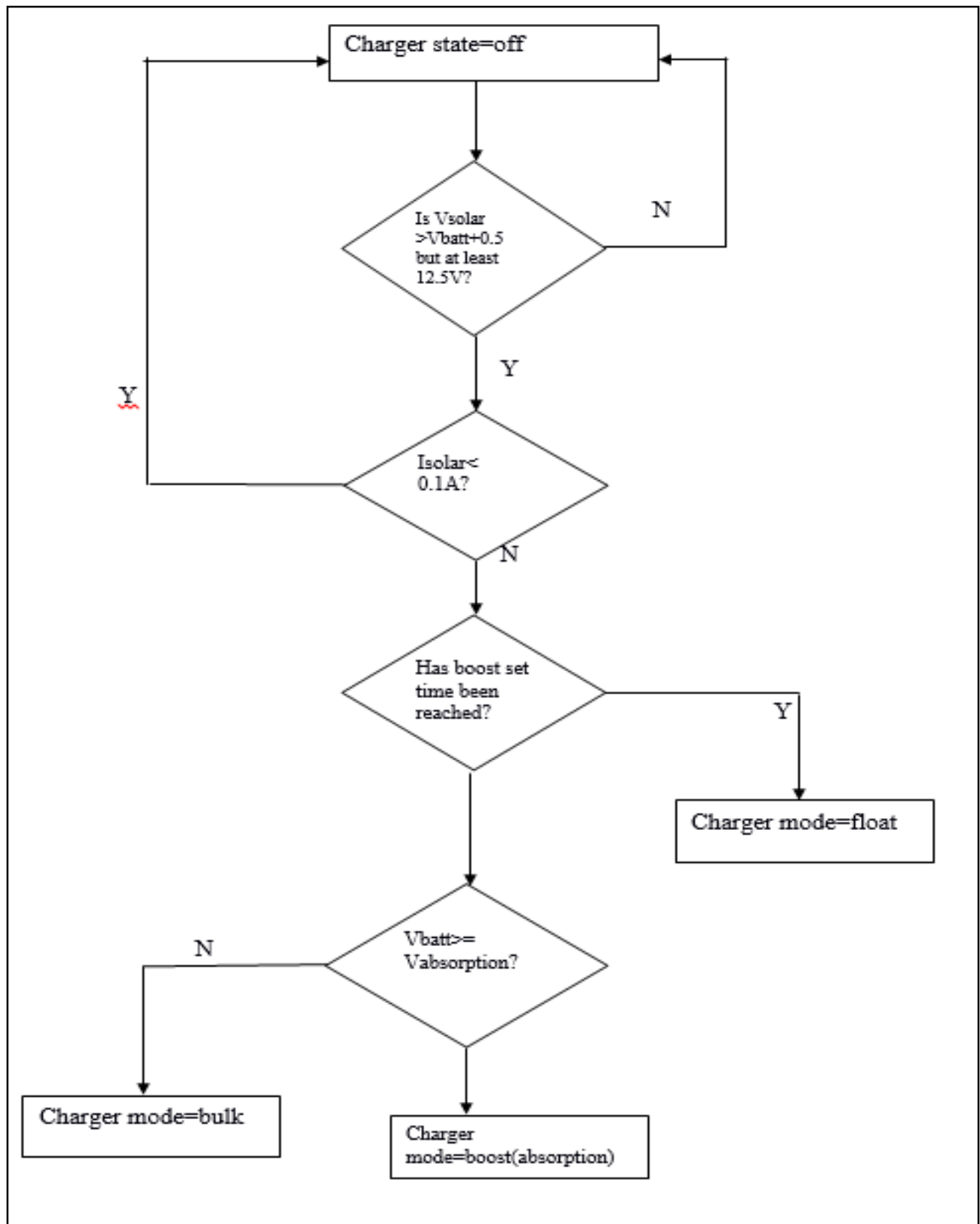


Figure 3-5: Flowchart showing the basic three stage charging being used

### 3.7 System Protection

The system is protected by a combination of hardware and software protection schemes

- Hardware protection.

To protect reverse current at the solar panel side MOSFET Q2 is used, this prevents current from flowing from the battery to the solar panel at night time or whenever the battery voltage is far greater than the solar panel voltage which could damage the array. MOSFET Q2 is an NMOS setup such that its source is at the solar panel side as shown in the schematic. Since each MOSFET has a body diode, setting it up this way ensures that when Q2 is off its body diode restricts flow of current from battery to solar panel. A MOSFET is used in place of a diode to reduce the losses since diodes have a relatively larger voltage drop of about 0.7V hence when passing current of about 5A they have a power loss of 3.5W, MOSFETs on the other hand have a low  $R_{ds(On)}$ , the one selected had a static-on resistance of 19.5m $\Omega$  hence when passing current it has a power loss of 0.5W. MOSFETs are thus more efficient by saving on losses.

Wire selection was also important for efficiency and protecting the system from overheating. Using too thin wire connections increase resistance to current due to less cross-section area and this leads to large power ( $I^2R$ ) losses that cause excessive heating. The wire gauge that connects the solar panel to the charge controller was selected to withstand 10A, (worst case  $I_{sc}$  for a single 240W system is about 8A) a 4mm<sup>2</sup> wire was chosen as it handles this comfortably. The wire connecting the charge controller to the battery was also chosen as 6mm<sup>2</sup> to withstand the maximum charging current of 20A. On the PCB, traces of 1.5 inches were used to handle the solar panel current of 10A same case for the battery. Using to thinner traces could cause the copper traces to overheat when conducting and may vaporize very thin traces if conditions persist for long.

For the case of polarity reversal protection, high voltage diodes are used across the PV and battery inputs of the MPPT charge controller to the circuit from user mistakes of interchanging the positive and negative terminals. The polarity on the charge controller was also clearly marked (+ and -) on the terminal blocks inputs. Dual ultra-fast rectifier diodes 1N5819 were placed between the positive and negative terminals of the PV voltage (input) and battery voltage (output) as they could withstand voltages of up to 50V which could support our  $V_{oc}$  of 45V and for the battery bank it gave room for expansion into a 24V system. By placing the diodes in parallel, the overall resistance decreased, and allowed a greater amount of current to pass through.

A push button switch S2 that resets and forces the MPPT algorithm to restart was added. This technique helped in removing transients that may be caused in the system or software bugs and malfunctions.

A 20A fuse is also used to protect the battery from the specified maximum charging current of 20A. The fuse is designed to burn out and disconnect, if the current through the battery's positive terminal exceeds the current rating of the fuse.

- Software protection.

Once the battery is fully charged, the output current of the charge converter has to be decreased in order to maintain the voltage across the battery at a constant 13.6V, float state as discussed under batteries to replenish charge lost due to leakage. Also when charging at the absorption stage, the voltage across the battery is maintained at 14.4V while current into the battery reduced. In both of these absorption and float constant voltages the algorithm achieves this by reducing the duty cycle (pwm) till near null hence forcing the solar panel to operate at almost  $V_{oc}$  where the output current of the solar panel is minimized. The following code snippet shows the protection.

```
float Vfloat=13.6;//float voltage
float Vboost=14.4;//absorption voltage
float pwm=0;//the duty cycle
if (Vbatt>Vboost+0.08) {
    error1=Vbatt-(Vboost+0.08);
    inc=delta*300*error1;//if battery voltage >14.48 decrease
pwm by the %error
    pwm-=inc;
    set_pwm_duty_cycle(pwm);
if (Vbatt>Vfloat+0.1) {
    error2=Vbatt-(Vfloat+0.1);
    inc=delta*300*error2;
    pwm-=inc;
    set_pwm_duty_cycle(pwm);
```

Monitoring the battery voltage & current and PV voltage & current by the microcontroller is essential since it gives battery and solar panel status

If the battery or solar panel is disconnected, the algorithm also prevents MOSFET Q1 from switching by shutting down the MOSFET driver, because otherwise for the former case the voltage at the output would increase linearly and hence damage the system -the battery maintains the output of the buck converter approximately fixed at battery voltage.(The LED lights blue in this case)

Other conditions that cause the MOSFET Q1 to be switched off are:

Overvoltage protection: When the battery voltage exceeds the bulk charge set point and reaches 14.6V, at this point further increase in voltage would lead to overcharging and gassing of the battery if sustained especially at high temperatures.(The LED lights purple in this case)

Reverse current protection: The algorithm also turns off the MOSFET Q1 when solar panel voltage isn't 0.5V above battery voltage as this may lead to inefficient charging and if significantly lower by turning the MOSFET driver, it enables the body diode of Q2 to prevent the battery from charging the solar panel.

Overcurrent protection: To protect the battery from the maximum charging current of 20A, the MOSFET is also switched off for currents exceeding the set limit.

Overheating protection: With the DSB1820 incorporated, the charger was automatically turned off for temperatures exceeding 40° C since this is the upper threshold of healthy stable battery charging.

The following code snippet shows the above software protection.

```
#define MOSFET_OFF digitalWrite(SD_pin,HIGH)
int Imax=20;int Tmax=40;
if(( (Vbatt>12) &&(Vsolar<Vbatt+0.5) || (Vbatt<=12) &&(Vsolar<12.5) ||
(Isolar<0.1) || (Vbatt>Vboost+0.15) || Psolar<0.5 || Ibatt>Imax || Tbatt
>Tmax)) {
    charger_mode=off;           MOSFET_OFF;           break; }
```

### 3.8 Complete Schematic

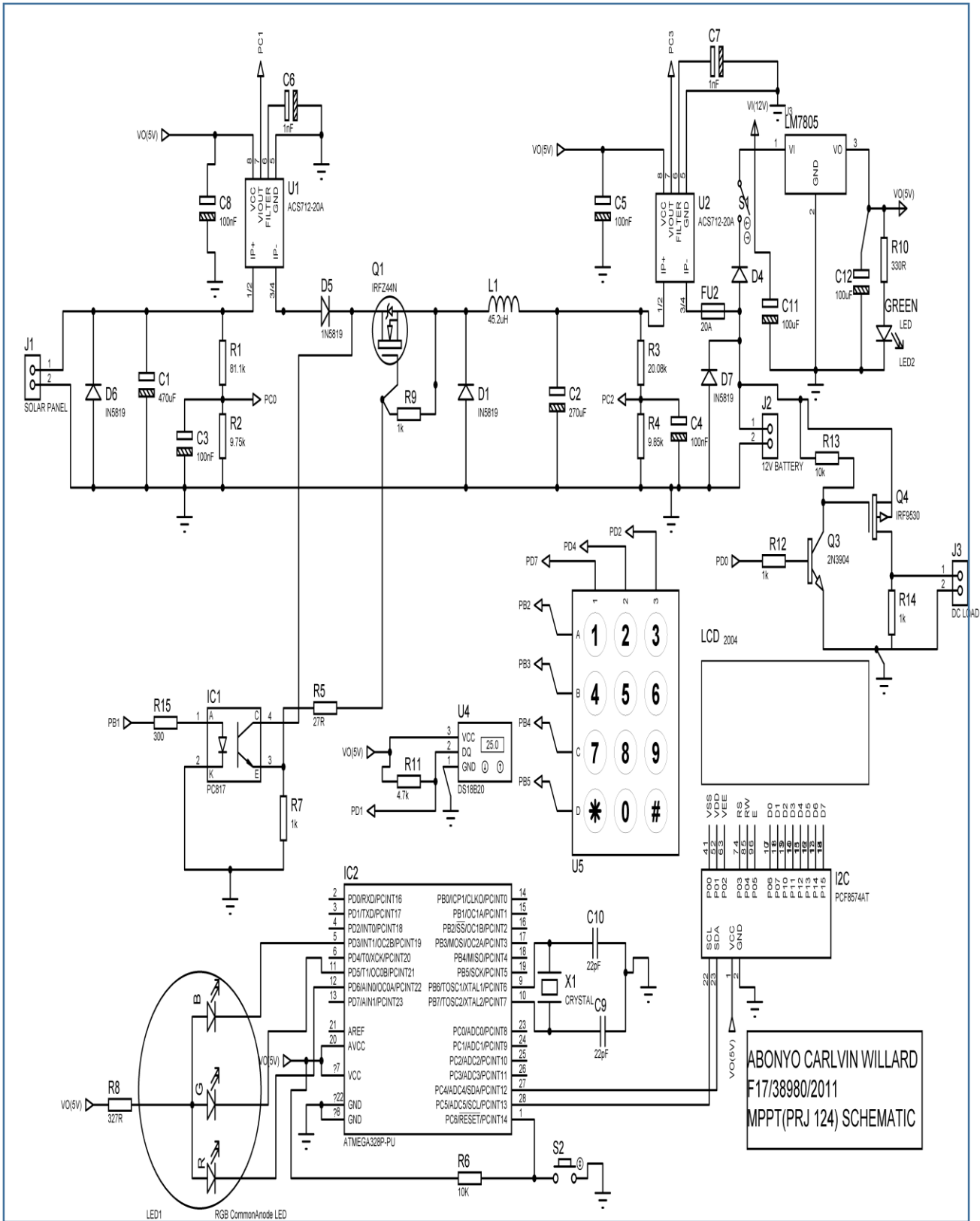
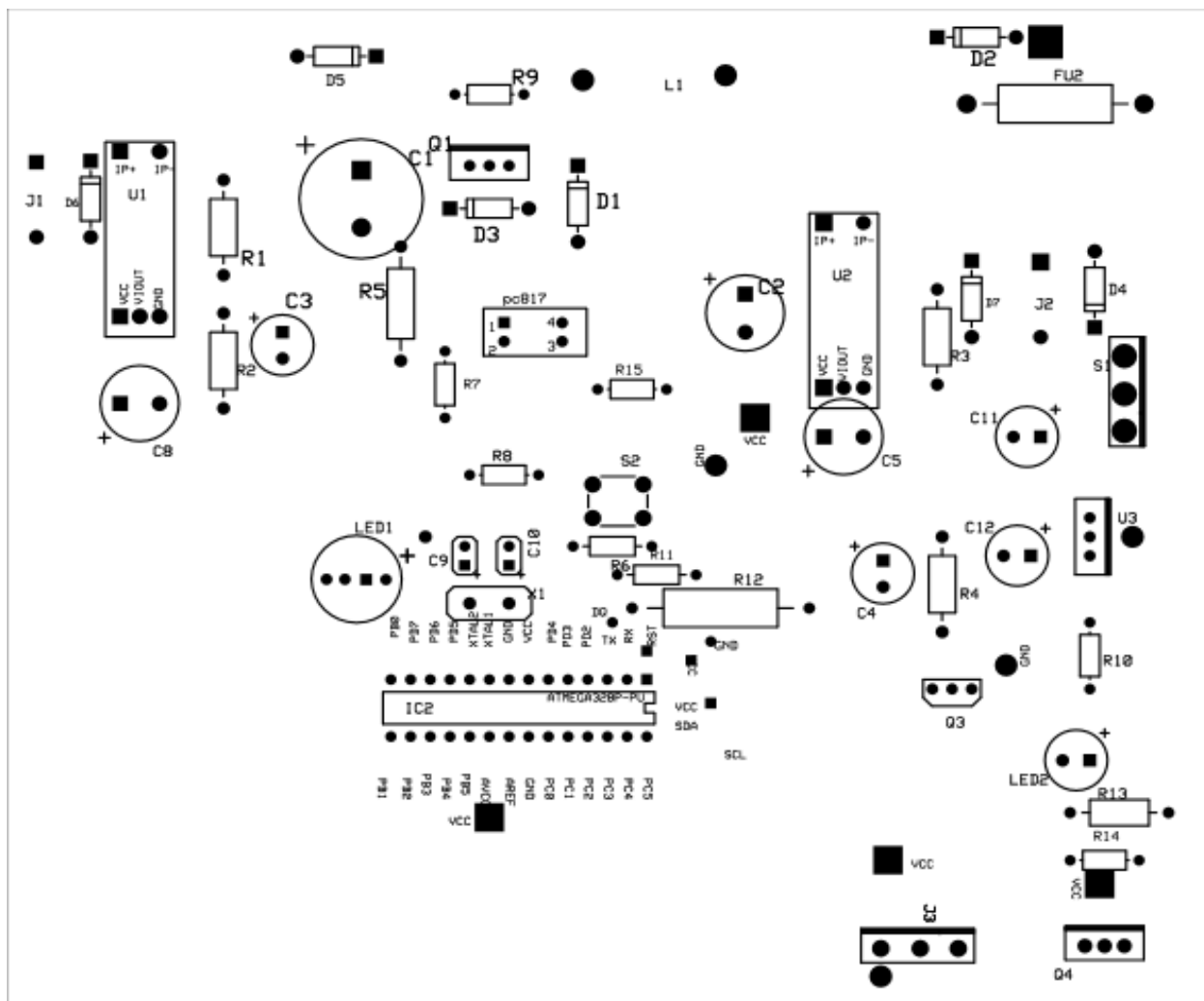


### Figure 3-6: MPPT Charge Controller Schematic

After the circuit in the schematic was tested and verified to be working properly on a breadboard, a double-sided printed circuit board was printed out and components soldered on to produce a neat marketable module.

- The PCB mechanical drawing is shown below. Figure 3-7 shows how the components in the schematic were laid the top and bottom copper layer traces are shown in the appendix 3.



53

## 4 TESTING, RESULTS AND ANALYSIS

Hardware and software portions of the project were separated into stages while developing the overall system. The portions consisted of panel testing, battery testing, sensor testing and MPPT charge controller software testing. Building and testing smaller individual sections of the system on the breadboard made the project more manageable and increased efficiency by decreasing debugging time.

### 4.1 Solar Panel Testing

Solar panel testing is important in determining the I-V and P-V characteristics of a solar panel. The characteristics of the solar panel are tested by the sweep method; the duty cycle is varied from near 100% to 0%, from the background research this varies the solar panel's operating voltage from  $V_{oc}$  to near the battery's voltage of 12V. This enables us to generate its curves of PVvoltage vs pwm, PVcurrent vs PVvoltage and PVpower vs PVvoltage.

Also the above tests are done at different times of day to see the effect of various weather conditions such as insolation and clouds on the P-V characteristics and peak power produced by a solar panel. The solar panel used was the one below (SOLARTEC SOLAR MODULE NE-20). Some important specs are  $V_{oc}=21.6V$ ,  $V_{mp}=17.2V$ ,  $I_{sc}= 3.5A$

To plot the readings the LCD was recorded and the also the program MegunoLink Pro was used to read data being transferred between the ATMEGA 328P and the port on my computer (COM25). The data was tapped on the serial connection and the values recorded pasted onto Excel 2013 to generate a compound line graph.

On 5/04/2016 tests were made. A code was written to sweep the duty cycle of the buck converter from 100% to 0% while the solar panel power, current and voltage were recorded from the serial monitor. Figure 4-1 shows the solar panel power ( $P_{solar}$ ) and current( $I_{solar}$ ) as a function of solar panel voltage ( $V_{solar}$ ) while Figure 4-2 shows the same parameters as a function of the duty cycle of switching MOSFET Q1 ; both tests carried out at 1415 hrs. Figure 4-3 shows the peak solar panel wattage displayed on the LCD taken at six different times of that day.

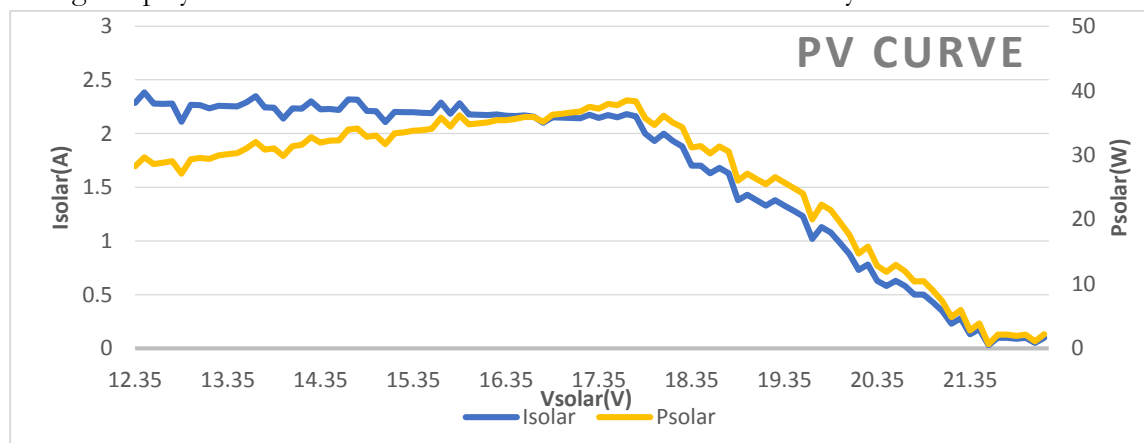
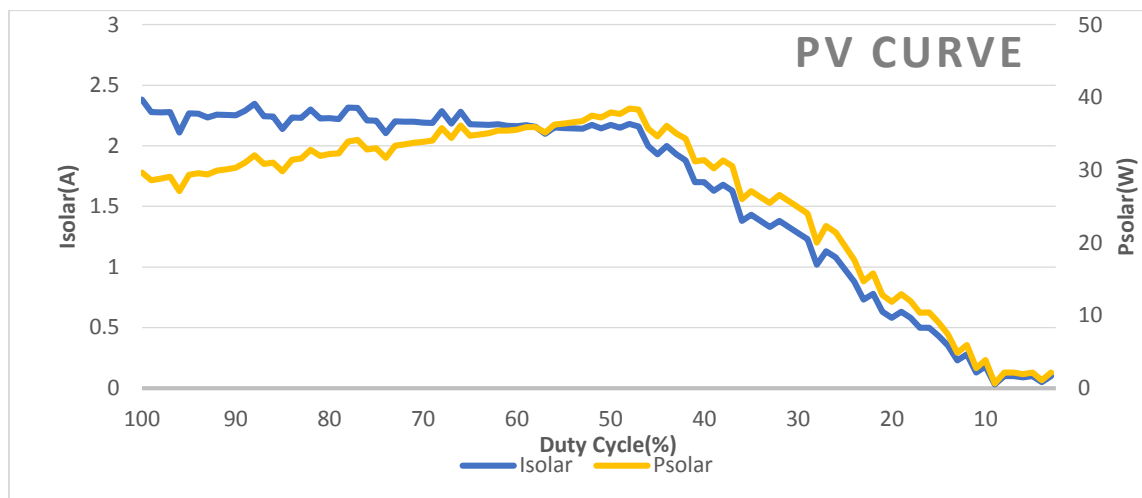
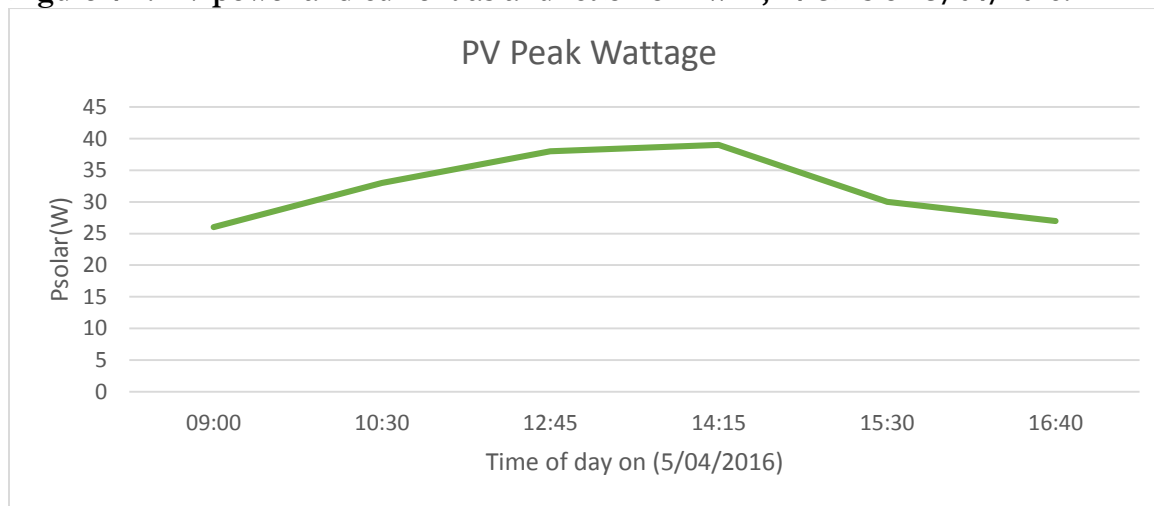


Figure 4-1: PV power and current as a function of PV Voltage; 1415hrs on 5/04/2016.





**Figure 4-2: PV power and current as a function of PWM; 1415hrs on 5/04/2016.**



**Figure 4-3: PV wattage at different periods of the day on 5/04/2016.**

## 4.2 Battery Testing

The battery voltage, temperature and current was tested and verified to correspond to the charging state displayed on the LCD and LED as per the table 5 and 6. The battery used for testing was FIAMM 12FGL100.

## 4.3 Sensor Testing

The voltage and current sensors were the key to determining the solar panel output power which is key in the P&O Algorithm and also to determine the charging mode of the battery. The sensors thus had to inadvertently be accurate for efficient and effective performance. The voltages and currents

displayed on the LCD as measured by the microcontroller was compared to those measured by the DMM and the results found an outstanding degree of accuracy as shown in the tables below.

**Table 4-1: Voltage Sensor test**

| ATMEGA328 |          | DMM       |          | % Difference |          |
|-----------|----------|-----------|----------|--------------|----------|
| Vsolar(V) | Vbatt(V) | Vsolar(V) | Vbatt(V) | Vsolar(%)    | Vbatt(%) |
| 21.60     | 13.55    | 21.61     | 13.51    | 0.04%        | 0.29%    |
| 17.48     | 12.82    | 17.50     | 12.81    | 0.11%        | 0.10%    |
| 22.10     | 13.10    | 22.15     | 13.13    | 0.23%        | 0.23%    |
| 18.01     | 13.00    | 17.95     | 13.10    | 0.33%        | 0.76%    |
| 21.46     | 12.76    | 21.47     | 12.80    | 0.04%        | 0.31%    |
| 21.42     | 12.46    | 21.55     | 12.46    | 0.60%        | 0.00%    |

**Table 4-2: Current Sensor test**

| ATMEGA328 |          | DMM       |           | % Difference |       |
|-----------|----------|-----------|-----------|--------------|-------|
| Isolar(A) | Ibatt(A) | Isolar(A) | Ibatt (A) | Isolar       | Ibatt |
| 1.5       | 2.13     | 1.6       | 2.12      | 6.25%        | 0.47% |
| 1.71      | 2.5      | 1.75      | 2.6       | 2.29%        | 3.85% |
| 2.30      | 3.35     | 2.19      | 3.37      | 5.02%        | 0.59% |
| 0.2       | 0.39     | 0.21      | 0.4       | 4.76%        | 2.5%  |
| 2.12      | 3.10     | 2.14      | 3.3       | 0.93%        | 6.06% |

## 4.4 Software Testing

The software was then tested at different times and different conditions to see if the system status indicators displayed the actual system status. The results were tabulated below.

| Table 4-3: Battery state test |            |              |
|-------------------------------|------------|--------------|
| Vbatt(V)                      | SoC on LCD | Expected SoC |
| 12.46                         | BULK       | BULK         |
| 12.76                         | BULK       | BULK         |
| 13.55                         | FLOAT      | FLOAT        |
| 14.42                         | BOOST      | BOOST        |

| Table 4-4: Charge algorithm test |            |           |           |               |          |               |          |
|----------------------------------|------------|-----------|-----------|---------------|----------|---------------|----------|
| Solar panel                      |            | Battery   |           | Charging Mode |          | LED Display   |          |
| Vsolar (V)                       | Isolar (A) | Vbatt (V) | Ibatt (A) | Actual on LCD | Expected | Actual on LED | Expected |
| 16.55                            | 1.5        | 13.55     | 1.55      | FLOAT         | FLOAT    | GREEN         | GREEN    |
| 18.01                            | 1.71       | 12.82     | 2.10      | BULK          | BULK     | GREEN         | GREEN    |
| 17.60                            | 2.30       | 13.10     | 2.6       | BULK          | BULK     | GREEN         | GREEN    |
| 21.6                             | 0.2        | 13.00     | 0.30      | OFF           | OFF      | GREEN         | GREEN    |
| 17.48                            | 2.18       | 12.3      | 2.8       | BULK          | BULK     | ORANGE        | ORANGE   |
| 0.00                             | 0.00       | 12.5      | 0.00      | OFF           | OFF      | BLUE          | BLUE     |

| Table 4-4: MPPT Charge controller efficiency test |            |           |           |                                |
|---|------------|-----------|-----------|--------------------------------|
| Solar panel                                       |            | Battery   |           | Efficiency                     |
| Vsolar (V)  | Isolar (A) | Vbatt (V) | Ibatt (A) | (Vbatt*Ibatt)/(Vsolar*Isolar)% |
| 16.55   | 1.5        | 13.55     | 1.55      | 84.6%                          |
| 18.01   | 1.71       | 12.82     | 2.10      | 87%                            |
| 17.60   | 2.30       | 13.10     | 2.6       | 84.1%                          |
| 21.6  | 0.2        | 13.00     | 0.30      | 90.2%                          |
| 17.48   | 2.18       | 12.3      | 2.8       | 90.3%                          |
| 0.00  | 0.00       | 12.5      | 0.00      | 100%                           |
| 16.30   | 0.12       | 12.56     | 0.12      | 77.10%                         |

| Table 4-5: Temperature compensation testing at 3mv/°C/Cell deviation from 25°C |                  |                           |                       |                                |
|--|------------------|---------------------------|-----------------------|--------------------------------|
| Battery Temperature  | Vfloat set-point | Compensated float voltage | Vabsorption set-point | Compensated absorption voltage |
| 24.00°C  | 13.6V            | 13.62V                    | 14.40V                | 14.42V                         |
| 24.96°C  | 13.6V            | 13.60V                    | 14.40V                | 14.40V                         |
| 22.55°C  | 13.6V            | 13.64V                    | 14.40V                | 14.44V                         |
| 26.12°C  | 13.6V            | 13.58V                    | 14.40V                | 14.38V                         |

Below is the bread-board implementation of the circuit before a PCB was made.

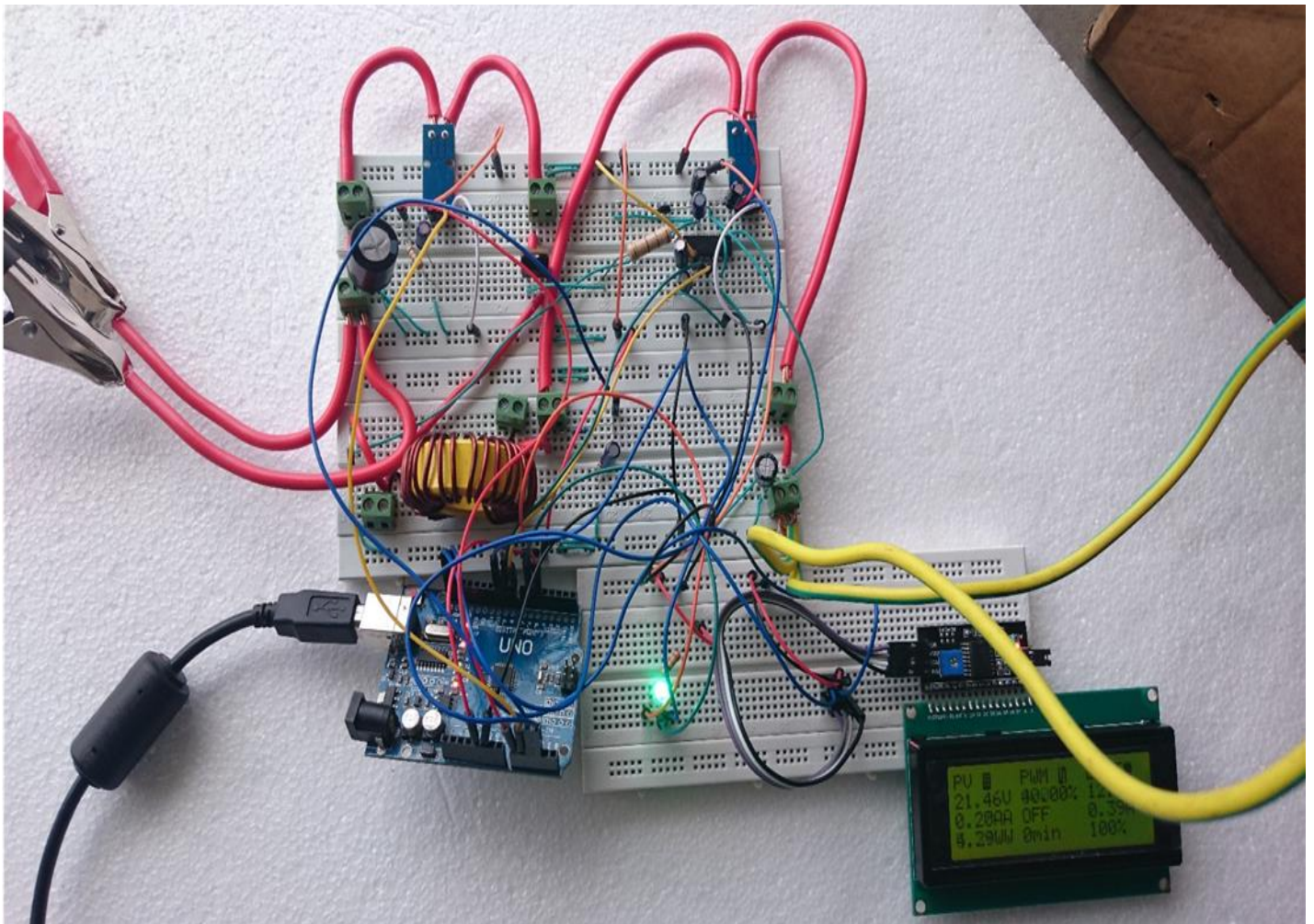


Figure 4-4: Breadboard implementation of MPPT Charge controller; 1555hrs on 5/04/2016.

Below is the PCB implementation of the MPPT Charge controller.

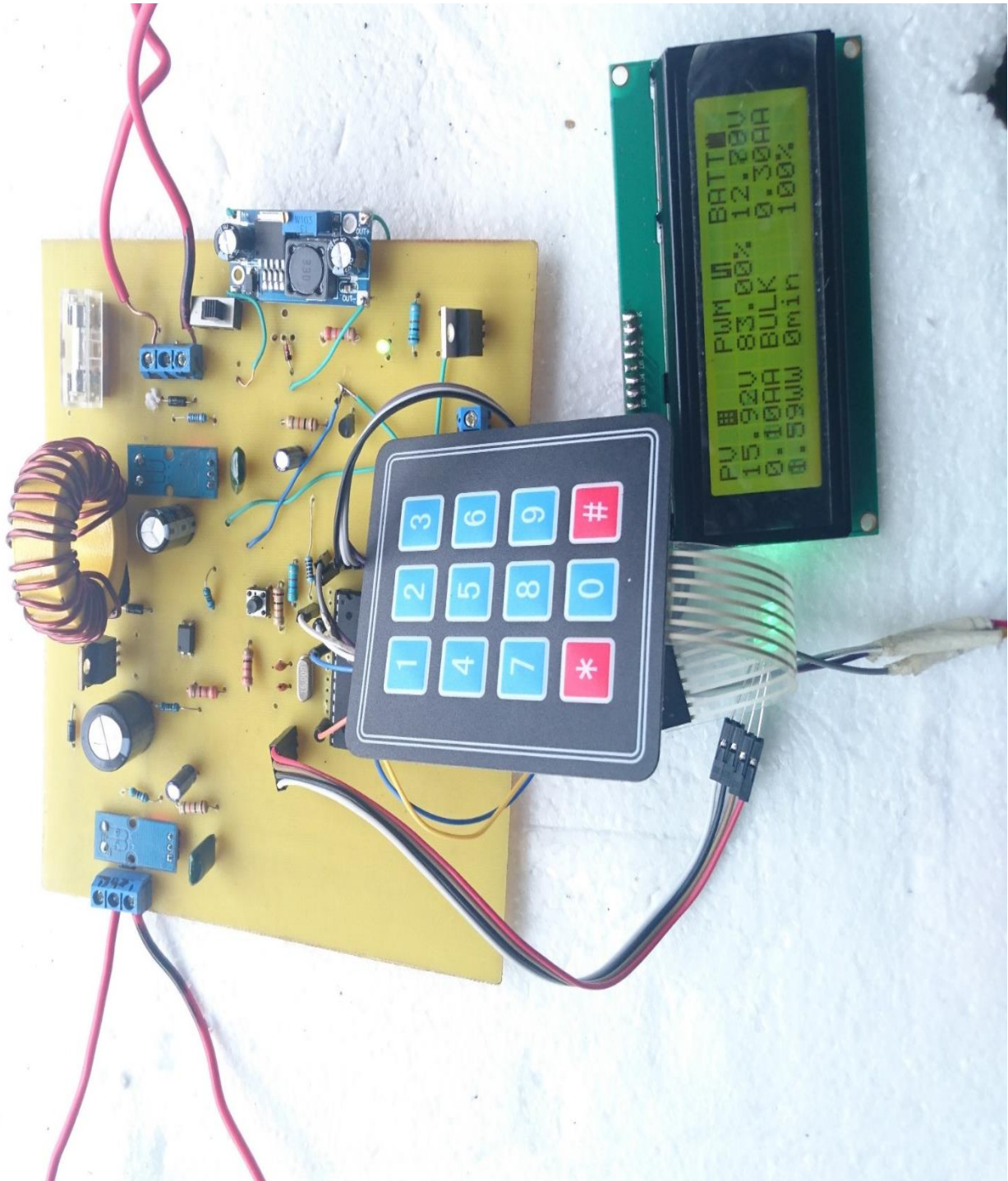


Figure 4-5: PCB circuit of MPPT Charge controller 12/05/2016.



## 4.5 Analysis

As it is evident for the curves, the solar panel operating point varies with the duty cycle of the MOSFET Q1 being switched on. The maximum power point is hence seen to be tracked by perturbing the duty cycle and observing if the output power of the solar panel has increased

Another observation was that the peak power from the solar panel varied with insolation as the sun moved across the sky during the day and as clouds came up. With peak power got at mid-day and less power got as clouds cast a shadow.

The system interface was also seen to be working well with the LED and LCD displaying correct information. The Keypad also worked well as shown by screenshots in Appendix 4.

The temperature compensated charging was seen to work well by lowering charge set points with increasing temperature and increasing charge set points with decreasing temperature as shown in Table 4-5.

The controller efficiency was also found to vary between 75%-90% as from table 4-4 depending on the power input and this was due to  $I^2R$  losses in the buck converter.

The standby current drain by the MPPT charge controller calculated when no solar panel was present was 40mA drained from the battery that was due to the power consumption of the MPPT charge controller devices such as LCD backlight.

## 5 FINANCIAL ANALYSIS

The aim of this project was to design, implementation and test an economical microcontroller based MPPT charge controller. Using the least number and size of circuit components allowable while maintaining a high efficiency margin the charge controller was built that allowed for a simple circuit that reduced the PCB size, hence production, packaging cost and the overall cost of the charge controller. An efficient, effective and economical charge controller was built by using basic components and eliminating anything superfluous. Table7 shows the table of list of components and the total price of the project.

**Table 5-1: Financial Analysis**

| <b>Component</b>  | <b>Units Required</b> | <b>Price per Unit(Kshs)</b> | <b>Total Price(Kshs)</b> |
|---|-----------------------|-----------------------------|--------------------------|
| <b>Terminal Blocks</b>                                  | 2 (J1,J2)             | 20.00                       | 40.00                    |
| <b>81.1K*1W resistor</b>                                | 1 (R1)                | 5.00                        | 5.00                     |
| <b>9.75K*1W resistor</b>                                | 1 (R2)                | 5.00                        | 5.00                     |
| <b>20.08K*1W resistor</b>                               | 1 (R3)                | 5.00                        | 5.00                     |
| <b>9.85K*1W resistor</b>                                | 1 (R4)                | 5.00                        | 5.00                     |
| <b>27R*2W resistor</b>                                  | 1 (R5)                | 10.00                       | 10.00                    |
| <b>10K*1/4W resistor</b>                                | 1 (R6)                | 3.00                        | 3.00                     |
| <b>4.7K*2W resistor</b>                                 | 1 (R7)                | 10.00                       | 10.00                    |
| <b>327R*1/2W resistor</b>                               | 2 (R8,R9)             | 3.00                        | 6.00                     |
| <b>1K*1W resistors</b>                                  | 2 (R10,R11)           | 5.00                        | 10.00                    |
| <b>470<math>\mu</math>F *50V electrolytic capacitor</b> | 1 (C1)                | 30.00                       | 30.00                    |
| <b>220<math>\mu</math>F*25 V electrolytic capacitor</b> | 1 (C2)                | 20.00                       | 20.00                    |
| <b>0.1<math>\mu</math>F*25V electrolytic capacitors</b> | 5(C3,C4,C5,C6,C7,C8)  | 15.00                       | 75.00                    |

|   |   |            |        |        |
|---|---|------------|--------|--------|
| <b>100μF*16V electrolytic capacitors</b>                | 2 | (C11,C12)  | 10.00  | 20.00  |
| <b>22pF capacitors</b>                                  | 2 | (C9,C10)   | 5.00   | 10.00  |
| <b>IRFZ44N MOSFET</b>                                   | 2 | (Q1,Q2)    | 100.00 | 200.00 |
| <b>PC 817 Opto Coupler</b>                              | 1 | (IC1)      | 20.00  | 20.00  |
| <b>Atmega328P-PU Microcontroller</b>                    | 1 | (IC2)      | 300.00 | 300.00 |
| <b>ACS712-20A Current Sensor</b>                        | 2 | (U1,U2)    | 450.00 | 900.00 |
| <b>45.2μH inductor(Iron powder core + 16 AWG wire )</b> | 1 | (L1)       | 300.00 | 300.00 |
| <b>1N5819 Schottky diode</b>                            | 1 | (D1)       | 10.00  | 10.00  |
| <b>UF4007 diode</b>                                     | 1 | (D2)       | 15.00  | 15.00  |
| <b>1N4742A Zener Diode</b>                              | 1 | (D3)       | 5.00   | 5.00   |
| <b>1N4148 Signal Diode</b>                              | 1 | (D5)       | 10.00  | 10.00  |
| <b>RGB LED</b>  | 1 | (LED1)     | 20.00  | 20.00  |
| <b>Green LED</b>  | 1 | (LED2)     | 5.00   | 5.00   |
| <b>LM7805 Voltage Regulator</b>                         | 1 | (U3)       | 30.00  | 30.00  |
| <b>4*3 Keypad</b>                                       | 1 | (U5)       | 150.00 | 150.00 |
| <b>DS18B20 Probe</b>                                    | 1 | (U4)       | 400.00 | 400.00 |
| <b>16MhZ Crystal</b>                                    | 1 | (X1)       | 15.00  | 15.00  |
| <b>PCF8574AT I<sup>2</sup>C</b>                         | 1 | (I2C)      | 400.00 | 400.00 |
| <b>LCD 20*04</b>  | 1 | (LCD 2004) | 800.00 | 800.00 |



|                           |   |       |        |                 |
|---------------------------|---|-------|--------|-----------------|
| <b>Tactile Switch</b>     | 1 | (S2)  | 10.00  | 10.00           |
| <b>Slide Switch</b>       | 1 | (S1)  | 10.00  | 10.00           |
| <b>28pin DIP Socket</b>   | 1 | (IC2) | 10.00  | 10.00           |
| <b>PCB Implementation</b> | 1 |       | 500.00 | 500.00          |
| <b>TOTAL</b>              |   |       |        | <b>4,386.00</b> |

As seen the MPPT charge controller built costs Kshs4, 386 (\$43.00); VAT-inclusive. In comparison, the average price of an MPPT on the market is about \$100(Kshs10, 000) for a PWM charge controller and at least \$220(Kshs25, 000) for an MPPT charge controller to do the same job from the market research already done. The savings depicted here are very significant (80% for MPPT charge controllers and 50% for PWM charge controllers) and can make solar power a reality to many consumers unable to use renewable energy due to financial constraints.

## 6 CONCLUSION AND RECOMMENDATIONS

### 6.1 Recommendations for further work

A technical design is always restricted by time, budget and resources. This is a pragmatic dilemma faced in any real world occupation. This MPPT project experience was no exception similar challenges erupted affecting the overall project design. Throughout the project duration many practical challenges were faced from applying electrical circuit theory, to troubleshooting components and making due with unavailable components, to debugging software bug and designing an efficient PCB layout. However, improvisation was key and the project provided exposure to a variety of technical, electrical and mechanical disciplines. Albeit the existing design of the MPPT charge controller proved to be a major success, there is still room for improvement in certain aspects and features of the product. Some of the future improvements are discussed below.

The only algorithm tested and used was the P&O algorithm ,though it tracks the maximum power point, it theoretically is not the fastest under rapidly varying atmospheric conditions . Testing other robust and complex algorithms such as current sweep, fuzzy logic and neural network methods and finding the most efficient way to track the maximum power point or even creating a hybrid can be a future improvement work to this project and greatly enhance the software design robustness.

A hardware design improvement could be using a synchronous buck converter which has been discussed under the design. The rectifier diode D1 in this case would be replaced by a MOSFET and a dedicated MOSFET driver IR2104 can be used to drive the synchronous buck by toggling between turning them on based on its shutdown button while receiving only one input signal from the microcontroller. The IR2104 isn't commercially readily available in the market and has to be imported. The synchronous buck converter is a trade-off between added cost of the MOSFET and improved efficiency by the MOSFET. The efficiency is improved since the diode has a large voltage drop of 0.7V while the MOSFET has a low static on resistance of about  $20\text{m}\Omega$  hence for large currents the diode has significantly larger power losses. The synchronous buck converter can thus be a future improvement work. A buck-boost converter could also be used so that the boost mode operation functions during low solar wattage periods.

The MPPT charge controller was implemented on a PCB. A design modification could be modifying and making the PCB layout more compact and effective in terms of spacing and hence saving copper losses with reduced track lengths. Maximizing the use of traces on both layers could create a neater project. More professional PCB design software which cost more can be used and the created product manufactured by experienced PCB manufacturers to create a more marketable product.

Several additional auxiliary devices can be added to increase the versatility. An irradiance sensor can be added to detect level of insolation so that the MPPT algorithm can account for power change due to change in insolation. The effects of partial shading can also be accounted for by the algorithm by use of particle swarm optimization incase clouds and tree/building shadows block solar cells from receiving the full sun insolation. Wi-Fi modules such as ESP8266, Xbee Modules and Bluetooth connectivity can also be incorporated to wirelessly transmit the data to a website or computer for

comprehensive data analysis. Since all analog pins have been used no additional analog devices may be used, unless an analog-to-digital (I2C) converter is added to the system. This shouldn't be a problem since all I2C devices have a unique address, and up to 127 unique devices may be contained on a single I2C bus.

There are many ventures that can emerge from the improvement design of the MPPT charge controller in the endeavor of building a more versatile product. No design is ever perfect and some of the imperfections that easily came to mind and their solutions have been discussed and there surely are more improvements not thought of that will come into horizon with future technology advances. All the improvements can be undertaken by increasing the budget, timeframe or even project scope. With such small improvements this can be the foundation of future contributions to small, mass-scale and affordable renewable energy projects in the energy discipline.

## **6.2 Conclusion**

The project goal focused on creating a MPPT charge controller with a maximum charging current of 20A to help encourage the use of renewable energy in the form of solar power throughout the world by building a basic, cheap, adaptable, elementary and durable one. An introduction to solar panels and their electrical characteristics has been presented in the literature review. The P-V and I-V curves of the solar panel were of noteworthy importance and based on these characteristics, the significance of maximum power point tracking has been shown. This was followed by carefully designing the hardware and software that constitute an MPPT charge controller in order to address the challenges of the non-linearity in a solar panel power curve. A buck converter was decided on, with a perturb and observe algorithm implementing the tracking. The controller was first tested in Proteus8.1 and PSIM, it was then assembled by testing of each of the module blocks that constituted the charge controller.

The experimental graphs and tables have been presented validating the performance and functionality of the MPPT charge controller in tracking and delivering peak power while also charging the battery healthily. The final product was then tested by connecting a 100W solar panel and a 12V battery load. Once the functionality of the MPPT charge controller was proven while on a breadboard, it was printed on a circuit board to save on space, have a neat simple outlay and for portability. From the results the values of current and voltages got from the solar panel were not as high as expected for a 100W solar panel but that was because the solar panel was faulty from the nameplate though it specified 100W peak, the  $V_{mp}$  was 17.2V and  $I_{mp}$  was 1.17A giving a maximum power of 20W. On carrying out open and short circuit tests  $V_{oc}$  was 21.6V and  $I_{sc}$  was 3.0A. The faulty rated solar panel coupled with cloudy weather gave relatively lower readings for a 100W solar panel, despite this a curve was able to be traced for the solar panel by changing the duty cycle of the MOSFET switch.

The design on the PCB was also done in a way to make the charge controller efficient, safe (by using protection devices) and adaptable - by using DIP sockets so that the microcontroller can be replaced easily and reprogrammed for updates; the incorporation of a keypad made the charge controller more adaptable and robust since the user can set different operating points for different battery and panel

ratings. Finally, a financial analysis of building the MPPT charge controller was done showing that it could be built at a relatively cheap price of \$43(Ksh4386), yet would still be robust enough to handle the power with the common added ancillary functionality such as temperature compensation ,low voltage disconnect when loaded and user customizable charging. The project was a success meeting the project goals of a simple, efficient, adaptable and affordable charge controller which has many applications in developing countries encouraging the use of renewable energy for cheaper energy and helping the global cause of keeping the environment clean. This is a huge milestone in combatting the world energy crisis and global warming.

## REFERENCES

1. A.Harish, M. (2013). Microcontroller based Photovoltaic MPPT Charge Controller. *IJETT*, 4(4).
2. *About Us:Arduino.* (n.d.). Retrieved from Arduino.cc: <https://www.arduino.cc/en/Hacking/PinMapping168>
3. *About Us:Blueskyenergyinc.* (n.d.). Retrieved from Blueskyenergyinc: [http://www.blueskyenergyinc.com/uploads/pdf/BSE\\_SB2512i\(X\)-HV\\_datasheet.pdf](http://www.blueskyenergyinc.com/uploads/pdf/BSE_SB2512i(X)-HV_datasheet.pdf)
4. *About Us:Midnitesolar.* (n.d.). Retrieved from Midnitesolar: [http://www.midnitesolar.com/pdfs/spec\\_sheet\\_kid\\_frontBack.pdf](http://www.midnitesolar.com/pdfs/spec_sheet_kid_frontBack.pdf)
5. *About Us:Morningstarcorp.* (n.d.). Retrieved from Morningstarcorp: [http://www.morningstarcorp.com/wp-content/uploads/2014/02/SunSaverENG\\_R3\\_5\\_12web1.pdf](http://www.morningstarcorp.com/wp-content/uploads/2014/02/SunSaverENG_R3_5_12web1.pdf)
6. *About US:Morningstarcorp.* (n.d.). Retrieved from Moningstarcorp: <http://support.morningstarcorp.com/wp-content/uploads/2015/10/MS-C-Data-Sheet-ProStar-MPPT-151020-10-MG-HIGH.pdf>
7. *Allegromicro.* (n.d.). Retrieved from Allegromicro: <http://www.allegromicro.com/en/Products/Current-Sensor-ICs/Zero-To-Fifty-Amp-Integrated-Conductor-Sensor-ICs/ACS712.aspx>
8. *Batterystuff.* (n.d.). Retrieved from Batterystuff: <http://www.batterystuff.com/blog/3-stages-of-smart-chargers.html#sthash.lxy5HzhU.dpuf>
9. *Chargingchargers.* (n.d.). Retrieved from Chargingchargers: <http://www.chargingchargers.com/tutorials/charging.html>
10. E. Koutroulis, K. K. (2001). Development of a microcontroller-based, photovoltaic maximum power point tracking control system. *IEEE Transactions Power Electronics*, 16, 46-54.
11. *International Rectifier.* (n.d.). Retrieved from International Rectifier: <http://www.irf.com/technical-info/appnotes/an-967.pdf>
12. *MaximIntegrated.* (n.d.). Retrieved from MaximIntegrated: <https://datasheets.maximintegrated.com/en/ds/DS18B20.pdf>
13. Md.Selim Hossain, M. H. (2012). Design,simulation and real-time implemrntation of amaximum power point tracker for a photovoltaic system. *IJSS*, 6(1), 25-29.
14. Mihnea Rosu-Hamzescu, S. O. (n.d.). *Microchip Technology Inc.* Retrieved from Microchip Technology Inc.: <http://ww1.microchip.com/downloads/en/AppNotes/00001521A.pdf>

15. Patrick L. Chapman, E. T. (2007). Comparison of Photovoltaic Array Maximum Power. *IEEE TRANSACTIONS ON ENERGY CONVERSION*, 22(2), 26-30.
16. Rashid, M. H. (n.d.). *Power Electronics Handbook* (Third ed.). Florida: Butterworth-Heinemann.
17. *Wikipedia*. (n.d.). Retrieved from Wikipedia:  
[https://en.wikipedia.org/wiki/Battery\\_\(electricity\)](https://en.wikipedia.org/wiki/Battery_(electricity))

## APPENDICES

### Appendix One: MPPT Charge Algorithm Code used in the ATMEGA328P

The following is the complete code for the MPPT charge controller.

```
/*PROJECT124-Microcontroller based MPPT Charge Controller
F17/38980/2011*/

/*Specs:
Maximum charging current=20A
Max rated Input Voltage=45V
Efficient Solar panel rating= 50-240W
Rated battery =12V battery by default,can tolerate also 6V and 24V
*/

//Arduino Pin Connectivity:
/*Analog input pins
A0-Solar panel voltage divider sensor
A1-Solar panel ACS-712 current sensor
A2-Battery voltage divider sensor
A3-Battery ACS-712 current sensor
SDA&SCL-LCD by I2C
Digital I/O pins
3-BLUE LED
5-RED LED
6-GREEN LED
8-PWM MOSFET DRIVER SD
9-PWM MOSFET DRIVER IN or PC817 anode pin1
1-Temp sensor
2,4,7,10-13-Keypad
*/

//Essential Libraries
```

```

#include<TimerOne.h>//http://playground.arduino.cc/Code/Timer1
#include<LiquidCrystal_I2C.h>//http://playground.arduino.cc/Code/LCDi2c
#include<Wire.h>
#include <DallasTemperature.h>//for dsb1820
#include <Keypad.h>
// Pin outs definitions
#define Vsolar_sensor 0
#define Isolar_sensor 1
#define Vbatt_sensor 2
#define Ibatt_sensor 3
#define SD_pin 8//IR2110 SD
#define IN_pin 9//IR2110 HIN
#define MPPT_PandO //choose method of implementation using either perturb or incremental
conductance by uncommenting the choice.
//#define MPPT_INCCOND
#define COMMON_ANODE //uncomment if its common cathode ,the RGB pin connectivities are
specified below
#define R 5
#define G 6
#define B 3
#define Vsolar_factor 0.045085461//((5/1024)*(R2+R1)/R1;R1=9.85K,R2=81.1K
#define Vbatt_factor 0.014938902//((5/1024)*(R2+R1)/R1;R1=9.75K,R2=20.08K
#define Isolar_factor 0.048828125//((5/1024)/0.1 „sensitivity of ACS712-20A is 100mV/A
#define Ibatt_factor 0.048828125//((5/1024)/0.1 „sensitivity of ACS712-20A is 100mV/A
#define Ioffset1 24.9 //((2.5/0.1 5/1024)/0.1 „sensitivity of ACS712-20A is 100mV/A & volatge at
0A is 2.5 V (but with the ones I used they had avoltage drop of 24.8 at 0A)
#define Ioffset2 24.9 //((2.5/0.1 5/1024)/0.1 „sensitivity of ACS712-20A is 100mV/A & volatge at
0A is 2.5 V (but with the ones I used they had avoltage drop of 24.4 at 0A)

//Pertinent constants

```



```

#define MOSFET_OFF digitalWrite(IN_pin,LOW)//because were using PC817 just turn off its
input
#define MOSFET_ON digitalWrite(SD_pin,LOW)
#define LOAD_ON digitalWrite(load_pin,HIGH)
#define LOAD_OFF digitalWrite(load_pin,LOW)
#define pwm_max 100 //100%
#define pwm_top 1023 //DAC value of max pwm by timer1.h
#define pwm_min 28 //worst case pwm for maximum rating open circuit voltage Voc=45V
#define pwm_stepsize 1//step size to be use in Perturb&Observe
#define pwm_start 60//Optimal starting pwm
#define sample_no 10

// Data wire is plugged into Dpin1 on the Arduino
#define ONE_WIRE_BUS 1
#define load_pin 0//for keypad
const byte ROWS = 4; //four rows
const byte COLS = 3; //three columns
char keys[ROWS][COLS] = {  {'1','2','3'}, {'4','5','6'}, {'7','8','9'}, {'.','0','#'}};

byte rowPins[ROWS] = {13, 12, 11, 10}; //connect to the row pinouts of the keypad
byte colPins[COLS] = {7, 4, 2}; //connect to the column pinouts of the keypad

//LCD BATTERY SoC ICONS
byte batt_icons [6][8]={ { 0b01010, 0b10001, 0b10001, 0b10001, 0b10001, 0b10001,
0b10001,
0b11111 }, { 0b01010, 0b10001, 0b10001, 0b10001, 0b10001, 0b10001, 0b11111,
0b11111
},
{ 0b01010, 0b10001, 0b10001, 0b10001, 0b10001, 0b11111, 0b11111, 0b11111 },
{ 0b01010, 0b10001, 0b10001, 0b10001, 0b11111, 0b11111, 0b11111, 0b11111 },
{ 0b01010, 0b10001, 0b10001, 0b11111, 0b11111, 0b11111, 0b11111, 0b11111

```

```

    }, { 0b01010, 0b11111, 0b11111, 0b11111, 0b11111, 0b11111, 0b11111, 0b11111 },
};

#define PV_ICON 6

byte pv_icon[8]={ 0b11111, 0b10101, 0b11111, 0b10101, 0b11111, 0b10101, 0b11111,
    0b11111 };

#define PWM_ICON 7

byte pwm_icon[8]= { 0b10111, 0b10111, 0b10101, 0b10101, 0b10101, 0b10101, 0b11101,
    0b11101
};

//Declaring variables and data types

float Vsolar; float PrevVsolar=0; float Isolar; float PrevIsolar=0; float Vbatt; float Ibatt; float
Tbatt=25;

float celcius; float Psolar; float Pleast=2; float PrevPsolar=0; unsigned int interrupt_counter=0;
unsigned long boost_millis=0;//stors the boost time(absorption/topping) time for the day
float delta=pwm_stepsize;//changes pwm in MPPT bulk mode
float inc=pwm_stepsize;//changes pwm in boost and float modes to maintain voltage constant
float error1=0;//error during maintain absorption voltage
float error2=0;//error during maintaining float voltage
float error3=0;//error during avoiding exceeding max charging current
float pwm=0;

//Battery set points

float Vfloat;//temp compensated float Vfloat1;//to be set by user
char strfloat[]={"13.60"}; float Vboost;//temp compensated
float Vboost1;//to be set by user
char strboost[]={"14.40"};

float LVD;//LOW VOLTAGE DISCONNECT

char strLVD[]={"11.20"}; unsigned long boost_settime; float boost_settime1; char
strboostTime[]={"060"}; unsigned long boost_time; char strBattType[]={"12"};

float temp_compensation; float tempComp1; char strtempComp[]={"3.0"};//3mV per cell

```

```

    int Imax=20;//max charging current    int Tmax=40;//max rated battery temperature    operating
condition
//keypad auxiliaries

enum charger_mode{off,initialize,bulk,boost,float_mode}charger_mode;
//SetLCD I2C address fot the 2004 diplay by syntax :hexaddress,en,rw,rs,D4,D5,D6,D7,bl,blpol
LiquidCrystal_I2C lcd(0x3F,2,1,0,4,5,6,7,3,POSITIVE);
//set keypad mapping matrix
Keypad keypad = Keypad( makeKeymap(keys), rowPins, colPins, ROWS, COLS );
// setup dsi8b20 Pass our oneWire reference to Dallas Temperature .
OneWire oneWire(ONE_WIRE_BUS); DallasTemperature sensors(&oneWire);
void setup() {
pinMode(SD_pin,OUTPUT);//Start in the off state by defining Shutdown Pin as an output and
turning it low
MOSFET_OFF;
charger_mode=off;
lcd.begin(20,4);//Initialize our LCD 2004 display (20 columns by 4 rows)
//Create LCD various SoC -state of charge icons and ensure backlight is on for all light conditions
visibility
lcd.backlight();
for (int baticon=1;baticon<7;baticon++){
    lcd.createChar(baticon,batt_icons[baticon]);
} lcd.createChar(PV_ICON,pv_icon); lcd.createChar(PWM_ICON,pwm_icon);
pinMode(R,OUTPUT); pinMode(G,OUTPUT); pinMode(B,OUTPUT);
led_mode=black; Timer1.initialize(20);//initialize timer1 at a 20microsecond period=50KHz
Timer1.pwm(IN_pin,0);//Set the PWM for the IN pin of MOSFET driver to0
//startpwm at an optimized start point
pwm=pwm_start;
keypad.addEventListener(keypadEvent); // Add an event listener for this keypad
//display constant icons of the key MPPT components
lcd.setCursor(0,0);lcd.print("PV");lcd.setCursor(3,0);lcd.write(PV_ICON);lcd.setCursor(7,0);
lcd.print("PWM");lcd.setCursor(11,0);lcd.write(PWM_ICON);lcd.setCursor(14,0);

```

```

lcd.print("BATT");

}

void loop() {
  read_sensors();//read various sensors to get data needed to run MPPT charge controller
  keypadmode();
  run_MPPTcharger();//run MPPT P&O Algorithm and battery charging algorithm
  lcd_display();//display system parameters on LCD
  led_display();//display system status via LEDs
  load_engage();resetting(); }

int sample_sensor(int Inputpin){
  int sum = 0; int temp;

  for (int k=0; k<sample_no ; k++){      temp=analogRead(Inputpin);      sum+=temp;
  delayMicroseconds(50);
  } return(sum/sample_no); }

void read_sensors(void){      Vsolar=sample_sensor(Vsolar_sensor)*Vsolar_factor;
Vbatt=sample_sensor(Vbatt_sensor)*Vbatt_factor;
Isolar=(sample_sensor(Isolar_sensor)*Isolar_factor)-Ioffset1;
Ibatt=(sample_sensor(Ibatt_sensor)*Ibatt_factor)-Ioffset2; sensors.begin();//to search for ds18b20

int b=(sensors.getDeviceCount()); if (b=10){ sensors.requestTemperatures();
celcius=sensors.getTempCByIndex(0); Tbatt=celcius;  }

else {Tbatt=25;}

Psolar=Vsolar*Isolar;

Vfloat=(Vfloat1+(25-Tbatt)*temp_compensation);//Just incase the user doesnt edit anything
Vboost=(Vboost1+(25-Tbatt)*temp_compensation);  }

//Setting the pwm duty cycle for the IN_pin using timer1.pwm on pin9
void set_pwm_dutycycle(float pwm){
  if (pwm<pwm_min){ pwm=pwm_min;  }

  else if (pwm>pwm_max || pwm==pwm_max){ pwm=pwm_max;

```

Timer1.pwm(IN\_pin,(pwm\_top-1),20); //operate at max99.9% duty cycle to allow bootstrap capacitor to recharge at off time

}if (pwm<pwm\_max&& pwm>pwm\_min){

Timer1.pwm(IN\_pin,(pwm\_top)\*(long)pwm/100,20); //set pwm at 50KHz

}}

void run\_MPPTcharger(){

switch(charger\_mode){ case off: MOSFET\_OFF; delay(1500);  
if(((Vbatt>12)&&(Vsolar>Vbatt+0.5) || (Vbatt<=12)&&(Vsolar>=12.5))) {

charger\_mode=initialize;

} break;

case initialize:

if

((Vbatt>12)&&(Vsolar<Vbatt+0.5) || (Vbatt<=12)&&(Vsolar<12.5) || (Isolar<0.1) || (Ibatt>Imax)  
|| (Vbatt>Vboost+0.15) || Psolar<Pleast || Tbat>Tmax)) { charger\_mode=off;  
MOSFET\_OFF; break;

}

else {if (boost\_time>boost\_settime){ charger\_mode=float\_mode;} else {if (Vbatt>Vboost){  
charger\_mode=boost; MOSFET\_ON; boost\_millis=millis(); break; }

else { charger\_mode=bulk; //if voltage is less than boost voltage and cant go to float since  
the boost time hasnt been reached

MOSFET\_ON; break;

} } } break;

case bulk:

if

((Vbatt>12)&&(Vsolar<Vbatt+0.5) || (Vbatt<=12)&&(Vsolar<12.5) || (Isolar<0.1) || (Ibatt>Imax)  
|| (Vbatt>Vboost+0.15) || Psolar<Pleast || Tbat>Tmax)) {

charger\_mode=off; MOSFET\_OFF; break;

}

else {if (Vbatt>Vboost+0.01){ if (boost\_time>boost\_settime){  
charger\_mode=float\_mode;

MOSFET\_ON; break; }

```

    else { charger_mode=boost;    MOSFET_ON;    boost_time=millis();    break;    }
}

else {    #ifdef MPPT_PandO        mppt_PandO();    #endif
    #ifdef MPPT_INCCOND        mppt_INCCOND();    #endif

if(Ibatt>Imax-1){
    error3=Ibatt-(Imax-1);    inc=300*delta*error3;    pwm-=inc;    set_pwmudutycycle(pwm);
    }    break; } }

case boost:
    boost_time=boost_time+millis()-boost_millis;    boost_millis=millis();
    if
(((Vbatt>12)&&(Vsolar<Vbatt+0.5) || (Vbatt<=12)&&(Vsolar<12.5) || (Ibatt>Imax) || (Isolar<0.1)
|| (Vbatt>Vboost+0.15) || Psolar<Pleast || Tbatt>Tmax)){
MOSFET_OFF;    break;
    }
    else {if (Vbatt< Vboost-0.25){    charger_mode=bulk;    MOSFET_ON;    break; }
    else{    if(boost_time>boost_settime){    charger_mode=float_mode;    MOSFET_ON;
break;
    }
    else {if(Vbatt>Vboost+0.02){    error1=Vbatt-(Vboost+0.02);
        inc=delta*500*error1;//if battery voltage >14.42 decrease pwm by the %error;we want thr pwm
to be zero by the time we get to 14.6
        pwm-=inc;    set_pwmudutycycle(pwm);    boost_time=boost_time+millis()-boost_millis;
    }

    if(Ibatt>Imax-1){
        error3=Ibatt-(Imax-1);    inc=300*delta*error3;//if battery current >19 decrease pwm by the
%error
        pwm-=inc;    set_pwmudutycycle(pwm);    }    break;    }    } }

```

```

    case float_mode:
        if
        (((Vbatt>12)&&(Vsolar<Vbatt+0.5) || (Vbatt<=12)&&(Vsolar<12.5) || (Isolar<0.1) || (Ibatt>Imax)
        || (Vbatt>Vboost+0.15) || Psolar<Pleast || Tbatt>Tmax)){
            charger_mode=off;    MOSFET_OFF;    break;    }
        else {if(Vbatt<(Vfloat-0.1)){
            charger_mode=bulk;    MOSFET_ON;    break;    }
        else {if (Vbatt>(Vfloat+0.02)){    error2=Vbatt-(Vfloat+0.02); inc=delta*500*error2; pwm-=inc;
        set_pwmduycycle(pwm);
        if(Ibatt>Imax-1){
            error3=Ibatt-(Imax-1);    inc=300*delta*error3;//if battery current >19 decrease pwm by the
        %error
            pwm-=inc;    set_pwmduycycle(pwm);    }    break;    } }
        default: charger_mode=off; MOSFET_OFF; break; }}

void mppt_PandO(){
    if (Psolar<PrevPsolar){
        pwm-=delta;//if solar power has reduced,change track direction and add this negated value to
        pwm
        PrevPsolar=Psolar;    set_pwmduycycle(pwm);    }
    else{    pwm+=delta;//else just add the normal pwm that is positive to pwm
        PrevPsolar=Psolar;    set_pwmduycycle(pwm);    }
}

void mppt_INCCOND(){
    float delta_P=Psolar-PrevPsolar; float delta_V=Vsolar-PrevVsolar; float delta_I=Isolar-PrevIsolar;
    float gradient=delta_P/delta_V;    if(delta_V!=0){    if(gradient>0){    pwm+=delta;
    PrevPsolar=Psolar;
        PrevVsolar=Vsolar;    PrevIsolar=Isolar;    set_pwmduycycle(pwm);    }
    else    if(gradient<0){    pwm-=delta;    PrevPsolar=Psolar;    PrevVsolar=Vsolar;
    PrevIsolar=Isolar;    set_pwmduycycle(pwm);    } }
    else { if(delta_I>0){    pwm+=delta;    PrevPsolar=Psolar;    PrevVsolar=Vsolar;    PrevIsolar=Isolar;
        set_pwmduycycle(pwm);}}

```

```

else if(delta_I<0){  pwm-=delta;  PrevPsolar=Psolar;  PrevVsolar=Vsolar;  PrevIsolar=Isolar;
    set_pwmudutycycle(pwm);}} }
/*led system status indication
red light= battery undervoltage <30% ,<11.75V// warning light
purple light=battery overvoltage >14.5V
orange light =30% to 90% 11.75-12.5V
green light=battery full charge >90% 12.5-13.6V
blue light= no solar panel/battery//warning light
small green led= MPPT charger on(will be done from lm7805 secondary side)*/
void led_display(void)
{  if(Vbatt>Vboost+0.2)          led_mode=purple;      else if (Vbatt>12.5&&Vbatt<Vfloat)
led_mode=green;
    else if(Vbatt<11.75)      led_mode=red; if (Vbatt<12.5 | Vsolar<0.25)  led_mode=blue;

    switch (led_mode){
        case red: setColor(255, 0, 0); break;case green:setColor(0, 255, 0);break;case blue:setColor(0, 0, 255);
break;case yellow:setColor(255, 255, 0); break ;case purple:setColor(80, 0, 80);break;case orange :
setColor(255,128,0);break;case black :setColor(0,0,0);break;}}
void setColor(int r, int g, int b)
{
#ifdef COMMON_ANODE r = 255 - r; g= 255 - g; b = 255 - b; #endif
analogWrite(R,r); analogWrite(G,g); analogWrite(B,b);}
//LCD display of system parameters
void lcd_display()
{  lcd.setCursor(0,0);lcd.print("PV");lcd.setCursor(3,0);lcd.write(PV_ICON);lcd.setCursor(7,0);
lcd.print("PWM");lcd.setCursor(11,0);lcd.write(PWM_ICON);lcd.setCursor(14,0);lcd.print("BATT");
    //solar parameters
    lcd.setCursor(0,1);  lcd.print(Vsolar);  lcd.print("V");  lcd.setCursor(0,2);  lcd.print(Isolar);
lcd.print("A");
    lcd.setCursor(0,3); lcd.print(Psolar); lcd.print("W");

```



```

//Duty cycle of pwm
lcd.setCursor(7,1);if (charger_mode==off){lcd.print("0"); lcd.print("."); lcd.print("00");}
else {lcd.print(pwm);lcd.print("%");}

//charging mode
lcd.setCursor(7,2);if (charger_mode==off){ lcd.print("OFF"); lcd.print(" "); lcd.print(" ");}
else if (charger_mode==bulk){ lcd.print("BULK"); lcd.print(" ");}else if (charger_mode==boost)
lcd.print("BOOST");else if (charger_mode==float_mode) lcd.print("FLOAT");

//boost time
lcd.setCursor(7,3);lcd.print(boost_time/60000);lcd.print ("min");

//battery parameters
lcd.setCursor(14,1); lcd.print(Vbatt); lcd.print("V"); lcd.setCursor(14,2); lcd.print(Ibatt);
lcd.print("A");

//Battery SoC
int pct=100*(Vbatt-10.5)/(12.7-10.5);//battery at 10% is 12.7V and at 0% is 10.5V
if (pct<0) pct=0; else if (pct>100) pct=100; lcd.setCursor(18,0); if (pct==0){ lcd.write(1);
} else {
lcd.print((char)(pct*5/100));//print battery icon based on battery SoC
} lcd.setCursor(14,3); pct=pct-(pct%10); lcd.print(pct); lcd.print("%"); lcd.print(" "); lcd.print("
");}

// Taking care of some special events.
void keypadEvent(KeypadEvent key){
switch (keypad.getState()){

char keypadmode(){
char key = keypad.getKey(); keypad.getState();
void settings(){ while(e<7){ editmode=e; if (editmode==0){ e++; setBattType();}else {if
editmode==1){ e++; setVboost();}else {if (editmode==2){ e++; setVfloat();}else {if
(editmode==3){
e++; setVboostTime();}else {if (editmode==4){e++; settempComp();}else
{if(editmode==5){e++;

```

```

void setBattType(){
lcd.clear(); lcd.setCursor(0,0); lcd.print("Set Battery Type"); lcd.setCursor(2,1);
lcd.print("V"); lcd.setCursor(3,1); lcd.print(":NEW VALUE"); lcd.setCursor(0,2); lcd.print(a);
lcd.print("V"); lcd.print(":CURRENT VALUE");

float cellboost=Vboost1/(a/2); //save per cell setpoint so that if we change battery type we can
respectively scale up depending on the no. of cells a/6

float cellfloat=Vfloat1/(a/2); //no need for adjusting temp compensation since its calculated per
cell

float cellLVD=LVD/(a/2); while(j<2){char key = keypad.getKey();

if (key){ strBattType[j]=key; lcd.setCursor(j,1); lcd.print(key); j++; } }
// j=0; //reset n incase we enter this loop again

lcd.clear(); Vboost1=cellboost*(a/2); Vfloat1=cellfloat*(a/2); LVD=cellLVD*(a/2);}

void setVboost(){ lcd.clear(); lcd.setCursor(0,0); lcd.print("Enter Boost Value"); lcd.setCursor(5,1);
lcd.print("V"); lcd.setCursor(6,1); lcd.print(":NEW VALUE"); lcd.setCursor(0,2);
lcd.print(Vboost1);

lcd.print("V"); lcd.print(":CURRENT VALUE"); while(k<5){char key = keypad.getKey();
if (key){ strboost[k]=key; lcd.setCursor(k,1); lcd.print(key); k++; } }
//k=0; //reset k incase we enter this loop again

lcd.clear(); Vboost=(Vboost1+(25-Tbatt)*temp_compensation);
}

void setVfloat(){ lcd.clear(); lcd.setCursor(0,0); lcd.print("Enter Float Value"); lcd.setCursor(5,1);
lcd.print("V"); lcd.setCursor(6,1); lcd.print(":NEW VALUE"); lcd.setCursor(0,2);
lcd.print(Vfloat1);

lcd.print("V"); lcd.print(":CURRENT VALUE");
while(l<5){char key = keypad.getKey();
if (key){ strfloat[l]=key; lcd.setCursor(l,1); lcd.print(key); l++; }
l=0; lcd.clear(); Vfloat=(Vfloat1+(25-Tbatt)*temp_compensation);}

void setLVD(){

```

```

    lcd.clear(); lcd.setCursor(0,0); lcd.print("Enter LVD Value"); lcd.setCursor(5,1); lcd.print("V");
    lcd.setCursor(6,1);    lcd.print(":NEW VALUE");    lcd.setCursor(0,2);    lcd.print(LVD);
    lcd.print("V");

```

```

    lcd.print(":CURRENT VALUE"); while(p<5){char key = keypad.getKey();
    if (key){    strLVD[p]=key;    lcd.setCursor(p,1); lcd.print(key); p++; } }
    p=0; lcd.clear();

```

```

void setVboostTime()

```

```

{ lcd.clear(); lcd.setCursor(0,0); lcd.print("Enter Boost minutes"); lcd.setCursor(3,1);
    lcd.print("min");    lcd.setCursor(6,1);    lcd.print(":NEW VALUE");    lcd.setCursor(0,2);
    lcd.print(strboostTime);    lcd.print("min");    lcd.print(":CURRENT VALUE"); while(m<3){
    char key = keypad.getKey();
    if (key){    strboostTime[m]=key;    lcd.setCursor(m,1); lcd.print(key);    m++;    } }
    lcd.clear(); ; boost_settime=((unsigned long)(boost_settime1*60000));}

```

```

void settempComp()

```

```

{    lcd.clear(); lcd.setCursor(0,0); lcd.print("Cell TempCompensation"); lcd.setCursor(3,1);
    lcd.print("mV/*C"); lcd.setCursor(8,1); lcd.print(":NEW VALUE"); lcd.setCursor(0,2);
    lcd.print(strtempComp);    lcd.print("mV/*C");    lcd.print(":CURRENT VAL"); while(n<3){
    char key = keypad.getKey();
    if (key){    strtempComp[n]=key;    lcd.setCursor(n,1); lcd.print(key);    n++; } }
    lcd.clear(); temp_compensation=(tempComp1*(a/2)/1000);}

```

```

void lcd_scroll(){ while(s<1){ lcd.clear(); lcd.home(); lcd.print("Batt Temp:"); lcd.print(Tbatt);
    lcd.print("*C"); lcd.setCursor(0,1); lcd.print("Vboost"); lcd.print(Vboost); lcd.print("V");
    lcd.setCursor(0,2); lcd.print("Vfloat"); lcd.print(Vfloat); lcd.print("V"); lcd.setCursor(0,3);
    lcd.print("LOAD:"); if (load){ lcd.print("ON"); }else { lcd.print("OFF"); } delay(3000); s++;
    lcd.clear(); } resetting();}

```

```

void load_engage(){ if(load){//only if user has activated load mode

```

```

    if(Psolar<Pleast&&Vbatt>LVD){    LOAD_ON; }else {if(Psolar>Pleast&&Vbatt>Vfloat){
    LOAD_ON; } else LOAD_OFF; }}elseLOAD_OFF;}

```

## Appendix Two: IC Datasheets

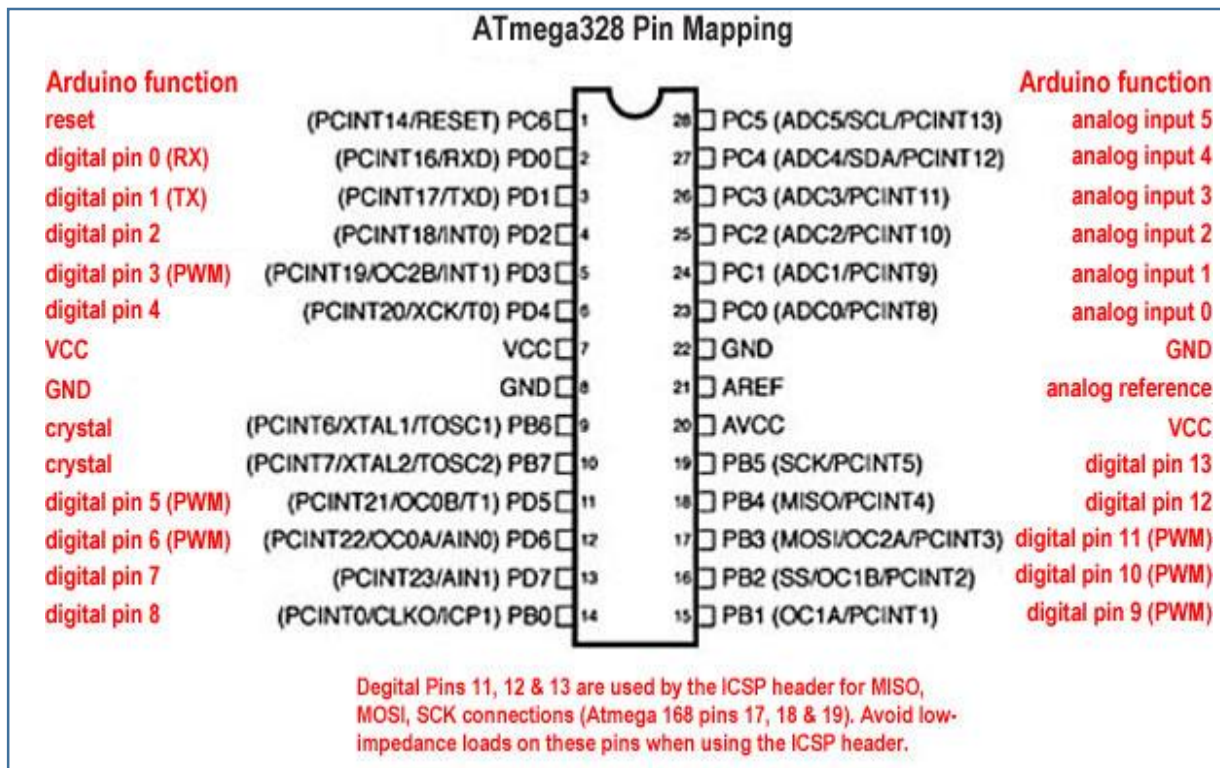


Figure A-1: ATMEGA328P Pin Mapping

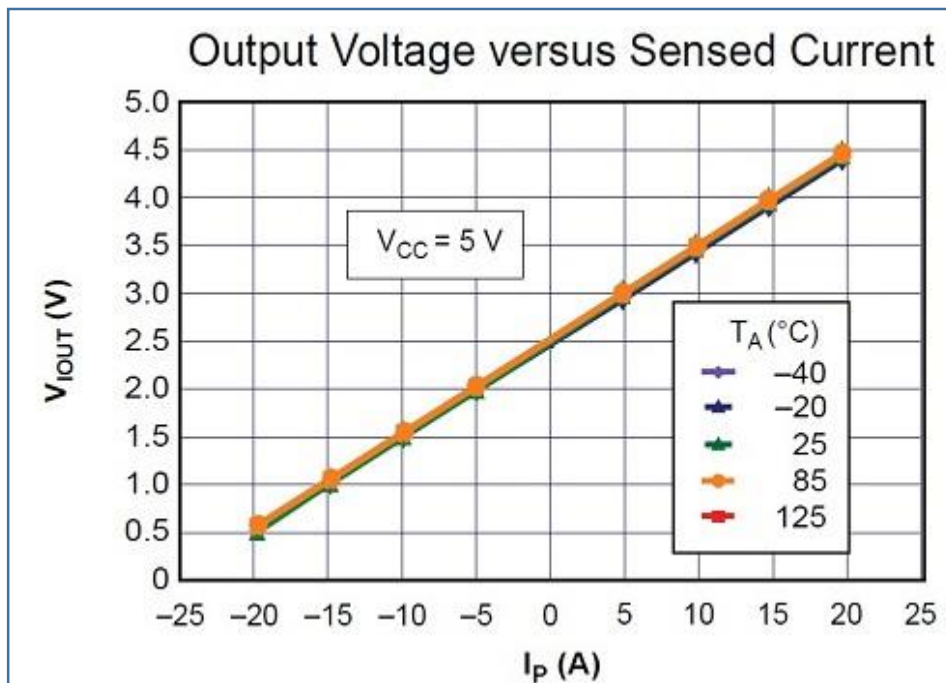


Figure A-2: ACS712 Sensitivity Graph

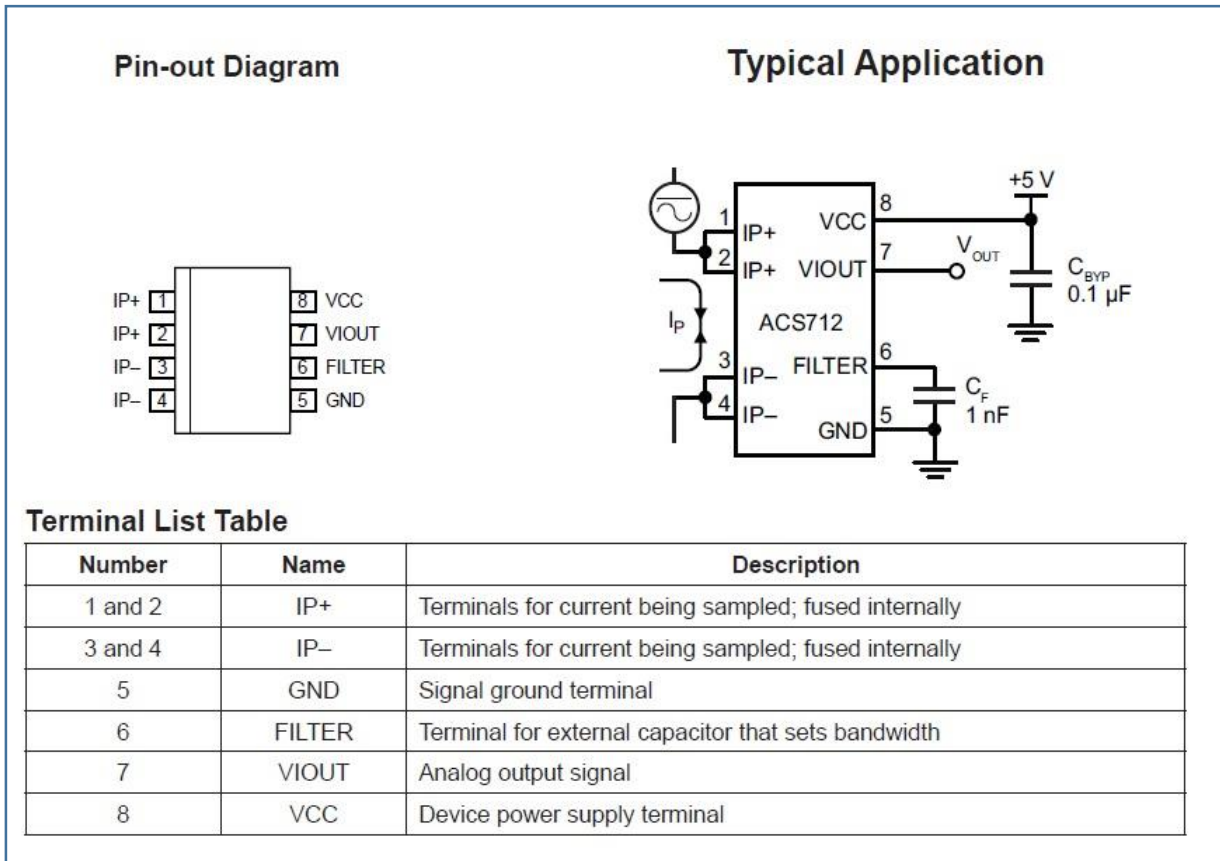


Figure A-3: ACS712 Pin out diagram and typical connection

## Pin Configurations

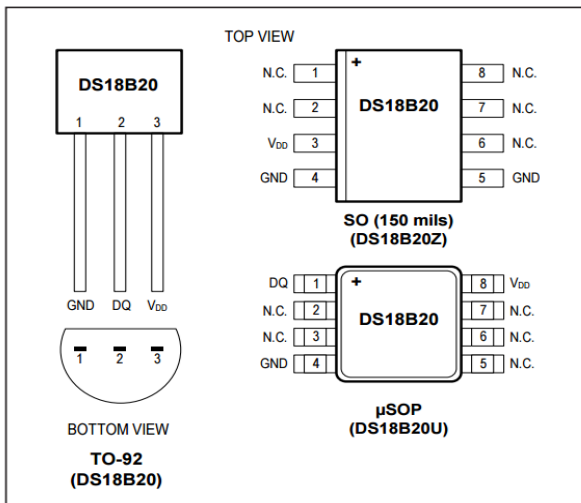


Figure A-4: DSB1820 Pin out diagram

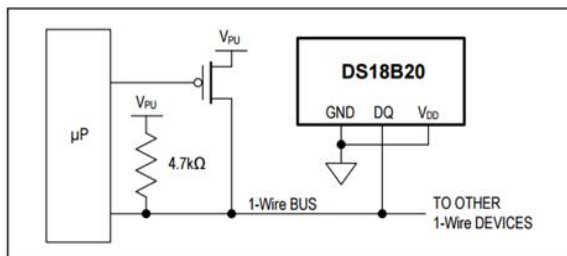


Figure 6. Supplying the Parasite-Powered DS18B20 During Temperature Conversions

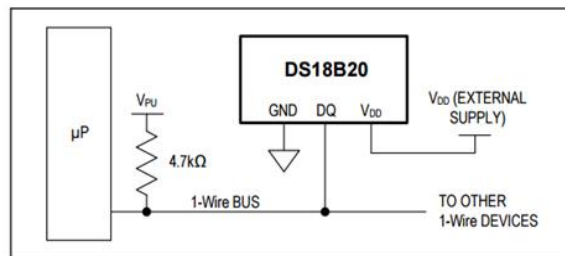


Figure 7. Powering the DS18B20 with an External Supply

Figure A-5: DS18B20 typical connection diagram

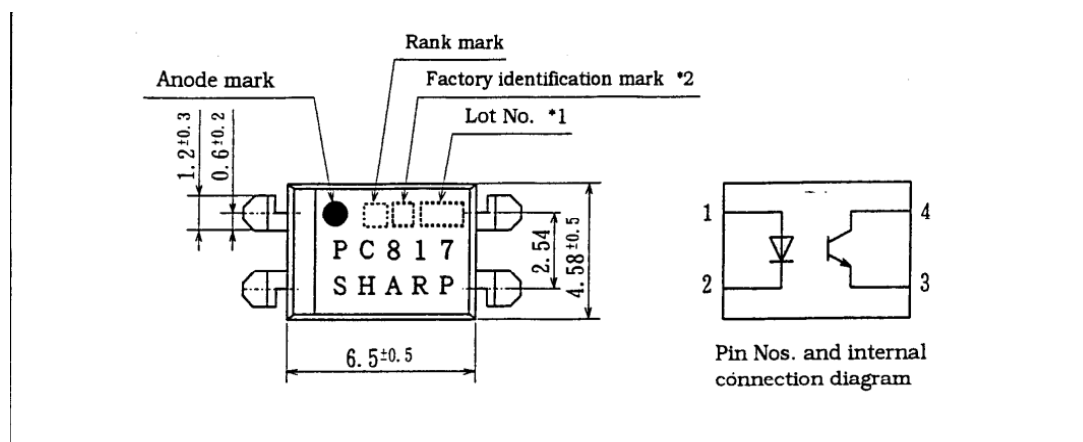


Figure A-6: PC817 typical connection diagram

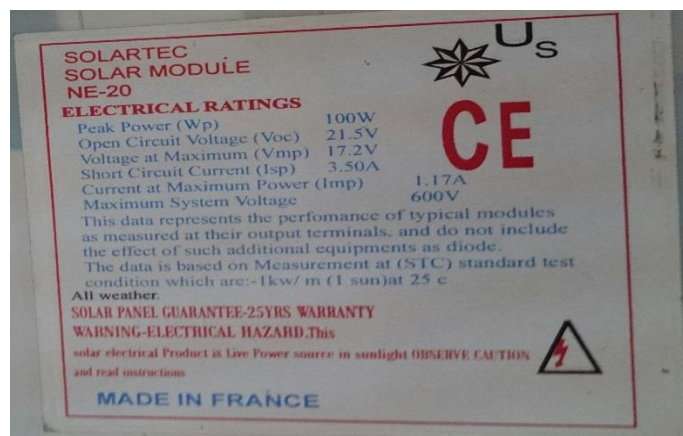


Figure A-7: SolarTec solar module name plate specifications



Figure A-8: FIAMM 12FGL100 Battery used



### Appendix Three: PCB traces

Below is the PCB bottom, top and silk screen layer

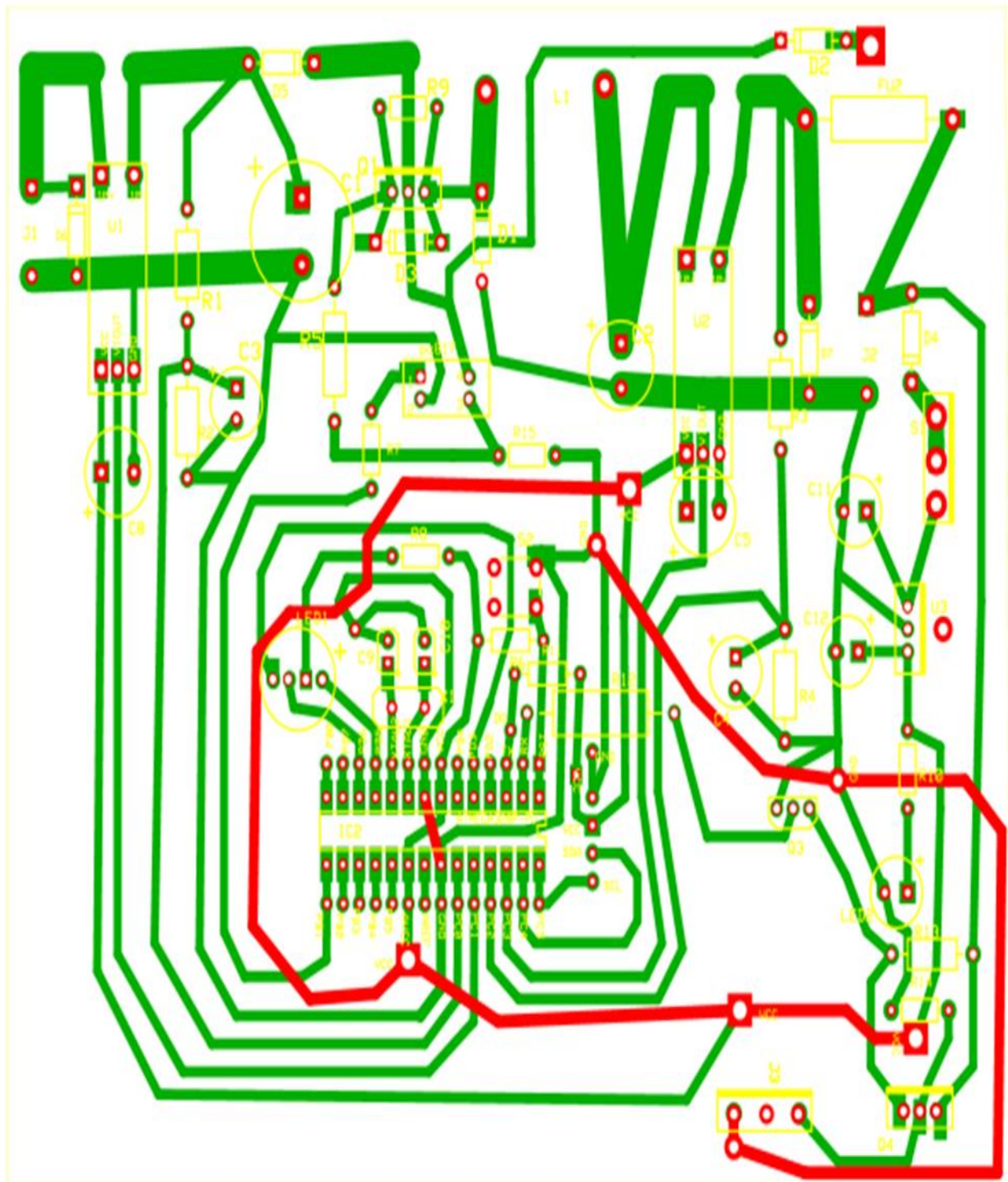


Figure A-9: PCB of top, bottom and silk screen layer

#### Appendix Four: Pictures of MPPT Charge Controller in various modes

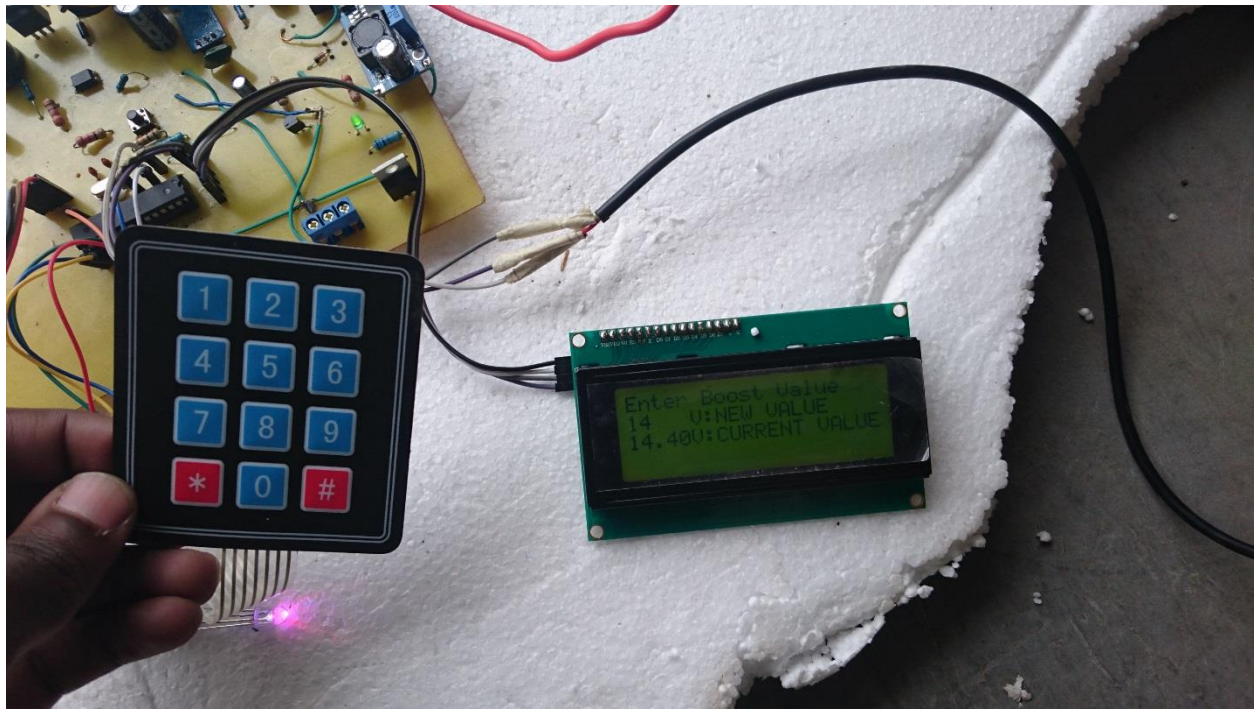


Figure A-10: Using Keypad to set absorption voltage value

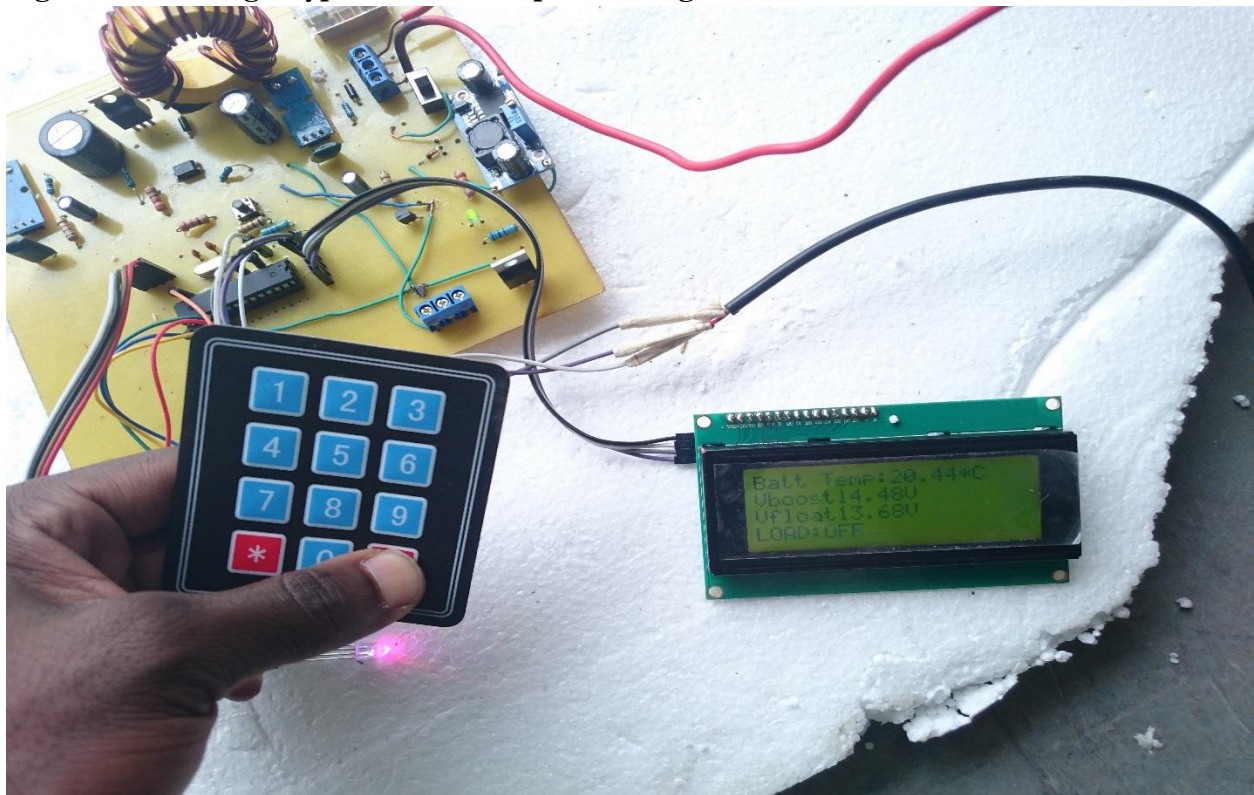


Figure A-11: Using Keypad to verify temperature compensation at 3mv/°C/Cell